

Distribution agreement

In presenting this thesis or dissertation as a partial fulfillment of the requirements for an advanced degree from Emory University, I hereby grant to Emory University and its agents the non-exclusive license to archive, make accessible, and display my thesis or dissertation in whole or in part in all forms of media, now or hereafter known, including display on the world wide web. I understand that I may select some access restrictions as part of the online submission of this thesis or dissertation. I retain all ownership rights to the copyright of the thesis or dissertation. I also retain the right to use in future works (such as articles or books) all or part of this thesis or dissertation.

signature

Lisa H. Kreiner

Date

Factors that modulate Ca^{2+} -dependent regulation of $\text{Ca}_v 2.1$ (P/Q-type) Ca^{2+} channels

By

Lisa H. Kreiner
Doctor of Philosophy

Graduate Division of Biological and Biomedical Sciences
Neuroscience Program

Amy Lee, Ph.D.
Advisor

Ronald Abercrombie, Ph.D.
Committee Member

Elizabeth Finch, Ph.D.
Committee Member

Criss Hartzell, Ph.D.
Committee Member

Stephen Traynelis, Ph.D.
Committee Member

Accepted:

Lisa A. Tedesco, Ph.D.
Dean of the Graduate School

Date

Factors that modulate Ca^{2+} -dependent regulation of $\text{Ca}_v 2.1$ (P/Q-type) Ca^{2+} channels

By

Lisa H. Kreiner
BS, Georgia Institute of Technology, 1992
MS, Georgia State University, 1997

Advisor: Amy Lee, Ph.D.

An Abstract of
A dissertation submitted to the Faculty of the Graduate
School of Emory University in partial fulfillment
of the requirements for the degree of
Doctor of Philosophy

Program in Neuroscience
Graduate Division of Biological and Biomedical Sciences

2008

Abstract

Factors that modulate Ca^{2+} -dependent regulation of $\text{Ca}_v 2.1$ (P/Q-type) Ca^{2+} channels

By Lisa H. Kreiner

Activity-dependent changes in the cytoplasmic Ca^{2+} concentration in neurons initiate a multitude of processes ranging from gene transcription to neurotransmitter release. Voltage-gated Ca^{2+} channels are important for these processes as they couple membrane depolarization to the influx of Ca^{2+} ions into the neuron. Since Ca^{2+} is a second messenger in many cellular pathways, factors that regulate Ca^{2+} signaling are essential for proper regulation of neuronal function. $\text{Ca}_v 2.1$ (P/Q-type) voltage-gated Ca^{2+} channels undergo a complex feedback regulation mediated by Ca^{2+} bound calmodulin, which can cause short-term alterations in synaptic efficacy. Ca^{2+} influx through $\text{Ca}_v 2.1$ produces an initial increase (Ca^{2+} -dependent facilitation (CDF)) and gradual decrease (Ca^{2+} -dependent inactivation (CDI)) in Ca^{2+} current amplitude during high frequency or prolonged stimulation. We investigated two factors that could potentially regulate CDF and/or CDI in neurons, Ca^{2+} buffering proteins and Ca^{2+} induced Ca^{2+} release from intracellular stores. Voltage clamp recordings from either $\text{Ca}_v 2.1$ transfected HEK 293T cells or dissociated Purkinje neurons were used to quantify CDF and CDI that occurs in response to depolarization. The effects of the Ca^{2+} buffering proteins parvalbumin (PV) and calbindin (CB), and the effects of caffeine-induced Ca^{2+} release from intracellular stores on CDF and CDI were characterized. We found that regulation of CDI by PV and CB is more complex than expected of simple Ca^{2+} buffers, and absence of these proteins in neurons results in altered $\text{Ca}_v 2.1$ subunit expression. Additionally, we found that caffeine, an activator of intracellular Ca^{2+} release, enhances CDI in transfected cells, suggesting that Ca^{2+} release from intracellular stores contributes to regulation of $\text{Ca}_v 2.1$. Overall, our results suggest that CDI is highly influenced by endogenous factors, which may allow tailoring of Ca^{2+} regulation to the needs of specific neurons. Manipulation of these factors may prove useful in developing therapeutic strategies to

treat diseases such as migraine, absence epilepsy, spinocerebellar ataxia and other diseases where Ca^{2+} signaling is altered.

Factors that modulate Ca^{2+} -dependent regulation of $\text{Ca}_v 2.1$ (P/Q-type) Ca^{2+} channels

By

Lisa H. Kreiner
BS, Georgia Institute of Technology, 1992
MS, Georgia State University, 1997

Advisor: Amy Lee, Ph.D.

A dissertation submitted to the Faculty of the Graduate
School of Emory University in partial fulfillment
of the requirements for the degree of
Doctor of Philosophy

Program in Neuroscience
Graduate Division of Biological and Biomedical Sciences

2008

Acknowledgements

I would like to thank the people who made this dissertation possible. First of all, I would like to extend my gratitude to my advisor Dr. Amy Lee for all of her help and support in guiding me through this process. I am also grateful for all of my friends and labmates who have provided support and laughter over the years. I am thankful for my family for their support and encouragement over the past 20 years, 15 of which have been spent pursuing some form of higher education. I would also like to thank my husband, Barrett, for standing by me through another 6 years of graduate school. And finally, I am grateful for my son Joshua, for being a little ray of sunshine.

Table of Contents	Page
Chapter 1: Introduction	1
Characterization of voltage-gated Ca ²⁺ currents	1
Ca _v 2.1 channels	5
Regulation of Ca _v channels by Ca ²⁺	10
Ca ²⁺ regulation of Ca _v 2.1	12
Physiological significance of Ca ²⁺ -dependent modulation of Ca _v 2.1	14
Regulation of CDI of Ca _v 2.1	15
Significance	22
Chapter 2: Endogenous and exogenous Ca²⁺ buffers differentially modulate Ca²⁺-dependent inactivation of Ca_v 2.1 Ca²⁺ channels	27
Abstract	27
Introduction	28
Materials and Methods	29
Results	32
Discussion	40
Chapter 3: Caffeine increases Ca²⁺-dependent inactivation of Ca_v 2.1 (P/Q-type) Ca²⁺ channels	61
Abstract	61
Introduction	61
Materials and Methods	63
Results	65
Discussion	68
Chapter 4: Altered Ca²⁺-feedback to Ca_v 2.1 Ca²⁺ channels in Purkinje neurons lacking parvalbumin and calbindin	79
Abstract	79
Introduction	80
Materials and Methods	81
Results	87
Discussion	94
Chapter 5: Discussion	116
I _{Ca} and Ca ²⁺ buffering proteins interact to regulate Ca _v 2.1	116
Factors that affect feedback regulation of Ca _v 2.1 by CICR	120
Potential consequences of altered Ca _v 2.1 feedback regulation for neuronal function	123
Role of Ca _v 2.1 in network function and pathological conditions	125
References	127

Tables and Figures		Page
Table 1.1	Comparison of $Ca_v 1$ and $Ca_v 2$ channels with respect to regulation by CaM	24
Figure 1.1	Schematic of Ca_v channels	25
Figure 1.2	CDF and CDI of Cav2.1 channels during repetitive depolarizations	26
Table 2.1	Effect of PV and CB on kinetics of inactivation of $Ca_v 2.1$ Ca^{2+} current	45
Figure 2.1	CDI depends on the amplitude of $Ca_v 2.1$ Ca^{2+} currents	47
Figure 2.2	Inactivation of $Ca_v 2.1$ Ca^{2+} currents is greater with BAPTA than with EGTA	49
Figure 2.3	PV has opposite effects on inactivation of small and large amplitude I_{Ca}	51
Figure 2.4	PV alters CDI during repetitive stimuli	53
Figure 2.5	Effects of PV require Ca^{2+} -binding to PV and are specific for CDI	54
Figure 2.6	CB inhibits inactivation of small-amplitude I_{Ca}	55
Figure 2.7	PV and CB do not influence levels of calmodulin or Ca^{2+} -dependent facilitation of $Ca_v 2.1$	57
Figure 2.8	Model for differential regulation of CDI by Ca^{2+} buffers	59
Figure 3.1	Caffeine enhances CDI	72
Figure 3.2	Effects of caffeine on CDF	74
Figure 3.3	Blocking intracellular Ca^{2+} release blocks the effect of caffeine on CDI	75
Figure 3.4	<i>IV</i> curves in the presence and absence of intracellular Ca^{2+} antagonists	76
Figure 3.5	IBMX mimics the effect of caffeine on CDI	77

Figure 3.6	Schematic representation of the effect of caffeine on pathways that could lead to increased CDI	78
Table 4.1	Differences in Ca _v 2.1 properties between WT and PV ^{-/-} /CB ^{-/-} Purkinje neurons	99
Table 4.2	Average maximal facilitation for action potential waveforms from Fig. 4.5	100
Figure 4.1	Facilitation and inactivation of Ca _v 2.1 in wild-type (WT) Purkinje neurons	101
Figure 4.2	Facilitation and inactivation in WT Purkinje neurons depend on stimulation frequency	103
Figure 4.3	Characterization of Cav2.1 currents in WT and PV ^{-/-} /CB ^{-/-} Purkinje neurons	105
Figure 4.4	Increased inactivation in PV ^{-/-} /CB ^{-/-} Purkinje neurons	107
Figure 4.5	Comparison of responses to action potential waveforms in WT and PV ^{-/-} /CB ^{-/-} Purkinje neurons	108
Figure 4.6	Comparison of Ca _v 2.1 α1 splice variants in WT and PV ^{-/-} /CB ^{-/-} neurons	110
Figure 4.7	Comparison of Ca _v β subunit expression in WT and PV ^{-/-} /CB ^{-/-} neurons	112
Figure 4.8	Characterization of Ca _v 2.1 currents in HEK 293T cells transfected with α _{1A} , α ₂ δ and either β _{2a} or β ₄ subunits	114

Chapter 1: Introduction

Voltage-gated Ca_v Ca^{2+} channels couple membrane depolarization to the influx of Ca^{2+} ions, which mediate such diverse physiological processes as excitation-contraction coupling in muscle and gene transcription and neurotransmitter release in neurons. Small changes in intracellular Ca^{2+} concentration can substantially affect cellular processes, but Ca^{2+} overloads can be toxic. Therefore, factors that regulate Ca_v channels may control the balance between normal and disease states. Ca^{2+} entry through Ca_v channels causes a feedback regulation of these channels that can significantly alter Ca^{2+} signaling. Considerable progress has been made in elucidating the molecular mechanism underlying Ca^{2+} -dependent regulation of Ca_v channels. However, little is known of the extent to which Ca_v channels undergo Ca^{2+} -feedback regulation and the factors that may affect this process in neurons. The goal of this dissertation is to fill this void in our understanding by analyzing how cellular factors such as Ca^{2+} buffering proteins and Ca^{2+} release from intracellular stores influence Ca^{2+} -feedback regulation of the Ca_v 2.1 (P/Q-type) Ca^{2+} channel.

Characterization of voltage-gated Ca^{2+} currents

Electrophysiological characterization in excitable cells

A role for Ca^{2+} for cellular excitability was first described in crustacean muscle tissue when Fatt and Katz (1953) found that action potentials could be evoked in the presence of Na^+ free media, thus challenging the idea that action potentials are Na^+ -dependent. Subsequently, in voltage-clamp studies of starfish eggs, Hagiwara et al. (1975) showed that inward current was carried by Ca^{2+} ions. This Ca^{2+} current showed

voltage-dependent activation was consistent with the activity of a voltage-gated channel selective for Ca^{2+} . Moreover, the current-voltage (I - V) relationship for Ca^{2+} currents (I_{Ca}) suggested the presence of two distinct Ca^{2+} channels, one which activated at a membrane potential of -55 mV (type I) and another that activated at -6 mV (type II). Additionally, type II channels were more sensitive to Ca^{2+} channel blockers such as Co^{2+} or Mg^{2+} . Single-channel recordings of vertebrate sensory neurons revealed similar low- and high-voltage activated (LVA and HVA) Ca^{2+} channels (Carbone and Lux, 1984).

The presence of functionally and pharmacologically distinct Ca^{2+} channels was further documented in single-channel recordings of chick dorsal root ganglion neurons by Nowycky et al., (1985). These authors characterized the LVA currents as T-type, for having a tiny conductance and rapid inactivation kinetics (“transient”). Two HVA currents were identified, one of which showed limited inactivation and a large conductance and so was named “L-type”. These currents were also blocked by dihydropyridine (DHP) analogs. The second HVA current was not sensitive to DHPs and was found in a subset of DRG neurons. Since this current exhibited properties distinct from those of T- and L-type currents, it was termed N-type, for “neither” (Nowycky et al., 1985). These studies were the first to demonstrate the existence of heterogeneous voltage-gated Ca^{2+} channels that could be expressed in a single neuronal cell-type.

Further evidence for pharmacologically distinct Ca^{2+} channels came from patch-clamp recordings of cerebellar Purkinje and granule neurons. Compared to N-type currents, HVA currents in Purkinje neurons were relatively insensitive to the N-type blocker ω -conotoxin MVIIC ($\text{IC}_{50} = 35$ nM compared to <1 nM for N-type currents, (Turner and Dunlap, 1995)), but were blocked by relatively low concentrations of the

spider toxin ω -agatoxin IVA (IC 50 = 1-2 nM (Mintz et al., 1992)). This current was named P-type (for Purkinje (Llinas et al., 1989)). A ω -conotoxin MVIIC -insensitive HVA current was also identified in cerebellar granule neurons, but was blocked by higher concentrations of ω -agatoxin IVA (IC 50 = 90 nM) than the P-type current and so was termed Q-type (Randall and Tsien, 1995). An additional HVA current was found in cerebellar granule cells and was termed R-type (for residual) since it was generally insensitive to known blockers of voltage-gated Ca^{2+} channels (Randall and Tsien, 1995).

Biochemical/ molecular characterization

The previous studies suggested the presence of diverse voltage-gated Ca^{2+} channels, which was further confirmed by biochemical and molecular studies. The first voltage-gated Ca^{2+} channel so characterized was the skeletal muscle L-type channel, which was purified from rabbit transverse tubule membranes by sucrose density gradient centrifugation. SDS/PAGE of proteins radiolabeled with the DHP analog, PN200-110, revealed three major bands corresponding to the α , β , and γ subunits that make up the channel. Cleavage of disulfide bonds yielded two α polypeptides, α_1 and α_2 , and a δ component (Takahashi et al., 1987). Tryptic digests of the purified DHP receptor from skeletal muscle yielded the amino acid sequences towards which oligonucleotide probes were generated and used to screen a skeletal muscle cDNA library. This led to the molecular cloning of the first Ca^{2+} channel pore-forming α_1 subunit (Tanabe et al., 1987). Subsequently, ten different genes that encode the α_1 subunit have been identified, each giving rise to channels with properties generally consistent with those described in native tissues. These Ca^{2+} channels have been recently renamed according to the identity

of the α_1 subunit (Birnbaumer et al., 1994; Ertel et al., 2000). Ca_v1 channels conduct L-type currents, while Ca_v2 family members conduct P/Q, N and R-type currents. The Ca_v3 channels correspond to the LVA channels and conduct T-type currents.

The α_1 subunit (Fig. 1.1) consists of a protein encoded by ~2000 amino acids arranged in four repeating domains, each with six helical transmembrane segments (Starr et al., 1991). Transmembrane segments 5 and 6, along with the membrane-associated loop between them, form the pore lining of the channel (Tanabe et al., 1987). The fourth transmembrane segment is positively charged and corresponds to the voltage sensor (reviewed by (Keynes and Elinder, 1999) and (Elinder et al., 2007)).

Four genes encode the β subunit, although alternative splicing can lead to many different isoforms with distinct properties (Takahashi et al., 2003; Cohen et al., 2005; Vendel et al., 2006). This 55 kDa protein interacts with a site (alpha interaction domain (AID)) on the cytoplasmic loop connecting domains I-II (I-II loop) of the α_1 subunit. The AID is highly conserved among HVA Ca^{2+} channels, but is not found on LVA Ca^{2+} channels (Pragnell et al., 1994). The β subunit is thought to be a cytoplasmic protein since it has no predicted transmembrane segments (Opatowsky et al., 2004). Structural analysis has shown that β subunits are composed of two protein interaction domains, a Src homology 3 (SH3) region and guanylate kinase (GK) region (Van Petegem et al., 2004). A hydrophobic groove in the GK domain allows it to interact with the AID on the α_1 subunit of Ca_v1 and Ca_v2 channels (Chen et al., 2004). Electrophysiological comparisons of $\text{Ca}_v \alpha_1$ subunits expressed with or without the β subunit show that β subunits can significantly alter voltage-dependent activation and inactivation of Ca_v channels (Varadi et al., 1991). Antisense depletion and single channel studies have shown

that β subunits also enhance Ca^{2+} current amplitude presumably by helping to target the channel complex to the plasma membrane (Berrow et al., 1995; Brice et al., 1997).

The $\alpha_2\delta$ subunit is a 170 kDa extracellular disulfide-linked complex that binds to extracellular domains of the α_1 subunit (Gurnett et al., 1997; Felix et al., 1997). α_2 and δ subunits are encoded by one gene and are held together by disulfide bonds following post-translational proteolytic cleavage (De Jongh et al., 1990; Jay et al., 1991). The α_2 subunit is heavily glycosylated and thought to be extracellular while the δ subunit has one transmembrane segment and serves to anchor the $\alpha_2\delta$ complex (Wiser et al., 1996). Coexpression of $\alpha_2\delta$ with α_1 increases the peak current amplitude and shifts the voltage dependence of $\text{Ca}_v 2.1$ activation and inactivation in the hyperpolarizing direction (Hobom et al., 2000).

$\text{Ca}_v 2.1$ channels

The α_1 subunit of $\text{Ca}_v 2.1$ ($\alpha_1 2.1$) was cloned initially from rabbit brain (Mori et al., 1991), which allowed characterization of the expression pattern of these channels by *in situ* hybridization. $\alpha_1 2.1$ mRNA was detected in the olfactory bulb, cerebral cortex, and hippocampus, with particularly prominent expression in the cerebellum (Stea et al., 1994). Immunohistochemical studies with antibodies targeted against $\alpha_1 2.1$ showed that the $\alpha_1 2.1$ protein was localized mainly in presynaptic terminals throughout the brain, but also in Purkinje cell bodies and cerebellar granule cells (Volsen et al., 1995; Nakanishi et al., 1995; Westenbroek et al., 1995). Electron microscopy with immunogold labeling has confirmed prominent localization of $\alpha_1 2.1$ at active zones of parallel fiber varicosities and the dendritic spines of Purkinje neurons (Kulik et al., 2004).

Consistent with the largely presynaptic localization of $\text{Ca}_v 2.1$, the importance of $\text{Ca}_v 2.1$ for neurotransmitter release is supported by multiple lines of evidence. First, $\text{Ca}_v 2.1$ interacts directly with proteins involved in synaptic vesicle release (Taverna et al., 2004). These interactions help position $\text{Ca}_v 2.1$ channels so that they can mediate Ca^{2+} influx that triggers docking and fusion of synaptic vesicles (Leveque et al., 1992; Rettig et al., 1996). Second, block of $\text{Ca}_v 2.1$ channels with ω -agatoxin IVA significantly inhibits the amplitude of evoked excitatory postsynaptic potentials (EPSPs), indicating the importance of $\text{Ca}_v 2.1$ for synaptic transmission (Takahashi and Momiyama, 1993; Luebke and Dunlap, 1993; Wheeler and Randall, 1994; Mintz et al., 1995). Finally, mice lacking $\alpha_1 2.1$ show defects in presynaptic neurotransmitter release consistent with a role for $\text{Ca}_v 2.1$ channels in this process (Inchauspe et al., 2004).

In addition to their presynaptic role, $\text{Ca}_v 2.1$ channels also contribute to postsynaptic processes, particularly in cerebellar Purkinje neurons. Llinas and Hess (1976) showed that action potentials in the dendrites of Purkinje neurons were Ca^{2+} -dependent, and were sensitive to ω -agatoxin IVA, indicating a role for $\text{Ca}_v 2.1$ (Llinas et al., 1989). Dual dendritic and somatic extracellular recordings showed that partial block of $\text{Ca}_v 2.1$ with submaximal ω -agatoxin IVA concentrations can terminate spontaneous bursts of Na^+ dependent action potentials (Womack and Khodakhah, 2004), either by promoting inactivation of Na^+ channels or activation of Ca^{2+} -activated (SK or BK) K^+ channels. The latter mechanism is involved in regulating spontaneous firing (pacemaking) of Purkinje cells. Pharmacological or pathological decreases in $\text{Ca}_v 2.1$ activity inhibit the precision of Purkinje cell pacemaking, an effect that can be reversed by SK channel opener EBIO (Walter et al., 2006).

In addition to regulating the intrinsic excitability of Purkinje neurons, $Ca_v 2.1$ channels have also been implicated in the development and maintenance of synaptic inputs onto Purkinje neurons. During development, there is competition among climbing fibers and parallel fibers that synapse onto Purkinje cell dendrites. This allows the innervation of a specific dendritic region by a single climbing fiber (Miyazaki et al., 2004). In $\alpha_1 2.1$ knockout mice, Purkinje cell dendrites were innervated by multiple climbing and excess parallel fibers. These results imply that $Ca_v 2.1$ is necessary for proper innervation of Purkinje neurons.

Long term depression (LTD) in Purkinje neurons results from paired stimulation of the presynaptic parallel and climbing fibers (Ito and Kano, 1982), and is mediated by postsynaptic Ca^{2+} signals (Konnerth et al., 1992). The involvement of AMPA receptors in the induction of LTD has been demonstrated by agonist-mediated stimulation of AMPA and metabotropic glutamate receptors paired with depolarization. In the presence of the AMPA receptor antagonist CNQX, LTD is not induced (Linden et al., 1991). A functional complex between postsynaptic AMPA receptors and $Ca_v 2.1$ has been demonstrated, which serves to inhibit $Ca_v 2.1$ channel function. This interaction may promote lateral diffusion of AMPA receptors away from postsynaptic sites, which could contribute to the induction of LTD (Kang et al., 2006). Thus, postsynaptic $Ca_v 2.1$ channels play multiple and diverse roles in cerebellar Purkinje neurons.

Ca_v 2.1 channelopathies

The physiological importance of $Ca_v 2.1$ is best illustrated by $\alpha_1 2.1$ mutations that cause neurological disease. Familial hemiplegic migraine (FHM) is an inherited autosomal dominant disorder that can be accompanied by moderate to severe headaches,

aura, ataxia, drowsiness and sometimes impaired consciousness (Black et al., 2004). FHM1 has been linked to at least 18 point mutations in $\alpha_1 2.1$. When introduced into recombinant $\text{Ca}_v 2.1$ channels, these mutations can inhibit or potentiate channel function. For example, when expressed in hippocampal neurons of mice lacking $\alpha_1 2.1$, human $\text{Ca}_v 2.1$ channels bearing FHM mutations mediate smaller-amplitude Ca^{2+} currents compared to wild-type channels (Cao and Tsien, 2005). FHM1 mutations also reduced the contribution of P/Q-type currents to GABAergic synaptic currents. These results suggest that FHM1 mutations may cause migraine symptoms by reducing inhibitory neurotransmission during heightened periods of neuronal activity.

A gain-of-function FHM mutation in $\alpha_1 2.1$ (R192Q) can lead to cortical spreading depression (CSD). CSD is caused by a wave of transient intense spike activity followed by long-lasting suppression of neural activity that spreads across the cortex. CSD may underlie the aura associated with the onset of migraines (Leao, 1944). Introduction of the R192Q mutation into the mouse $\alpha_1 2.1$ produced a mouse model of FHM that was susceptible to CSD. These mice had and had increased P/Q-type current density in cerebellar granule neurons, which activated at more negative voltages than in wild-type neurons (van den Maagdenberg et al., 2004). Gain-of-function in presynaptic $\text{Ca}_v 2.1$ channels would lead to increased glutamate release in the cortex, which can lead to a positive feedback cycle initiating CSD.

Mutations in $\alpha_1 2.1$ have also been associated with absence epilepsy, which is characterized by a generalized 3 Hz spike-wave abnormality in the electroencephalogram. The neurological defect seems to result from decreased $\text{Ca}_v 2.1$ function for the following reasons. First, $\alpha_1 2.1$ mutations causing absence epilepsy in

humans cause significantly smaller Ca^{2+} current through recombinant $\text{Ca}_v 2.1$ channels (Imbrici et al., 2004). Second, mouse models of absence epilepsy involve mutations of $\alpha_1 2.1$ (*leaner*, *tottering*, *rolling Nagoya*, and *rocker*), and all of these mutations cause reduced $\text{Ca}_v 2.1$ current density. Finally, other mouse models of absence epilepsy involve mutations in the $\text{Ca}_v \beta$, $\alpha_2 \delta$ or γ subunits (*lethargic*, *ducky*, and *stargazer*). Recordings of Purkinje neurons from these mice also reveal significant decreases in $\text{Ca}_v 2.1$ current density.

Consistent with the role of $\text{Ca}_v 2.1$ in Purkinje neurons, mutations in $\alpha_1 2.1$ have also been linked to various ataxias. Autosomal dominant spinocerebellar ataxia (SCA6), is characterized by degeneration of Purkinje neurons and progressive ataxia and is associated with expanded polyglutamine repeats in $\alpha_1 2.1$ (Zhuchenko et al., 1997). Electrophysiological recordings of recombinant $\text{Ca}_v 2.1$ channels with expanded polyglutamine repeats exhibited an 8 mV hyperpolarizing shift in inactivation which resulted in reduced Ca^{2+} influx into Purkinje neurons (Matsuyama et al., 1999). Furthermore, when these cells were challenged with serum starvation and K^+ -induced depolarization, mutants with expanded polyglutamine repeats were less likely to survive. These results suggest that the mutant Ca^{2+} channel renders them more susceptible to cell death (Matsuyama et al., 1999). A second disorder, episodic ataxia type 2 (EA2), has been linked to missense and nonsense mutations in $\alpha_1 2.1$. These mutations also result in diminished whole cell $\text{Ca}_v 2.1$ currents (Jen et al., 2001). These findings show how dysregulation of $\text{Ca}_v 2.1$ may lead to pathological conditions.

Regulation of Ca_v channels by Ca^{2+}

Initial characterization of CDI

The role of Ca^{2+} ions in the feedback regulation of Ca^{2+} channels was first demonstrated by Brehm and Eckert (1978) in voltage-clamp recordings from *Paramecium*. These authors described an inward Ca^{2+} current that progressively decreased in amplitude over time. This decrease was Ca^{2+} -dependent in that it was largely inhibited when extracellular Ca^{2+} was replaced with other divalent ions, such as Ba^{2+} or Sr^{2+} . To characterize this effect, the authors used a double pulse voltage protocol, in which a test current was evoked by a single voltage-step after a conditioning prepulse. If the decay of the test current was voltage-dependent, the amplitude of the test current should decline as a function of the prepulse voltage. Instead, the test current amplitude showed a U-shaped dependence of prepulse voltage that peaked at prepulses that evoked the maximal inward Ca^{2+} current. These results suggested that inactivation of the Ca^{2+} current was driven by Ca^{2+} influx during the prepulse. This process of Ca^{2+} -dependent inactivation (CDI) has since been described in many cell types, including cardiac myocytes and neurons, and characterizes both Ca_v1 and Ca_v2 classes of Ca^{2+} channels (Lee et al., 1985; Lee et al., 1999; Liang et al., 2003).

A major question was whether Ca^{2+} influx through Ca_v channels activated a second-messenger that then caused CDI, or could Ca^{2+} directly control this process. Evidence for the latter was obtained from single channel recordings of L-type currents in cardiac myocytes (Yue et al., 1990). Conditional open probability analysis revealed that the probability of channel opening in Ca^{2+} extracellular solution was affected by prior channel openings. Ca^{2+} entry produced alterations in gating transitions over the course of several hundred milliseconds. If Ca^{2+} were binding directly to the channel, equilibration

would occur too quickly to account for these slow transitions in gating. This finding suggested a second messenger was involved.

Role of the IQ domain

Efforts to uncover the mechanism underlying CDI revealed a role for the cytoplasmic C-terminal domain of the $\text{Ca}_v \alpha_1$ subunit. Soldatov et al. (1997) showed that deletions of part of the C-terminal sequence of $\alpha_1 1.2$ inhibited CDI of $\text{Ca}_v 1.2$ channels. Further analyses indicated the importance of a consensus sequence for CaM binding (IQ-domain) in the proximal third of the $\alpha_1 1.2$ C-terminal domain (Zuhlke et al., 1999; Qin et al., 1999; Peterson et al., 1999). The IQ domain is an 11 amino acid motif that begins with a highly conserved isoleucine and glutamine (IQXXXRGXXXR). It was first characterized in myosin light chains and shares sequence similarity with CaM binding regions in neuromodulin and neurongranin (Cheney and Mooseker, 1992).

Multiple lines of evidence have established that CaM is preassociated with Ca^{2+} channels (Erickson et al., 2001) and interacts with the IQ domain in $\alpha_1 1.2$. First, overexpression of a CaM mutant that lacks high affinity Ca^{2+} binding sites inhibited CDI of $\text{Ca}_v 1.2$ in transfected cells (Peterson et al., 1999). Second, I-E and I-A mutations in the IQ motif, which disrupt binding of CaM, inhibit CDI of $\text{Ca}_v 1.2$ (Peterson et al., 1999). Further studies showed that CaM binding to the IQ-domain of $\alpha_1 1.2$ also mediated Ca^{2+} -dependent facilitation (CDF), but only when CDI was disabled with the I-A mutation (Zuhlke et al., 1999; Zuhlke et al., 2000).

Ca^{2+} regulation of $\text{Ca}_v 2.1$

Structural determinants

The conservation of the IQ domain in the α_1 subunits of $\text{Ca}_v 2$ (N-, P/Q-, and R-type) channels suggested that CaM could modulate CDI and CDF in other HVA Ca^{2+} channels (Peterson et al., 1999). However, CDI was generally not thought to characterize non-L-type currents, in part due to the relatively high concentrations (5 mM) of Ca^{2+} chelators, such as BAPTA or EGTA, that are usually used in whole-cell patch clamp recordings. By reducing Ca^{2+} chelator concentration in the intracellular recording solution (e.g., 0.5 mM EGTA), Lee et al. (1999) showed significant CDF and CDI of $\text{Ca}_v 2.1$ in transfected cells. Moreover, CDI and CDF were more significant for $\text{Ca}_v 2.1$ channels containing the $\text{Ca}_v \beta_{2a}$ than the $\text{Ca}_v \beta_{1b}$ subunit (Stea et al., 1994). $\text{Ca}_v 2.1$ channels with the $\text{Ca}_v \beta_{2a}$ subunit show relatively little voltage-dependent inactivation, which has the effect of obscuring CDI and CDF in channels with $\text{Ca}_v \beta_{1b}$.

The role of CaM in regulation of CDF and CDI of $\text{Ca}_v 2.1$ was investigated in electrophysiological recordings of transfected HEK 293T cells. When extracellular Ca^{2+} was replaced with Ba^{2+} , CDF and CDI were abolished, showing that they are dependent on Ca^{2+} influx (Fig. 1.2). Unlike for $\text{Ca}_v 1$ channels, Ca^{2+} chelators affected feedback regulation of $\text{Ca}_v 2.1$. Increasing intracellular EGTA (0.5 to 10 mM) preserved CDF but dramatically reduced CDI. In contrast, a high concentration of intracellular BAPTA (10 mM) greatly reduced both CDF and CDI. In addition, the inclusion of a CaM inhibitor peptide abolished both CDF and CDI, demonstrating that CaM mediates the dual feedback regulation of $\text{Ca}_v 2.1$ (Lee et al., 2000).

Molecular characterization of the interaction between the C-terminal of $\alpha_1 2.1$ and CaM revealed a more complex mechanism by which Ca^{2+} /CaM initiates CDF and

CDI. Mutational analysis of CaM showed that Ca^{2+} binding to the C-terminal and N-terminal lobes of CaM is necessary for CDF, while only the N-terminal lobe is necessary for CDI. Furthermore, mutation of the IQ-like domain of the $\alpha_1 2.1$ subunit showed that it was necessary for CDF, but not CDI. However, deletion of a CaM-binding sequence downstream of the IQ-domain (CBD) prevented both CDF and CDI. Lee et al. (2003) proposed that Ca^{2+} binding to the C-terminal lobe of CaM supports CDF via interaction with the IQ domain, while Ca^{2+} binding to the N-terminal lobe of CaM promotes secondary interactions with the CBD of the $\alpha_1 2.1$ subunit, which enhances facilitation and causes a conformational change that initiates CDI. However, work from other labs suggests a more dominant role for the IQ-domain in mediating both CDF and CDI (DeMaria et al., 2001; Mori et al., 2008). Such discrepancies may result from the different isoforms of $\alpha_1 2.1$ used, since sequence variations between α_1 subunits can significantly influence CDI and CDF of Ca_v channels (Krovetz et al., 2000; Soong et al., 2002; Chaudhuri et al., 2004).

Ca^{2+} sensitivity of CDF and CDI of $\text{Ca}_v 2.1$

The fact that CDI of $\text{Ca}_v 2$ but not $\text{Ca}_v 1$ channels is abolished by high concentrations of BAPTA and EGTA (Charnet et al., 1994) indicates a difference in the Ca^{2+} sensing mechanism between these channels (Lee et al., 2000). This is further supported by the reliance of CDI for $\text{Ca}_v 2$ on the low-affinity Ca^{2+} binding sites in the N-lobe of CaM while CDI for $\text{Ca}_v 1$ requires the higher Ca^{2+} affinity of the C-lobe of CaM (summarized in Table 1.1). Dick et al. (2008) proposed that this difference is due to an additional Ca^{2+} /CaM binding site within the cytoplasmic N-terminal domain of $\text{Ca}_v 1$

α_1 subunit. Deletion of this site causes $\text{Ca}_v 1$ channels to undergo CDI that can be blocked by high concentrations of BAPTA and by Ca^{2+} -binding mutations in the N-lobe of CaM. This N-terminal spatial Ca^{2+} transforming element may act as a molecular switch for selectivity of the CDI process for local vs global Ca^{2+} elevations.

The BAPTA and EGTA-insensitivity of CDF for $\text{Ca}_v 2.1$ suggests that unlike CDI, CDF depends on local Ca^{2+} influx through individual channels. Single channel studies of $\text{Ca}_v 2.1$ have shown that CDF represents an enhancement of the open probability of the channel, without a change in the activation kinetics (Chaudhuri et al., 2007). However, CDI is lacking at the single channel level, which is consistent with the idea that global Ca^{2+} signals initiate CDI of $\text{Ca}_v 2.1$, and are too distant to be detected by single channels.

Physiological significance of Ca^{2+} -dependent modulation of $\text{Ca}_v 2.1$

CDI and CDF were first characterized for $\text{Ca}_v 2.1$ in neurons in patch-clamp recordings of the nerve terminals at the Calyx of Held, a giant synapse in the auditory brainstem. Pharmacological studies show that most of the Ca^{2+} current in these nerve terminals is mediated by $\text{Ca}_v 2.1$ (Forsythe et al., 1998). During trains of action potential waveforms, Ca^{2+} currents initially increased with successive stimulations. Unlike in recombinant $\text{Ca}_v 2.1$ channels, this process (CDF) was proportional to Ca^{2+} influx and could be reduced by the addition of high concentrations of intracellular BAPTA (10 mM) (Borst and Sakmann, 1998). However, like recombinant $\text{Ca}_v 2.1$ channels, the presynaptic Ca^{2+} current did undergo CDI (Forsythe et al., 1998). Simultaneous postsynaptic recordings showed that CDF and CDI could cause facilitation and

depression, respectively, of the EPSC (Forsythe et al., 1998; Borst and Sakmann, 1998). Because of the widespread presynaptic distribution of $\text{Ca}_v 2.1$, these studies suggested that CDF and CDI of $\text{Ca}_v 2.1$ may fundamentally contribute to short term synaptic plasticity.

However, CDI is not necessarily characteristic of all $\text{Ca}_v 2.1$ channels (Wykes et al., 2007). In chromaffin cells, $\text{Ca}_v 2.1$ channels do not undergo CDI, even at high stimulus intensities. Molecular analyses revealed $\alpha_1 2.1$ splice variants that lacked the IQ-domain, and thus may have been unable to bind CaM and undergo CDI. The consequences of this lack of CDI on $\text{Ca}_v 2.1$ -mediated exocytosis were investigated with perforated patch voltage clamp recordings and membrane capacitance measurements. These experiments revealed that while $\text{Ca}_v 2.2$ channels in these cells underwent strong CDI at high stimulus intensities, $\text{Ca}_v 2.1$ channels remained open under these conditions, which strengthened their contributions to Ca^{2+} signals that support exocytosis. These findings show that CDI may play a role in depressing Ca^{2+} signals underlying exocytosis of hormone or neurotransmitters.

Regulation of CDI of $\text{Ca}_v 2.1$

1. CaM-like Ca^{2+} -binding proteins

CaM-like Ca^{2+} -binding proteins may regulate $\text{Ca}_v 2.1$ and other HVA Ca^{2+} channels by competing with CaM for binding to the α_1 subunit. For example, the neuronal Ca^{2+} -binding protein-1 (CaBP1) interacts with the CBD region on the $\alpha_1 2.1$ subunit. This interaction enhances inactivation, causes a depolarizing shift in activation and does not support facilitation of $\text{Ca}_v 2.1$ (Lee et al., 2002). CaBP1 has also been

shown to oppose CaM by blocking CDI for Ca_v 1.2 and Ca_v 1.3 (Zhou et al., 2004; Zhou et al., 2005; Yang et al., 2006; Cui et al., 2007). A splice variant of CaBP1, caldendrin, causes a more modest suppression of CDI for Cav1.2 channels (Tippens and Lee, 2007). These effects of CaBP1 and caldendrin may result from their ability to compete with CaM for binding to the IQ domain. Unlike CaM, CaBP1 and other CaBP family members are expressed primarily in the nervous system, such that their regulation of voltage-gated Ca²⁺ channels may underlie distinct Ca²⁺ signaling events in specific populations of neurons.

In some cases, modification of a Ca²⁺ binding protein is necessary to produce an effect on channel regulation. CaBP1 and Visinin-like protein 2 (VILIP-2) both are N-terminally myristoylated, which is important for their effects on Ca_v 2.1 (Lautermilch et al., 2005). Like CaBP1, VILIP-2 is a Ca²⁺-binding protein that binds to Ca_v 2.1 via the CBD and IQ domains, resulting in slowed inactivation during stimulus trains. However, in the absence of myristoylation, both proteins produce an effect similar to CaM on Ca_v 2.1 (Few et al., 2005). Post translational modification of Ca²⁺ binding proteins may underlie differential regulation of Ca_v channels by CaBPs.

The physiological significance of CaBP modulation of Ca_v 2.1 for short term synaptic plasticity was demonstrated in the calyx of held. Here, one CaBP, neuronal calcium sensor 1 (NCS-1) is highly expressed. Loading the presynaptic terminal with purified NCS-1 resulted in a gradual increase in amplitude of presynaptic Ca²⁺ current, mimicking activity-dependent facilitation seen during repetitive stimulations. Furthermore, blocking the interaction of NCS-1 with Ca_v 2.1 by injecting a fragment of the C-terminal portion of NCS-1 lacking the Ca²⁺ binding EF hand partially occluded the

effect of NCS-1, suggesting that binding of NCS-1 is necessary for activity-dependent facilitation of presynaptic P/Q-type currents (Tsujimoto et al., 2002). The role of Ca^{2+} binding protein binding to $\text{Ca}_v 2.1$ in short-term synaptic plasticity was further demonstrated by expression of $\text{Ca}_v 2.1$ mutants with altered IQ-like domain or deleted CBD in sympathetic neurons (Mochida et al., 2008). Paired pulse facilitation between synaptically connected pairs of neurons, normally observed in wild-type (WT) $\text{Ca}_v 2.1$ at longer time points (75 ms intervals), was eliminated in the IQ-like domain mutant, but preserved in a mutant where the CBD was deleted. In contrast, deletion of the CBD eliminated paired pulse depression observed during shorter time scales with WT $\text{Ca}_v 2.1$ (<50 ms). These results suggested that Ca^{2+} binding protein/ $\text{Ca}_v 2.1$ interactions contribute to a molecular mechanism that links presynaptic Ca^{2+} entry to short-term synaptic plasticity.

2. Ca^{2+} -buffering proteins (CBPs)

CBPs are similar to Ca^{2+} binding proteins like CaM in containing EF hand Ca^{2+} binding motifs. However CBPs are generally not thought to undergo Ca^{2+} -dependent conformational changes that allow them to interact with and modulate effector proteins. Acting in a similar manner to Ca^{2+} chelators, such as EGTA or BAPTA, CBPs bind free Ca^{2+} in the cytoplasm with distinct Ca^{2+} binding kinetics. CBPs are widely expressed throughout the nervous system, but parvalbumin (PV), calbindin-D28k (CB), and calretinin (CR) in particular are highly expressed in the cerebellar cortex (Celio, 1990).

CB and CR have 4 and 5 EF-hand Ca^{2+} binding sites, respectively. Both are considered fast Ca^{2+} buffers, with on-rates similar to BAPTA ($k_{\text{on}} = 4 \times 10^7 \text{ M}^{-1}\text{s}^{-1}$ for

CB (Roberts, 1994) and $k_{on} = 100-1000 \mu\text{M}^{-1}\text{s}^{-1}$ for CR (Edmonds et al., 2000)). In contrast, PV has 2 Ca^{2+} binding sites and is considered a much slower Ca^{2+} buffer since it has a higher affinity for Mg^{2+} rather than Ca^{2+} ions. Under resting conditions, the cytoplasmic concentration of Mg^{2+} (~1.15 mM (Darrow et al., 1991)) will be over 1000 times greater than that for Ca^{2+} , such that Mg^{2+} ions will be bound to the PV EF-hands and will have to dissociate before Ca^{2+} can bind (for Mg^{2+} : $k_d = 41.8 \mu\text{M}$ (Eberhard and Erne, 1994) and offrate = 0.93 s^{-1} (Hou et al., 1991) for Ca^{2+} : $K_d = 50-150 \text{ nM}$, $k_{on} = 6 \text{ mM}^{-1} \text{ s}^{-1}$, depending on the concentration of Mg^{2+} (Lee et al., 2000b; Schwaller et al., 2002; Dargan et al., 2004)).

The slow Ca^{2+} binding properties of PV are evident when examining Ca^{2+} signals in Purkinje neurons, where PV and CB are highly expressed. High speed confocal Ca^{2+} imaging has been used to determine the time course and decay of Ca^{2+} transients in the soma of Purkinje cells from wild-type (WT) mice and those lacking PV or PV and CB ($\text{PV}^{-/-}$ and $\text{PV}^{-/-}/\text{CB}^{-/-}$). Ca^{2+} signals were evoked by stimulation of the climbing fiber inputs to the Purkinje neurons. Compared to in WT neurons, the evoked Ca^{2+} transient in $\text{PV}^{-/-}$ neurons was similar in amplitude but showed a significantly slower rate of decay (Chard et al., 1993; Schmidt et al., 2003b). This suggests that PV limits the accumulation of free Ca^{2+} in the cytoplasm during repetitive stimulations. Ca^{2+} transients in double knockout ($\text{PV}^{-/-}/\text{CB}^{-/-}$) neurons were greater in amplitude and showed a faster decay compared to $\text{PV}^{-/-}$ neurons, suggesting that the fast buffering properties of CB will have an effect on controlling the size of the initial Ca^{2+} signal (Chard et al., 1993; Schmidt et al., 2003b).

These different Ca^{2+} handling properties of PV and CB may underlie different cellular responses in mice lacking PV or CB. Paired pulses (30-300 ms intervals) applied to GABAergic neurons forming synapses with Purkinje neurons produced depression in $\text{PV}^{+/+}$ mice, but facilitation occurred in $\text{PV}^{-/-}$ mice (Caillard et al., 2000). This result may be due to the effect of PV in accelerating the initial rate of decay of the Ca^{2+} transient. A possible role in paired-pulse facilitation (PPF) for CB has been demonstrated in recordings from synaptically connected neurons in the neocortex. These experiments revealed less PPF in $\text{CB}^{-/-}$ than in WT, suggesting that PPF relies on the fast Ca^{2+} binding and rapid saturation of CB as a Ca^{2+} buffer (Blatow et al., 2003). Mutant mice lacking CB generally have a more severe neurological phenotype than those lacking PV, with deficits in sensory processing (Barski et al., 2003) and motor coordination (Airaksinen et al., 1997).

3. Ca^{2+} release from intracellular stores

In addition to voltage-gated Ca^{2+} channels, release of Ca^{2+} from intracellular stores, such as the endoplasmic reticulum (ER), can rapidly change the cytoplasmic Ca^{2+} concentration. In cardiac cells, L-type Ca^{2+} channels are opened by depolarization which allows influx of Ca^{2+} . This increase in cytoplasmic Ca^{2+} concentration triggers the opening of intracellular Ca^{2+} channels located on the ER membrane which releases additional Ca^{2+} into the cytoplasm. Ca^{2+} -induced Ca^{2+} release (CICR) has also been demonstrated in neurons (Carter et al., 2002), and may be important for burst firing and synchronous oscillation of neuronal populations (Li and Hatton, 1997; Yoshimura et al., 2001). Two receptors mediate Ca^{2+} release from intracellular stores, inositol 1,4,5-

triphosphate receptors (IP₃ R) and ryanodine receptors (RyR). These receptors act independently to release Ca²⁺ from the ER. It is believed that for Purkinje cells, and possibly other types of neurons, IP₃ Rs and RyRs release Ca²⁺ from a common pool, even though the receptors have different agonists and antagonists (Khodakhah and Armstrong, 1997).

IP₃ Rs can be indirectly activated by G-protein coupled receptors and receptor tyrosine kinases. Activation of these receptors by neurotransmitters, hormones, and growth factors can activate the enzyme phospholipase C (PLC) (Nishizuka, 1988), resulting in the hydrolysis of PIP₂ into IP₃ and diacylglycerol (DAG) (Huang et al., 1988). Three major isoforms of the IP₃ R have been characterized, which correspond to tetramers of identical 310 kDa subunits (Maeda et al., 1990). IP₃ Rs are activated by IP₃, with Ca²⁺ functioning as a cofactor (Finch et al., 1991). Opening of the channel shows a biphasic dependence on Ca²⁺ concentration, but both IP₃ and Ca²⁺ must be present to open the channel. Ca²⁺ at low concentrations (0.1-10 μM) activates the channel and increases open probability (P_o). At high concentrations (>10 μM) of Ca²⁺, channel opening is inhibited (Finch et al., 1991).

Inhibition of IP₃ Rs is important physiologically to limit the amount of Ca²⁺ released into the cytoplasm. Endogenous inhibition can occur via CaM, which inhibits IP₃ Rs in a Ca²⁺-independent manner by competitively binding to the IP₃ binding site (Hirota et al., 1999; Adkins et al., 2000). However a second CaM binding site on the receptor may inhibit IP₃-induced Ca²⁺ release in a Ca²⁺-dependent manner (Patel et al., 1997; Cardy and Taylor, 1998). Pharmacological inhibition IP₃ Rs by heparin has been

used to characterize the effects of Ca^{2+} release by these receptors. Heparin competitively inhibits the binding of IP_3 to the IP_3 R (Bultynck et al., 2003).

Ryanodine receptors (RYRs) are a second type of channel responsible for Ca^{2+} release from the endoplasmic reticulum. Like IP_3 Rs, RyRs are made up of four subunits which form a receptor complex, and three major isoforms of the receptor have been characterized (Anderson et al., 1989; Takeshima, 1993). The first isoform, RyR1 is mainly present in skeletal muscle and is conformationally coupled to Ca_v 1.1 channels in the plasma membrane. This interaction permits membrane depolarization to open RyRs independent of Ca^{2+} influx through Ca_v 1.1 (Schneider and Chandler, 1973). RyR2 was originally characterized in cardiac muscle and RyR3 is found in the brain and at low levels in striated muscle (Imagawa et al., 1987; Mikami et al., 1989; Takeshima, 1993; Sorrentino et al., 1993). Although the RyR3 isoform is mainly expressed in the nervous system it is present at low levels. RyR2 is the predominant form of the receptor found in the brain, but Purkinje neurons mainly contain RyR1 (Kuwajima et al., 1992).

Unlike IP_3 Rs, RyRs can be directly activated by cytosolic Ca^{2+} in the absence of other second messengers. In non-skeletal muscle cells, RyRs are activated by low concentrations of Ca^{2+} (1-10 μM) and inhibited by high concentrations (1-10 mM), with little spontaneous channel activity occurring at resting cytosolic Ca^{2+} concentrations (<100 nM) (Copello et al., 1997). The average K_d for Ca^{2+} of the three RyR isoforms has been estimated to be between 0.5 and 5 μM , and deactivation can occur in response to rapidly decaying Ca^{2+} transients. In the RyR2 isoform, the deactivation time constant has been estimated to be about 5-6 ms (Schiefer et al., 1995; Velez et al., 1997).

Caffeine causes the release of Ca^{2+} from intracellular stores by reducing the threshold for Ca^{2+} activation of RyRs (Anderson et al., 1989). In the RyR2 isoform, single channel studies have shown that caffeine increases the sensitivity of receptors to luminal, but not cytosolic Ca^{2+} (Kong et al., 2008). Additional RyR agonists include cytosolic free ATP, which has isoform specific effects, and cyclic ADP-ribose, which may indirectly activate the RyR by activating the Ca^{2+} -ATPase and increasing luminal Ca^{2+} levels (Copello et al., 2002; Lukyanenko et al., 2001). RyRs may also be activated by phosphorylation, but the mechanism and the effects of this remain controversial.

Inhibition of RyRs is important physiologically to limit intracellular Ca^{2+} release and pharmacologically to treat cardiac arrhythmias associated with RyR mutations. RyRs are endogenously inhibited by CaM (Fuentes et al., 1994) and Mg^{2+} , which can compete with Ca^{2+} at the Ca^{2+} inhibition site on the receptor (Laver et al., 1997). Since the RyR1 isoform is coupled to L-type Ca^{2+} channels via the CaM binding regions of both proteins, high concentrations of CaM may disrupt this interaction thus inhibiting RyR, but low levels of CaM may activate the receptor (Sencer et al., 2001; Tang et al., 2002). A commonly used pharmacological inhibitor of RyRs, ruthenium red, binds directly to the receptor and blocks Ca^{2+} release by lodging in the pore, but may also block some voltage-gated Ca^{2+} channels (Cibulsky and Sather, 1999).

Significance

The ability of $\text{Ca}_v2.1$ channels to self-regulate depends on Ca^{2+} levels that we hypothesize can be affected both by Ca^{2+} buffers and Ca^{2+} release from intracellular stores. The studies presented here will test this hypothesis first by characterizing the

effects of CBPs and Ca^{2+} release pathways on CDF and CDI of $\text{Ca}_v2.1$. These studies utilize transfected $\text{Ca}_v2.1$ channels in HEK 293T cells, where the number of confounding factors is limited compared to cells such as neurons in which these channels are endogenously expressed. The physiological significance of regulation by Ca^{2+} buffering proteins will be examined in neurons. For these experiments, cerebellar Purkinje neurons will be used because Ca^{2+} current in these neurons is predominately carried through $\text{Ca}_v2.1$ channels, and both PV and CB are present in appreciable quantities. Additionally, these neurons have been well characterized with respect to Ca^{2+} signaling kinetics and the resulting changes in synaptic plasticity. Purkinje neurons lacking PV and CB can be directly compared to those with full Ca^{2+} -buffering protein expression to determine the role of these proteins in Ca^{2+} signaling. The goal of this work is to determine if and how Ca^{2+} buffering proteins fine-tune neuronal $\text{Ca}_v2.1$ channels.

$\text{Ca}_v2.1$ dysregulation causes cellular pathologies leading to migraine, epilepsy, and ataxia. Detailed knowledge of the regulation of $\text{Ca}_v2.1$ may lead to alternative therapeutic strategies for these and other disorders involving altered Ca^{2+} signaling in the central nervous system.

Table 1.1: Comparison of Ca_v1 and Ca_v2 channels with respect to regulation by CaM.

	Ca_v1 channels	Ca_v2 channels
CDF	Mediated by N-lobe of CaM ¹	Mediated by C-lobe of CaM ^{2,3}
CDI	Mediated by C-lobe of CaM ⁴	Mediated by N-lobe of CaM ^{2,3}
Ca²⁺ buffer sensitivity	BAPTA insensitive CDI ⁵	EGTA sensitive CDI ^{2,3} BAPTA sensitive CDI
CaM lobe specific regulation	C-lobe sensitive to local Ca ²⁺	C-lobe sensitive to local Ca ²⁺ N-lobe sensitive to global Ca ²⁺

References: 1, (Van Petegem et al., 2005) 2, (Lee et al., 1999) 3, (DeMaria et al., 2001)
4, (Peterson et al., 1999) 5, (Cens et al., 1999).

Figure 1.1

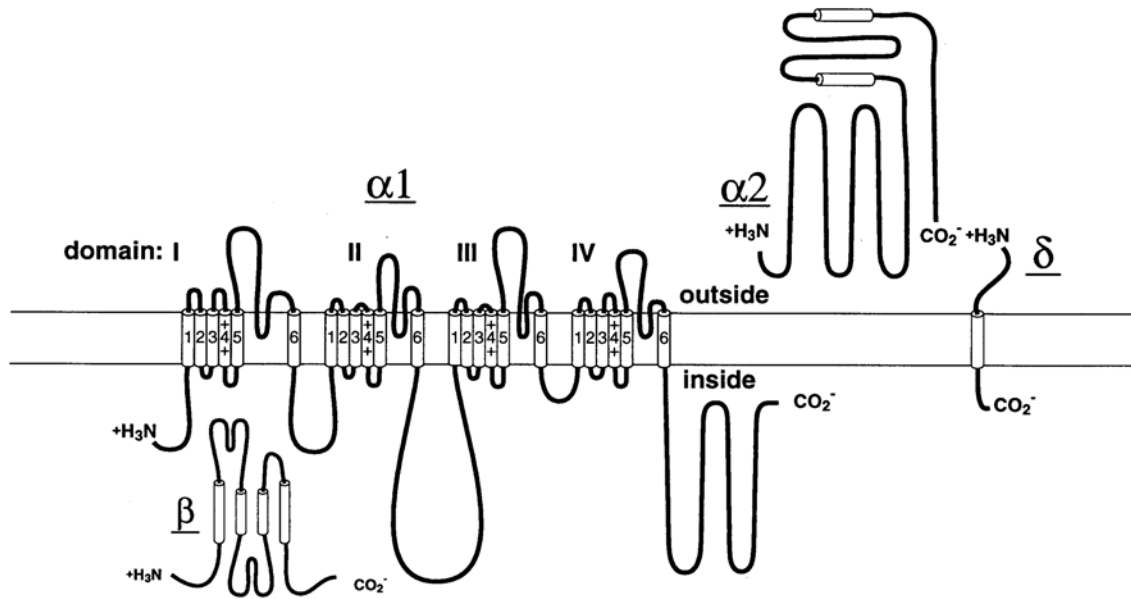


Figure 1.1 (from Catterall, 1999) Schematic showing α_1 , β and α_2 δ subunits of Ca_v channels.

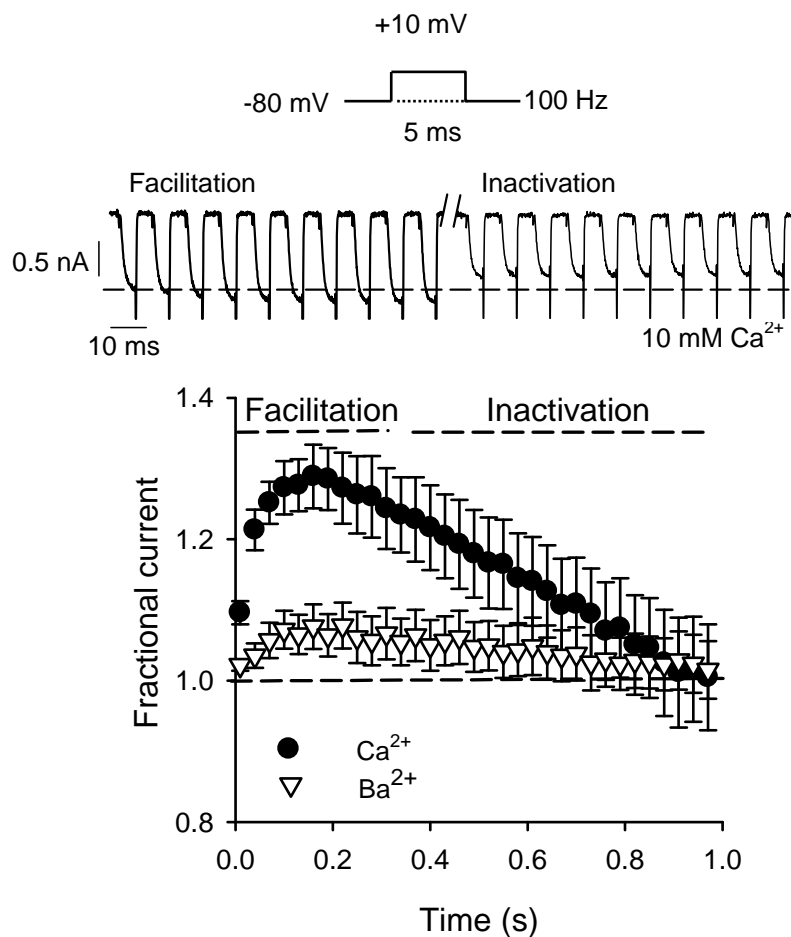
Figure 1.2

Figure 1.2 CDF and CDI of Cav2.1 channels during repetitive depolarizations. Results are from whole-cell patch clamp recordings of HEK 293T cells transfected with Cav2.1 with 0.5 mM EGTA in the recording pipette and 10 mM extracellular Ca²⁺ (n=7) or Ba²⁺ (n=8). Currents were elicited by 100-Hz trains of 5-ms pulses to +10 mV (0 mV for Ba²⁺). Voltage protocol and representative Ca²⁺ currents evoked by first and last 10 pulses are shown above, with dotted line indicating initial current amplitude. CDF is seen in first 10 pulses and CDI in the last 10 pulses. Fractional current is the mean peak current normalized to the first of the train \pm SEM. Every third point is plotted.

Chapter 2: Endogenous and exogenous Ca²⁺ buffers differentially modulate Ca²⁺-dependent inactivation of Ca_v2.1 Ca²⁺ channels

Abstract

Voltage-gated Ca²⁺ channels undergo a negative feedback regulation by Ca²⁺ ions, Ca²⁺-dependent inactivation, which is important for restricting Ca²⁺ signals in nerve and muscle. Although the molecular details underlying Ca²⁺-dependent inactivation have been characterized, little is known about how this process might be modulated in excitable cells. Based on previous findings that Ca²⁺-dependent inactivation of Ca_v2.1 (P/Q-type) Ca²⁺ channels is suppressed by strong cytoplasmic Ca²⁺ buffering, we investigated how factors that regulate cellular Ca²⁺ levels affect inactivation of Ca_v2.1 Ca²⁺ currents in transfected HEK 293T cells. We found that inactivation of Ca_v2.1 Ca²⁺ currents increased exponentially with current amplitude, but not with high intracellular concentrations of the fast Ca²⁺ buffer BAPTA. However, with low concentrations of BAPTA (0.5 mM), inactivation of Ca²⁺ currents was significantly greater than with an equivalent concentration of the slow Ca²⁺ buffer EGTA, indicating the importance of buffer kinetics in modulating Ca²⁺-dependent inactivation of Ca_v2.1. Cotransfection of Ca_v2.1 with the EF-hand Ca²⁺-binding proteins, parvalbumin and calbindin, significantly altered the relationship between Ca²⁺ current amplitude and inactivation, in ways that were unexpected from behavior as passive Ca²⁺ buffers. We conclude that Ca²⁺-dependent inactivation of Ca_v2.1 depends on a subplasmalemmal Ca²⁺ microdomain that is affected by the amplitude of the Ca²⁺ current and differentially modulated by distinct Ca²⁺-buffers.

Introduction

Ca_v2.1 (P/Q-type) voltage-gated Ca²⁺ channels mediate Ca²⁺ signals that regulate neuronal excitability, synapse formation, and neurotransmitter release (Dunlap et al., 1995; Wheeler et al., 1996; Jun et al., 1999; Cavelier et al., 2002; Miyazaki et al., 2004). Fidelity of Ca²⁺ signaling by Ca_v2.1 requires fine-control of voltage-gated Ca²⁺ entry, in part by the Ca²⁺ ions that permeate the channel. Self-regulation of Ca_v2.1 channels by Ca²⁺ is manifest as an initial increase (facilitation) and gradual decrease (inactivation) in Ca²⁺ current amplitude during high-frequency stimuli (Forsythe et al., 1998; Lee et al., 1999; Lee et al., 2000). Ca²⁺-dependent facilitation (CDF) and inactivation (CDI) of Ca_v2.1 channels depend on calmodulin binding to the pore-forming α_1 -subunit of Ca_v2.1 (Lee et al., 1999; DeMaria et al., 2001), and can cause activity-dependent changes in synaptic efficacy (Cuttle et al., 1998; Forsythe et al., 1998; Borst and Sakmann, 1998).

A fundamental distinction between CDF and CDI is their sensitivity to cytoplasmic Ca²⁺ buffering. The blockade of CDI, but not CDF, by high concentrations of the Ca²⁺ chelators EGTA and BAPTA (Lee et al., 2000; Soong et al., 2002), suggests that the extent to which Ca_v2.1 channels undergo CDI may largely be influenced by factors that regulate intracellular Ca²⁺ concentrations. Such factors include parvalbumin (PV) and calbindin (CB), which are EF-hand Ca²⁺ binding proteins that alter the amplitude and time course of Ca²⁺ signals in some nerve and muscle cells (Li et al., 1995; Schwaller et al., 1999; Lee et al., 2000a; Lee et al., 2000b; Schmidt et al., 2003b). Unlike calmodulin, which directly interacts with and confers Ca²⁺-dependent regulation to numerous effectors (Chin and Means, 2000), PV and CB were generally thought to act as

passive Ca^{2+} buffers which help protect cells from Ca^{2+} overloads. However, by modifying the spatial and temporal aspects of intracellular Ca^{2+} elevations, PV and CB can influence Ca^{2+} signals that modulate the activity of inositol 1,4,5 trisphosphate receptors (John et al., 2001; Dargan et al., 2004). Similarly, PV and CB might physiologically regulate Ca^{2+} -dependent modulation of $\text{Ca}_v2.1$, as PV and CB are concentrated in subsets of neurons, such as cerebellar Purkinje neurons, where $\text{Ca}_v2.1$ channels are also highly expressed (Mintz et al., 1992; Kadowaki et al., 1993; Schwaller et al., 2002; Chaudhuri et al., 2005). Previous studies implicate a role for PV and CB in modulating CDI of L-type voltage-gated Ca^{2+} channels in neurons (Nagerl et al., 2000a; Meuth et al., 2005), but whether these proteins also affect $\text{Ca}_v2.1$ (P/Q-type) channels is not known.

In this study, we compared the effects of Ca^{2+} buffers (EGTA and BAPTA) and Ca^{2+} buffering proteins (PV and CB) on CDI of $\text{Ca}_v2.1$ in transfected HEK 293T cells. Our analyses indicate that inactivation of $\text{Ca}_v2.1$ Ca^{2+} current varies significantly with current amplitude and is more sensitive to Ca^{2+} buffering by EGTA than BAPTA. PV and CB do not simply replicate the effects of EGTA and BAPTA, but differentially altered the current-dependence of CDI. These findings reveal the importance of cellular Ca^{2+} buffering mechanisms in the negative feedback regulation of $\text{Ca}_v2.1$ channels by Ca^{2+} , which may further diversify the properties of these channels in different neuronal cell-types (Llinas et al., 1992).

Materials and Methods

cDNA expression constructs. Ca_v2.1 subunits used in electrophysiological experiments were $\alpha_12.1$ (rbA isoform), β_{2a} and $\alpha_2\delta$ (Starr et al., 1991; Perez-Reyes et al., 1992; Stea et al., 1994). cDNAs corresponding to rat parvalbumin and calbindin were isolated by PCR amplification with specific primers from a rat brain cDNA library. Parvalbumin was subcloned into the *HindIII/BamHI* sites of pcDNA3.1+, and calbindin was subcloned into the *BamHI/XhoI* sites of pcDNA3.1 topo. The PV_{CDEF} mutant containing amino acid substitutions D51A, E62V, D90A, and E101V was based on that described by Pauls et al. (1994) and generated by multiple rounds of quick-change mutagenesis and subcloning into pcDNA3.1+. The identity of all cDNA constructs was confirmed by sequencing prior to use in electrophysiological experiments.

Cell culture and transfection. HEK 293T cells were maintained in Dulbecco's Modified Eagle's Medium supplemented with 10% fetal bovine serum at 37 °C under 5% CO₂. Cells plated in 35 mm tissue culture dishes were grown to 65-80% confluency and transfected with GenePORTER transfection reagent (Gene Therapy Systems Inc., San Diego, CA) according to the manufacturer's protocol with a 1:1 molar ratio of cDNAs for Ca²⁺ channel subunits (total of 5 μ g) and 0.7 μ g of a CD8 expression plasmid for identification of transfected cells. Parvalbumin and calbindin cDNAs were transfected at a 1:1 molar ratio with Ca²⁺ channel subunits.

Western blots. HEK 293T cells, plated and transfected as for electrophysiological experiments, were homogenized in ice-cold lysis buffer (25 mM Tris (pH. 7.4), 137 mM NaCl, 2.7 mM KCl, 0.1% PMSF, and 1% Triton X-100) and stored at -20 °C until use.

Cell lysates (50 μg) were electrophoresced on denaturing 4-20% tris-glycine gels (Invitrogen, Carlsbad, CA) and transferred to a nitrocellulose membrane that was blocked in 3% milk/TBS and incubated with antibodies against PV (1:1000, Chemicon International, Temecala, CA), CB (1:1000, Chemicon International, Temecala, CA), or CaM (1:500, Upstate, Lake Placid, NY). Chemiluminescent detection was achieved with HRP-conjugated secondary antibodies (1:2000, Amersham Biosciences, Piscataway, NJ) and ECL reagents (Amersham).

Electrophysiological recordings. At least 48 h after transfection, HEK 293T cells were incubated with CD8 antibody-coated microspheres (Dynal, Oslo, Norway) for identification of transfected cells. Ca^{2+} or Ba^{2+} currents were recorded in whole-cell patch-clamp recordings with a HEKA EPC-9 patch-clamp amplifier driven by PULSE software (HEKA Electronics, Lambrecht/Pfalz, Germany). Leak and capacitive transients were subtracted using a P/-4 protocol. Extracellular recording solutions contained (in mM): 150 Tris, 1 MgCl_2 , and 10 CaCl_2 or 10 BaCl_2 . Intracellular recording solutions contained (in mM): 130 N-methyl-D-glucamine, 60 HEPES, 1 MgCl_2 , 2 Mg-ATP, and EGTA (0.5 mM unless otherwise indicated) or BAPTA (0.5 mM or 10 mM). The pH of extracellular and intracellular recording solutions was adjusted to 7.3 with methanesulfonic acid. Due to shifts in the activation curve of -10 and $+10$ mV when extracellular Ba^{2+} or intracellular BAPTA were used, respectively, voltage protocols were adjusted to compensate for this difference as noted.

Data analysis. All data were analyzed using custom written procedures in IGOR Pro software (Wavemetrics, Portland, OR). Averaged data represent the mean \pm SEM. Statistical differences in averaged inactivation (I_{res}/I_{pk}) between groups were determined by Student's t-test. Normalized tail current-voltage curves were fit with a single Boltzmann function: $A/\{1 + \exp [(V - V_{1/2})/k] + b\}$ where V is test pulse voltage, $V_{1/2}$ is the midpoint of the activation curve, k is a slope factor, A is the amplitude, and b is the baseline. I - V curves were fit with the function: $g(V - E)/\{1 + \exp[(V - V_{1/2})/k] + b\}$ where g is the maximum conductance, V is the test potential, E is the apparent reversal potential, $V_{1/2}$ is the potential of half activation, k is the slope factor, and b is the baseline. Linear and nonlinear regression and statistical analyses were done with Sigma Plot (SPSS, Inc., Chicago, IL). Significant deviations of percent inactivation data from regression models were determined by Runs test. Data describing current-dependence of I_{Ca} inactivation were fit with a nonlinear regression equation, $y=ax^b$ where y is % inactivation, x is the current amplitude, and a and b are constants. F-tests were used for comparisons of nonlinear regression curves, with statistical significance considered as $p < 0.05$.

Results

Current-dependence of CDI and sensitivity to EGTA. Ca^{2+} microdomains near the pore of individual Ca^{2+} channels may reach micromolar concentrations, are too short-lived to be significantly buffered by high concentrations of slow Ca^{2+} buffers such as EGTA, or low concentrations of fast Ca^{2+} buffers such as BAPTA (Stern, 1992). For this reason, the blockade of CDI of $Ca_v2.1$ by high intracellular concentrations of EGTA and BAPTA (10 mM) implies a requirement for a "global" Ca^{2+} signal that is supported by multiple

open channels (Lee et al., 2000; DeMaria et al., 2001; Soong et al., 2002). A simple prediction of this model is that CDI should increase to some extent with the amplitude of the whole-cell Ca^{2+} current (I_{Ca}). In support of this prediction, human splice variants of $\alpha_12.1$ with poor expression levels in transfected cells, as reflected by low-amplitude I_{Ca} , exhibited less CDI than channel variants with higher mean current amplitudes (Soong et al., 2002).

In the present study, we also observed a similar relationship between current amplitude and CDI for channels containing the rat brain (rbA) $\alpha_12.1$ variant (2.1). In transfected HEK 293T cells, inactivation of currents carried by Ca^{2+} (I_{Ca}) or Ba^{2+} (I_{Ba}) was measured as $I_{\text{res}}/I_{\text{pk}}$, which was the amplitude of the current at the end of a 2-s pulse normalized to the peak current amplitude. With minimal Ca^{2+} buffering of the intracellular recording solution (0.5 mM EGTA), we found that inactivation was significantly greater (smaller $I_{\text{res}}/I_{\text{pk}}$) for large I_{Ca} (>0.4 nA) than for small I_{Ca} (<0.4 nA) ($p<0.01$; Fig. 2.1A,B) and that the increase in I_{Ca} inactivation with current amplitude was significantly nonlinear ($p<0.05$) (Fig. 2.1C). Because Ba^{2+} does not support CaM-dependent conformational changes that underlie CDI of voltage-gated Ca^{2+} channels (Brehm and Eckert, 1978; Qin et al., 1999; Zuhlke et al., 1999; Lee et al., 1999; Peterson et al., 1999), $\text{Ca}_v2.1$ currents carried by Ba^{2+} ions did not vary significantly with current amplitude (Fig. 2.1B). High concentrations (10 mM) of BAPTA in the intracellular recording solution, which block CDI of $\text{Ca}_v2.1$ (Lee et al., 1999; Lee et al., 2000), also prevented the current-dependent increase in inactivation (Fig. 2.1B), such that the relationship between current amplitude and inactivation for for I_{Ca} + 10 mM BAPTA and for I_{Ba} did not significantly deviate from a straight line ($p=0.83$ for I_{Ca} +10 BAPTA and

$p=0.53$ for I_{Ba} ; Fig.2.1C). The positive slope for the current-dependence of I_{Ba} inactivation (0.02 ± 0.01) could have resulted from Ba^{2+} -dependent effects on inactivation that have been described for L-type Ca^{2+} channels (Ferreira et al., 1997). It is not clear why the corresponding relationship for I_{Ca} with 10 mM BAPTA exhibited a negative slope (-0.01 ± 0.01), although stimulatory effects of BAPTA on the amplitude of $Ca_v2.1$ currents, have been reported in previous studies (Bodding and Penner, 1999; Rousset et al., 2004). The difference between inactivation for I_{Ca} and I_{Ba} , which reflects the magnitude of CDI, was significantly greater for larger currents ($\sim 20\%$, $p < 0.05$, Fig.2.1A,B), primarily as a consequence of stronger, current-dependent inactivation of I_{Ca} . Our analyses demonstrate that Ca^{2+} influx and its intracellular accumulation cause nonlinear increases in $Ca_v2.1$ inactivation and that current-dependent variations in CDI should be considered when evaluating factors that regulate this process.

To evaluate the modulatory potential of Ca^{2+} buffers on CDI, we compared the effects of BAPTA and EGTA at concentrations (0.5 mM) that are permissive for CDI. While EGTA and BAPTA bind Ca^{2+} with nearly equal affinity, Ca^{2+} on- and off-rates for BAPTA are at least 100 times faster than for EGTA (Tsien, 1980). Although BAPTA binds Ca^{2+} faster than EGTA, it will also retain it for shorter periods of time. This will cause a faster increase in Ca^{2+} concentration, such that CDI may be more evident with BAPTA than with EGTA. Consistent with this prediction, I_{res}/I_{pk} was significantly smaller with BAPTA (0.5 mM) than with the same concentration of EGTA ($\sim 54\%$ for $I_{Ca} < 0.4$ nA and $\sim 60\%$ for $I_{Ca} > 0.4$ nA, $p < 0.01$; Fig.2.2A). For $I_{Ca} > 0.4$ nA, the rate of inactivation with BAPTA (0.5 mM) was significantly faster than with EGTA ($\sim 36\%$, Table 1). The effect of BAPTA was evident as an upward shift in the relationship

between I_{Ca} inactivation and current amplitude, which was significantly different than that with EGTA ($p < 0.001$, Fig. 2.2A). Greater inactivation with BAPTA than with EGTA was particularly apparent during repetitive depolarizations (Fig. 2.2B). With this voltage-protocol and low EGTA (0.5 mM), I_{Ca} underwent initial facilitation, which is also calmodulin-dependent (Lee et al., 2000), followed by inactivation. However, with BAPTA (0.5 mM), only strong inactivation of I_{Ca} was observed, such that I_{Ca} was reduced ~23% by the end of the train compared to I_{Ca} recorded with EGTA (Fig. 2.2B). These results show that the ability of I_{Ca} to generate Ca^{2+} signals that cause CDI of $Ca_v2.1$ is greater in the presence of fast Ca^{2+} buffers like BAPTA, than with slow Ca^{2+} buffers like EGTA.

Effects of PV on CDI of $Ca_v2.1$. To determine if Ca^{2+} buffering proteins might similarly regulate inactivation of $Ca_v2.1$ Ca^{2+} currents, we investigated the effect of coexpressing $Ca_v2.1$ with parvalbumin (PV). We chose PV since its Ca^{2+} binding properties and effects on Ca^{2+} signals are well-characterized (Schwaller et al., 2002). The EF-hands of PV can bind Ca^{2+} with high affinity and Mg^{2+} with lower affinity (Haiech et al., 1979; Pauls et al., 1994). Under resting conditions, the concentration of Mg^{2+} in cells is generally far greater than that for Ca^{2+} (Li-Smerin et al., 2001), so that the rate of Ca^{2+} binding is slow due to a requirement for Mg^{2+} to first unbind (Hou et al., 1991). As a consequence, PV is considered a slow Ca^{2+} buffer in cells, with similar Ca^{2+} binding kinetics as EGTA (Nagerl et al., 2000b; Schwaller et al., 2002).

Based on our results with EGTA and BAPTA, we expected that PV, like EGTA, should decrease I_{Ca} inactivation. While this was true for $I_{Ca} < 0.4$ nA (~32% increase in

I_{res}/I_{pk} for PV-transfected cells, $p<0.05$; Fig. 2.3A), PV had the opposite effect for $I_{Ca}>0.4$ nA, causing significantly greater inactivation of I_{Ca} than in cells transfected with $Ca_v2.1$ alone (~50% decrease in I_{res}/I_{pk} , $p<0.04$; Fig. 2.3A). Kinetic analyses showed that these effects of PV were due to a slowing and acceleration of the rate of inactivation for small- and large-amplitude currents, respectively (Table 2.1). The dual effects of PV on I_{Ca} inactivation resulted in a significant deviation in the relationship between I_{Ca} inactivation and current amplitude relative to that for $Ca_v2.1$ alone ($p<0.005$, Fig. 2.3B). The peak I_{Ca} and shape of the I-V curves for cells transfected with $Ca_v2.1$ alone or cotransfected with PV were not different for either small or large I_{Ca} (Fig. 2.3C), excluding the possibility that the dual effects of PV on I_{Ca} inactivation were caused by alterations in voltage-dependent activation of $Ca_v2.1$, or variability in channel expression between groups. The effects of PV on the current-dependence of I_{Ca} inactivation were especially apparent during trains of repetitive stimuli (Fig. 2.4). In these experiments, inactivation of I_{Ca} in cells transfected with $Ca_v2.1$ alone varied less with peak I_{Ca} amplitude than during sustained test pulses (Fig. 2.1). Because Ca^{2+} -dependent facilitation as well as inactivation is evident with this voltage-protocol, temporal overlap of both forms of Ca^{2+} regulation may have minimized the current-dependence of I_{Ca} inactivation in cells transfected with $Ca_v2.1$ alone (Fig. 2.4A). However, in cells cotransfected with PV, the dependence of I_{Ca} inactivation on current amplitude was more pronounced (Fig. 2.4B). Consistent with results obtained with sustained test pulses (Fig. 2.3A,B), PV inhibited inactivation of small I_{Ca} and had the opposite effect on large I_{Ca} . The net effect of PV was to significantly augment differences in inactivation for I_{Ca} of different peak amplitudes (Fig. 2.4B).

The Ca^{2+} buffering properties of PV could account for the suppression of inactivation of small currents, but we wondered if the opposite effect of PV on large currents could have resulted from Ca^{2+} unbinding from PV. Large I_{Ca} through $\text{Ca}_v2.1$ channels could rapidly saturate the EF-hand Ca^{2+} binding sites on PV, and subsequent Ca^{2+} release from PV might then facilitate CDI. At the concentration of intracellular Mg^{2+} in our experiments (~ 3 mM), estimated rates of Ca^{2+} unbinding from PV ($\sim 0.9/\text{s}$, (Schmidt et al., 2003a)) are consistent with the potential for Ca^{2+} release from PV to occur within the 2-s depolarizing pulse in our experiments (Fig. 2.3A). In this context, both the inhibitory and stimulatory effects of PV on I_{Ca} inactivation should depend critically on the ability of PV to bind Ca^{2+} . To test this, we generated a PV construct with mutations in the second and third EF-hands (PV_{CDEF}). Because these alterations prevent binding of Ca^{2+} and Mg^{2+} (Pauls et al., 1993; Pauls et al., 1994), PV_{CDEF} should not replicate Ca^{2+} -dependent effects of PV on $\text{Ca}_v2.1$ inactivation. In these experiments, $I_{\text{res}}/I_{\text{pk}}$ for I_{Ca} was not affected by PV_{CDEF} for either small or large-amplitude I_{Ca} ($p=0.52$ and 0.71 , respectively), and the relationship between I_{Ca} inactivation and current amplitude was not significantly different from that for $\text{Ca}_v2.1$ channels expressed alone ($p=0.62$, Fig. 2.5A). These results were not due to limited expression levels of PV_{CDEF} , since Western blots indicated similar amounts of PV and PV_{CDEF} in lysates harvested from the cotransfected cells (not shown). The dual effects of wild-type PV on I_{Ca} inactivation were also not observed when CDI was blocked by a high intracellular concentration (10 mM) of BAPTA ($p=0.17$ for $I_{\text{Ca}} < 0.4$ nA, $p=0.45$ for $I_{\text{Ca}} > 0.4$ nA; Fig. 2.5B). Moreover, there was no effect of PV on the dependence of I_{Ca} inactivation on current amplitude in the presence of 10 mM BAPTA (Fig. 2.5B). These results argued

against the possibility that PV influenced Ca^{2+} -independent (i.e., voltage-dependent) mechanisms of $\text{Ca}_v2.1$ inactivation, since such actions would have been spared by BAPTA. We conclude that the opposing effects of PV on inactivation of large and small I_{Ca} are a consequence of Ca^{2+} binding to PV, which can either stabilize or diffuse Ca^{2+} pools that underlie CDI, depending on the amplitude of I_{Ca} .

Effects of CB on CDI. We investigated further the role of Ca^{2+} buffer kinetics and CDI in cells cotransfected with calbindin-D28k (CB), a protein with physiological Ca^{2+} -binding and unbinding rates that are faster, by an order of magnitude, than those for PV (Nagerl et al., 2000b). CB also differs from PV in possessing four functional EF-hands, which have relatively low affinity for Ca^{2+} compared to those in PV, and do not significantly bind Mg^{2+} (Nagerl et al., 2000b). In analyses of I_{Ca} evoked by step depolarizations, CB significantly inhibited inactivation of $I_{\text{Ca}} < 0.4$ nA (~35% increase in $I_{\text{res}}/I_{\text{pk}}$ compared to $\text{Ca}_v2.1$ alone, $p < 0.02$, Fig. 2.6A) and caused an even greater slowing of inactivation rate than PV (~52% for CB, and ~36% for PV, Table 2.1). Perhaps because of an inhibitory effect of CB on $\text{Ca}_v2.1$ expression, $\text{Ca}_v2.1$ Ca^{2+} currents in cells cotransfected with CB did not exceed 0.8 nA. Therefore, analysis of $I_{\text{Ca}} > 0.4$ nA in cells transfected with $\text{Ca}_v2.1$ alone or cotransfected with CB was restricted to currents with amplitude from 0.4 to 0.8 nA. In this current range, CB did not significantly influence the magnitude or rate of inactivation ($p = 0.39$, Fig. 2.6A, Table 2.1). The suppression of inactivation of low-amplitude currents caused a significant downward shift in the relationship between inactivation and I_{Ca} amplitude in cells cotransfected with CB compared to that in cells transfected with $\text{Ca}_v2.1$ alone ($p < 0.02$, Fig. 2.6B). The absence of $I_{\text{Ca}} > 0.8$ nA in cells

cotransfected with $\text{Ca}_v2.1$ and CB precluded determination if, like PV, CB had a stimulatory effect on inactivation of large-amplitude currents, as these effects were generally observed in cells cotransfected with PV for $I_{\text{Ca}} > 0.8$ nA (Fig. 2.3B). However, the inhibitory effects of both PV and CB on inactivation of small-amplitude $\text{Ca}_v2.1$ Ca^{2+} currents is consistent with a modulatory role for these Ca^{2+} buffering proteins in the negative feedback of $\text{Ca}_v2.1$ by Ca^{2+} .

Besides increasing the Ca^{2+} buffering capacity of the cell, PV and CB in the transfected HEK 293T cells may have had secondary effects that might influence $\text{Ca}_v2.1$ properties in our experiments. For example, overexpression of PV and CB could have reduced the levels of endogenous calmodulin required for CDI, which could also explain the inhibition of I_{Ca} inactivation in cells cotransfected with $\text{Ca}_v2.1$ and PV or CB (Figs. 2.3, 2.6). However, western blots indicated equivalent levels of calmodulin in cells transfected with $\text{Ca}_v2.1$ alone and in cells cotransfected with PV or CB (Fig. 2.7A). In addition, cotransfection of $\text{Ca}_v2.1$ with PV and CB did not alter the magnitude of Ca^{2+} -dependent facilitation of I_{Ca} , which also depends on calmodulin (Fig. 2.7B-D). The enhancement of I_{Ca} amplitude during the first 200 ms of a repetitive stimulus protocol was not significantly different in cells transfected with $\text{Ca}_v2.1$ alone and those cotransfected with PV ($p=0.30$) or CB ($p=0.54$). The ineffectiveness of PV and CB in these experiments can be explained by a reliance of facilitation on local Ca^{2+} increases that are not able to be suppressed by even high concentrations of EGTA and BAPTA (Lee et al., 2000; Soong et al., 2002; Chaudhuri et al., 2004). These results also show that calmodulin was not likely to be a limiting factor contributing to the reduced CDI in cells

expressing $\text{Ca}_v2.1$ with PV or CB. Taken together, our findings indicate that PV and CB modulate $\text{Ca}_v2.1$ Ca^{2+} currents by regulating global Ca^{2+} microdomains that support CDI.

Discussion

In the present study, the use of endogenous and exogenous Ca^{2+} buffers revealed new insights into the feedback regulation of $\text{Ca}_v2.1$ channels by Ca^{2+} . First, we confirmed and extended previous findings (Soong et al., 2002) that $\text{Ca}_v2.1$ inactivation increases nonlinearly with the amplitude of I_{Ca} , an effect not observed when intracellular Ca^{2+} is buffered with BAPTA (10 mM) or when Ba^{2+} is the charge carrier. Second, BAPTA, at submaximal concentrations, strengthens the relationship between current amplitude and CDI compared to EGTA, perhaps due to its faster Ca^{2+} unbinding kinetics. Third, the Ca^{2+} buffering proteins PV and CB also alter the Ca^{2+} current-dependence of $\text{Ca}_v2.1$ inactivation. These findings illustrate how factors affecting $\text{Ca}_v2.1$ expression and Ca^{2+} homeostasis may dynamically regulate $\text{Ca}_v2.1$ properties and Ca^{2+} signaling in excitable cells.

Differential modulation of $\text{Ca}_v2.1$ inactivation by Ca^{2+} buffers. Based on our results and those published previously, we propose a qualitative model to account for the Ca^{2+} -dependence of $\text{Ca}_v2.1$ inactivation (Fig. 2.8). Unlike the relative invariance of the local Ca^{2+} microdomain associated with individual channel openings, Ca^{2+} pools that support CDI may be enhanced by larger I_{Ca} due to increased overlap of global Ca^{2+} signals emanating from neighboring channels (Fig. 2.8A). Small I_{Ca} may inactivate less than large I_{Ca} because, when not supported by multiple channels, these Ca^{2+} pools dissipate

rapidly due to diffusion of Ca^{2+} (Figs. 2.1, 2.8A). These Ca^{2+} gradients surrounding individual channels are collapsed by high concentrations of BAPTA (Fig. 2.1) or EGTA (Lee et al., 2000), thus abolishing the dependence of CDI on current amplitude (Figs. 2.1C, 2.8A). However, at concentrations of Ca^{2+} buffers that are permissive for CDI, Ca^{2+} unbinding from the buffer may paradoxically stabilize the Ca^{2+} pool supporting CDI (Figs. 2.8B,C). Considering first the increased CDI seen with BAPTA compared to EGTA (0.5 mM, Fig. 2.2), the 100-fold faster association and dissociation rate of Ca^{2+} from BAPTA allows it to capture but also unload Ca^{2+} more rapidly than EGTA (Tsien, 1980). Therefore, the time that Ca^{2+} will remain bound before dissociating is considerably less for BAPTA (~6-60 ms), than for EGTA (~700-2000 ms) (Dargan and Parker, 2003), such that BAPTA (0.5 mM) is ultimately less efficient than EGTA in removing Ca^{2+} supporting CDI of both small and large I_{Ca} (Figs. 2.2, 2.8B).

The dual effects of PV on $\text{Ca}_v2.1$ inactivation may result not only from its slow Ca^{2+} binding properties but also more limited mobility of PV relative to EGTA and BAPTA. Owing to its larger size, PV has a diffusional range (~43 $\mu\text{m}^2\text{s}^{-1}$) that is about five times less than that for EGTA (~200 $\mu\text{m}^2\text{s}^{-1}$) (Schmidt et al., 2003a). When $\text{Ca}_v2.1$ channels are sparsely distributed in the plasma membrane (small I_{Ca}), PV may have a net Ca^{2+} buffering effect in reducing CDI (Fig. 2.3), as PV may bind and shuttle Ca^{2+} away from channels prior to releasing it (Lee et al., 2000b). However, with increased channel density (large I_{Ca}), Ca^{2+} -saturated PV may unload Ca^{2+} within microdomains that support CDI of neighboring channels (Fig. 2.8C), therefore increasing inactivation of large-amplitude I_{Ca} compared to cells transfected with $\text{Ca}_v2.1$ alone (Figs. 2.3, 2.4). Although CB has fast Ca^{2+} binding kinetics more comparable to BAPTA than EGTA, CB also has

considerably lower Ca^{2+} binding affinity ($\sim 1.5 \mu\text{M}$) and diffusional range ($< 40 \mu\text{m}^2\text{s}^{-1}$) than BAPTA (Nagerl et al., 2000b). Together, these factors may explain why CB behaved more like a slow Ca^{2+} buffer in inhibiting CDI only for low amplitude currents (Fig. 2.6).

For the following reasons, we consider the relatively modest effects of PV and CB on CDI in our experiments to underestimate the potential for these Ca^{2+} buffering proteins to influence $\text{Ca}_v2.1$ channels in neurons. First, the impact of PV was likely attenuated by the concentration of Mg^{2+} in our intracellular recording solution (3 mM). Due to the mixed $\text{Ca}^{2+}/\text{Mg}^{2+}$ affinity of PV EF-hands (Gillis et al., 1982; Pauls et al., 1994), PV would be occupied mainly by Mg^{2+} ions prior to evoking I_{Ca} in our experiments. Mg^{2+} unbinding from PV would therefore retard the rate of Ca^{2+} binding. Given that the estimated concentration of Mg^{2+} in brain synaptosomes is $\sim 0.3\text{-}0.6 \text{ mM}$ (Stout et al., 1996; Li-Smerin et al., 2001), we would predict more rapid Ca^{2+} binding by PV in neurons than in our transfected cell recordings, which should enhance its current-dependent modulation of CDI (Figs. 2.3, 2.4). Second, PV and CB are found at concentrations in neurons (100 μM -5 mM) (Kosaka et al., 1993; Plogmann and Celio, 1993; Fierro and Llano, 1996; Hackney et al., 2005) that may exceed that in our transfected cells. While western blots of transfected cell lysates indicated strong levels of overexpressed PV and CB (Figs. 2.3D, 2.6A), heterogeneous levels of PV and CB between cells could have contributed to intercellular variability and weakened the average impact on CDI. Finally, washout of PV and CB from transfected cells into the recording pipette solution during whole-cell recordings may have diminished the intracellular content of Ca^{2+} buffering proteins. Whole-cell patch clamp recordings of

dentate granule cells in hippocampal slices suggest considerable dilution of endogenous CB within the first 5 minutes of obtaining whole-cell configuration (Muller et al., 2005). Although we measured inactivation at similar time points between cells to limit variability, initial washout of PV or CB upon patch rupture could have significantly reduced the overall impact of these proteins on CDI.

Ca²⁺ buffering proteins as regulators of Ca²⁺ signaling. The effects of PV in altering feedback regulation of Ca_v2.1 channels parallels its modulation of inositol 1,4,5 trisphosphate receptors (IP₃Rs), which mediate Ca²⁺ release from intracellular stores (John et al., 2001; Dargan and Parker, 2003; Dargan et al., 2004). Overexpression of PV in *Xenopus* oocytes was found to stimulate Ca²⁺-dependent activation of IP₃Rs by facilitating Ca²⁺ diffusion between neighboring channels (John et al., 2001). That BAPTA, but not CB, replicated the effect of PV in this system was interpreted as a sign that the Ca²⁺ binding affinity and diffusional range of a Ca²⁺ buffering protein were important determinants of the ability to enhance IP₃R activation by Ca²⁺ (John et al., 2001). The similar effects of PV in stimulating Ca²⁺-feedback of Ca_v2.1 channels and IP₃Rs may exemplify fundamental mechanisms controlling Ca²⁺-dependent activation of other signaling pathways. In addition, the dual potential for PV to act as a passive Ca²⁺ buffer and a facilitator of intracellular and plasma membrane Ca²⁺ channels may contribute to the paradox that PV can be neuroprotective from pathological Ca²⁺ overloads in some neurons (Van Den Bosch et al., 2002), but can also exacerbate excitotoxic cell death in others (Hartley et al., 1996; Maetzler et al., 2004).

Our findings also provide direct support for previous observations that Ca^{2+} buffering proteins inhibit CDI of voltage-gated Ca^{2+} channels in neurons. Infusion of PV and CB in thalamic relay neurons caused an inhibition of CDI of high-voltage activated Ca^{2+} current, although this effect was primarily on L-type channels (Meuth et al., 2005). In addition, loss of CB from surviving granule cells isolated from the hippocampus of patients with mesial temporal lobe epilepsy correlated with increased CDI of voltage-gated Ca^{2+} currents, which was restored by inclusion of CB in the recording electrode (Nagerl et al., 2000a). Interestingly, Chaudhuri et al. (2005) found that $\text{Ca}_v2.1$ channels in cerebellar Purkinje neurons show highly variable CDI, which may result partly from cellular variations in $\text{Ca}_v2.1$ subunits expressed. Our results suggest that developmental or pathological alterations in PV and CB, as well as in the levels of $\text{Ca}_v2.1$ expression, could add to the heterogeneity of $\text{Ca}_v2.1$ inactivation in these and other neurons. Such variations in $\text{Ca}_v2.1$ properties may be important for tailoring Ca^{2+} influx according to particular physiological contexts.

Table 2.1. Effect of PV and CB on kinetics of inactivation of Ca_v2.1 Ca²⁺ current

		n	τ (s)	p-value (relative to Ca _v 2.1+0.5EGTA)	Fraction of I _{Ca}	p-value (relative to Ca _v 2.1+0.5EGTA)
I _{Ca} <0.4 nA	Ca _v 2.1 +0.5 EGTA	12	1.237 ± 0.107	--	0.943 ± 0.017	--
	Ca _v 2.1 +0.5 BAPTA	6	0.956 ± 0.088	0.11	0.980 ± 0.013	0.09
	Ca _v 2.1 +10 BAPTA	18	1.532 ± 0.084	<0.05	0.707 ± 0.030	<0.01
	Ca _v 2.1+PV	9	1.690 ± 0.177	<0.05	0.967 ± 0.033	0.18
	Ca _v 2.1+CB	17	1.884 ± 0.141	<0.01	0.977 ± 0.011	<0.05
	Ca _v 2.1 +0.5 EGTA	7	1.123 ± 0.098	--	1.000 ± 0.000	--
I _{Ca} >0.4 nA	Ca _v 2.1 +0.5 BAPTA	5	0.721 ± 0.064	<0.05	0.997 ± 0.002	0.11
	Ca _v 2.1 +10 BAPTA	13	1.771 ± 0.192	<0.05	0.875 ± 0.040	<0.05
	Ca _v 2.1+PV	5	0.747 ± 0.104	<0.05	0.977 ± 0.014	<0.05
	Ca _v 2.1+CB	11	1.109 ± 0.045	0.89	0.994 ± 0.005	0.39

Table 2.1: I_{Ca} was evoked by a test pulse from -80 mV to +10 mV (EGTA) or +20 mV (BAPTA), and inactivation time constants (τ) were estimated by fitting the current trace to the following equation: $I = I_0 + I_1 \exp(-t/\tau_1)$, where I_0 is the residual current amplitude at equilibrium and I_1 is the amplitude of the current. Fraction of I_1 is percent contribution of τ_1 to total inactivation, calculated as $I_1/(I_0 + I_1)$. Values are means ±

SEM; n= number of cells tested. *, $I_{Ca} > 0.4$ nA for cells cotransfected with $Ca_v2.1+CB$ represents I_{Ca} greater than 0.4 nA but less than 0.8 nA.

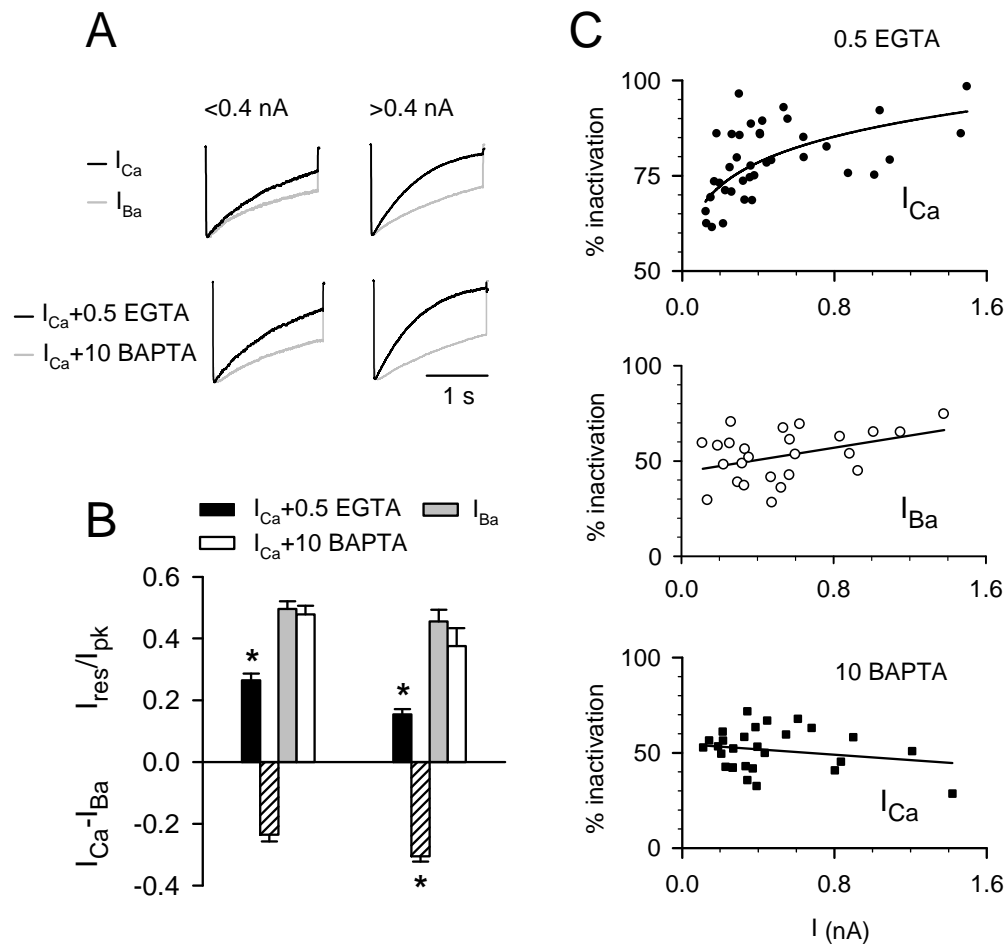
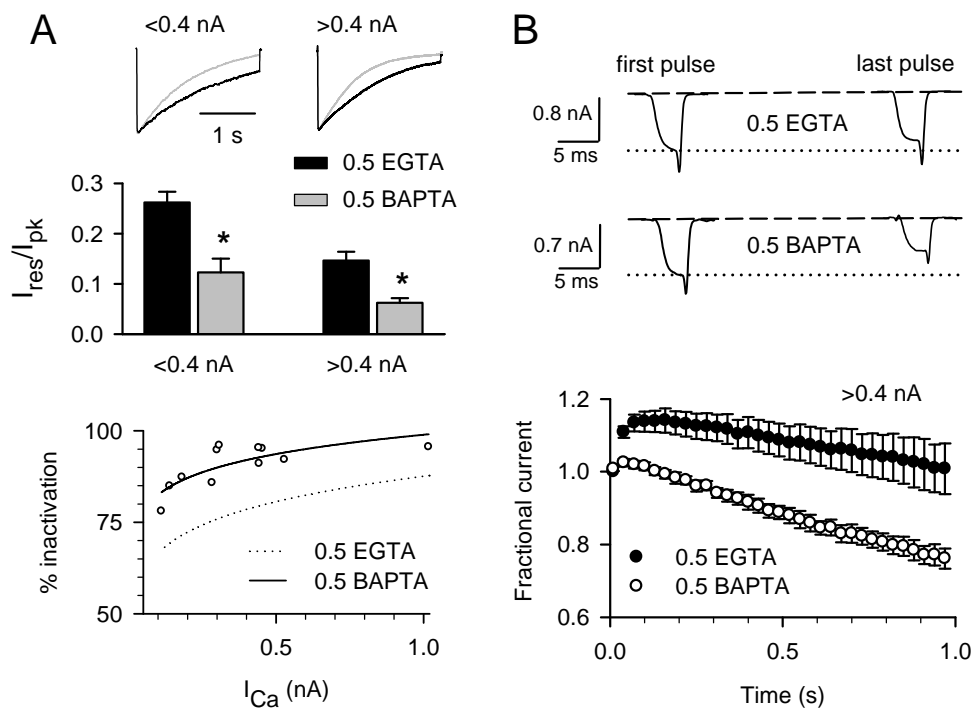
Figure 2.1

Figure 2.1. CDI depends on the amplitude of $Ca_v2.1$ Ca^{2+} currents. *A*, Normalized current traces showing $Ca_v2.1$ currents evoked by 2-s pulses from -80 mV to $+10$ mV ($I_{Ca}+0.5$ mM EGTA), 0 mV (I_{Ba}), or $+20$ mV ($I_{Ca}+10$ mM BAPTA) in HEK 293T cells transfected with $Ca_v2.1$. Top traces represent I_{Ca} (black) and I_{Ba} (grey) with 0.5 mM EGTA in the intracellular recording solution. Bottom traces show I_{Ca} recorded with either 0.5 mM EGTA (black) or 10 mM BAPTA (grey). *B*, For currents evoked as in *A*, I_{res}/I_{pk}

was determined as the current amplitude at the end of the pulse normalized to the peak current amplitude. $I_{Ca}-I_{Ba}$ was determined by subtracting I_{res}/I_{pk} of I_{Ba} from that for I_{Ca} . *, $p < 0.05$. *C*, Relationship between peak current amplitude and inactivation. For data obtained in *A* and *B*, % inactivation, which was calculated as $(1 - I_{res}/I_{pk}) * 100$, was plotted against peak current amplitude for I_{Ca} (●, ■) or I_{Ba} (○) recorded with 0.5 mM intracellular EGTA (●, ○) or 10 mM BAPTA (■). Each point represents a different cell. Smooth line represents fit from nonlinear ($I_{Ca}+0.5$ EGTA) or linear (I_{Ba} , $I_{Ca}+10$ BAPTA) regression.

Figure 2.2**Figure 2.2.** Inactivation of $Ca_v2.1$ Ca^{2+} currents is greater with BAPTA than with EGTA.

A, Inactivation during sustained depolarization. I_{Ca} was evoked and I_{res}/I_{pk} determined as in Fig. 2.1, but intracellular solution contained EGTA (black bars) or BAPTA (grey bars) at 0.5 mM. Current traces show normalized I_{Ca} from cells recorded with 0.5 mM EGTA (black) or BAPTA (grey). *, $p < 0.01$. Lower panel shows relationship between % inactivation and current amplitude for individual cells. % inactivation and nonlinear curve-fitting was the same as in Fig. 2.1C. Dotted line indicates curve-fit of data in Fig. 2.1C obtained for I_{Ca} with 0.5 mM EGTA. **B**, Inactivation during repetitive stimuli. I_{Ca} was evoked by 5-ms pulses from -80 mV to $+10$ mV (0.5 EGTA, ●) or $+20$ mV (0.5

BAPTA, ○) at a frequency of 100 Hz. Fractional current represents test current amplitude normalized to that for the first pulse in the train. Each point represents mean \pm SEM for $I_{Ca} > 0.4$ nA. Every second point is plotted against time during the train. Traces above show representative currents evoked by the first and last pulses. Dotted line indicates initial current amplitude.

Figure 2.3

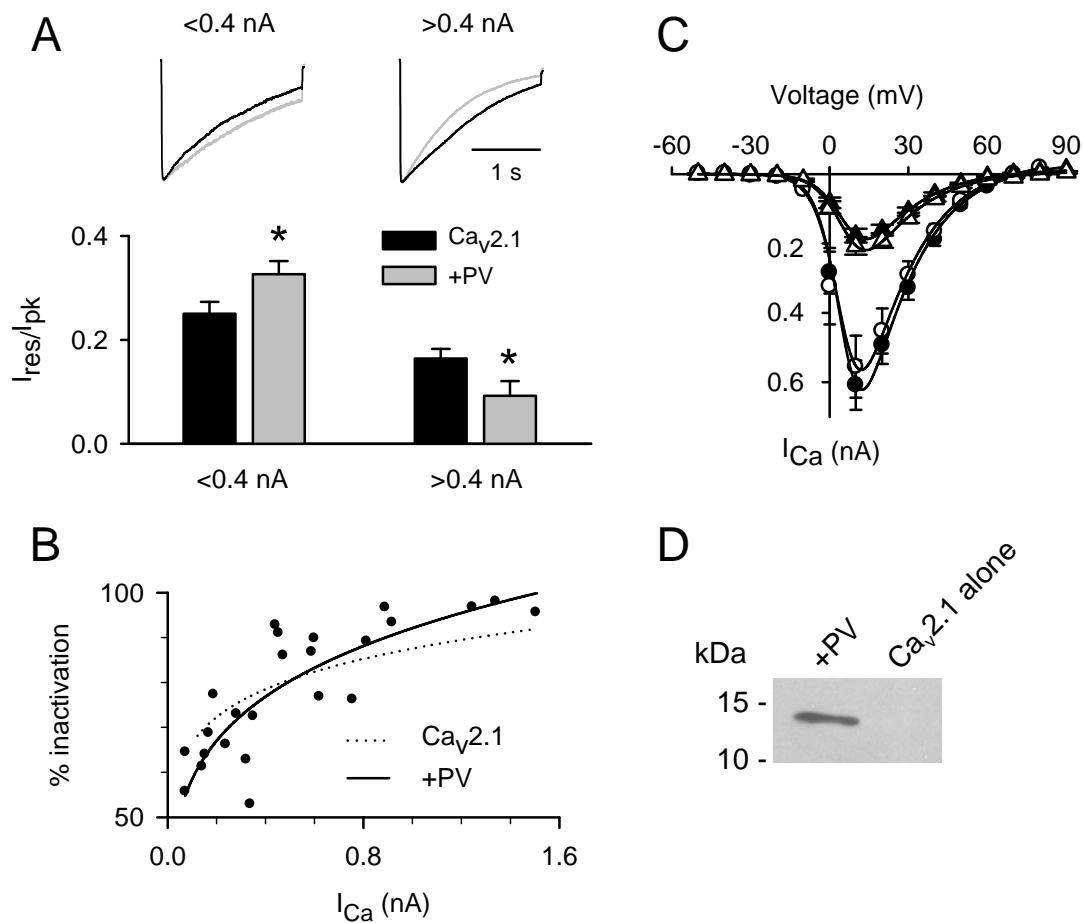


Figure 2.3. PV has opposite effects on inactivation of small and large-amplitude I_{Ca} . **A**, I_{res}/I_{pk} was determined as in Fig. 2.1 for I_{Ca} in cells transfected with Ca_v2.1 alone (black) or cotransfected with PV (grey) for I_{Ca} less than or greater than 0.4 nA. Representative normalized current traces are shown above. Intracellular solution contained 0.5 mM EGTA and extracellular solution contained 10 mM Ca²⁺. *, $p<0.05$. **B**, Current-dependence of I_{Ca} inactivation with PV. Dotted line indicates curve-fit of data in Fig. 2.1C obtained for I_{Ca} (+0.5 EGTA) in cells transfected with Ca_v2.1 alone. Solid line indicates curve-fit of data for cells cotransfected with PV. **C**, Current-voltage (I - V) curves

for cells transfected with $Ca_v2.1$ alone (open symbols) or cotransfected with PV (filled symbols) are shown for $I_{Ca} < 0.4$ nA (triangles) or > 0.4 nA (circles). *D*, Western blot detection of PV in cells cotransfected with PV but not in cells transfected with $Ca_v2.1$ alone.

Figure 2.4

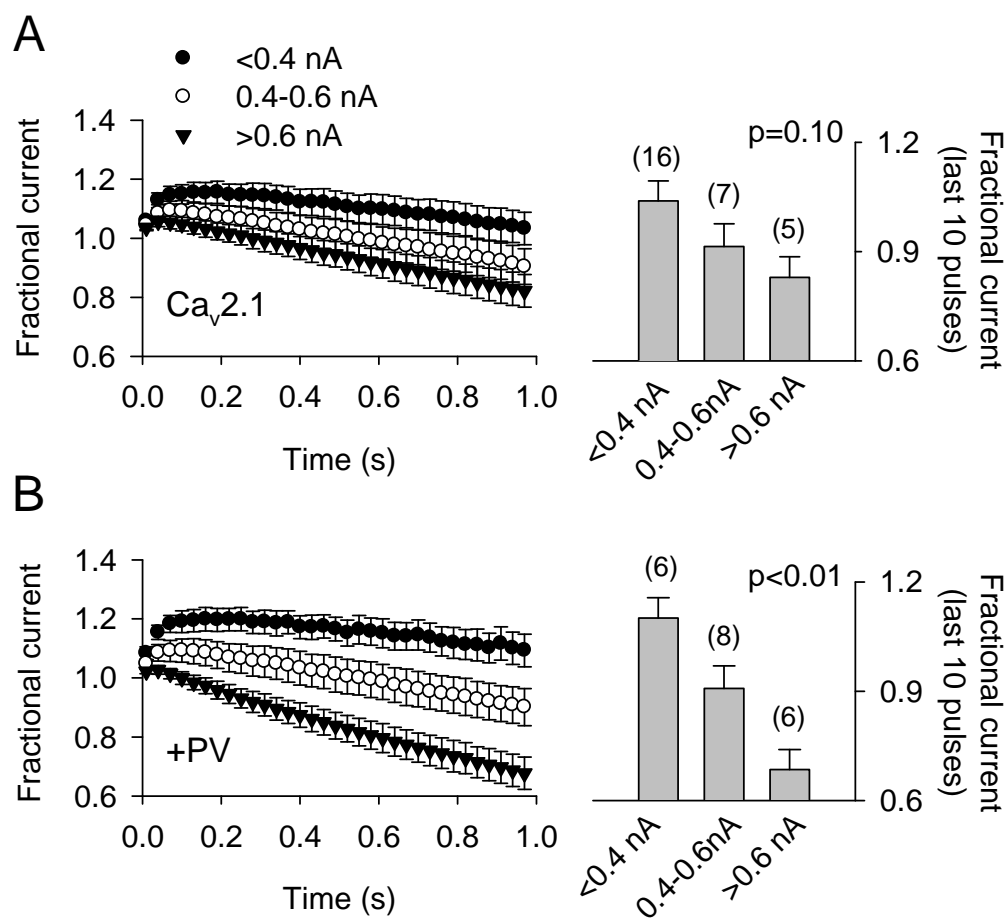


Figure 2.4. PV alters CDI during repetitive stimuli. *A,B, left panels*, Fractional current was determined as in Fig. 2.2B and plotted against time for cells transfected with Ca_v2.1 alone (*A*) or cotransfected with PV (*B*) for I_{Ca} of different amplitudes indicated in *A*. *Right panels*: Fractional current for the last 10 pulses were averaged and compared for the different groups. Numbers of cells are shown in parentheses and *p*-values from one-way analysis of variance are indicated.

Figure 2.5

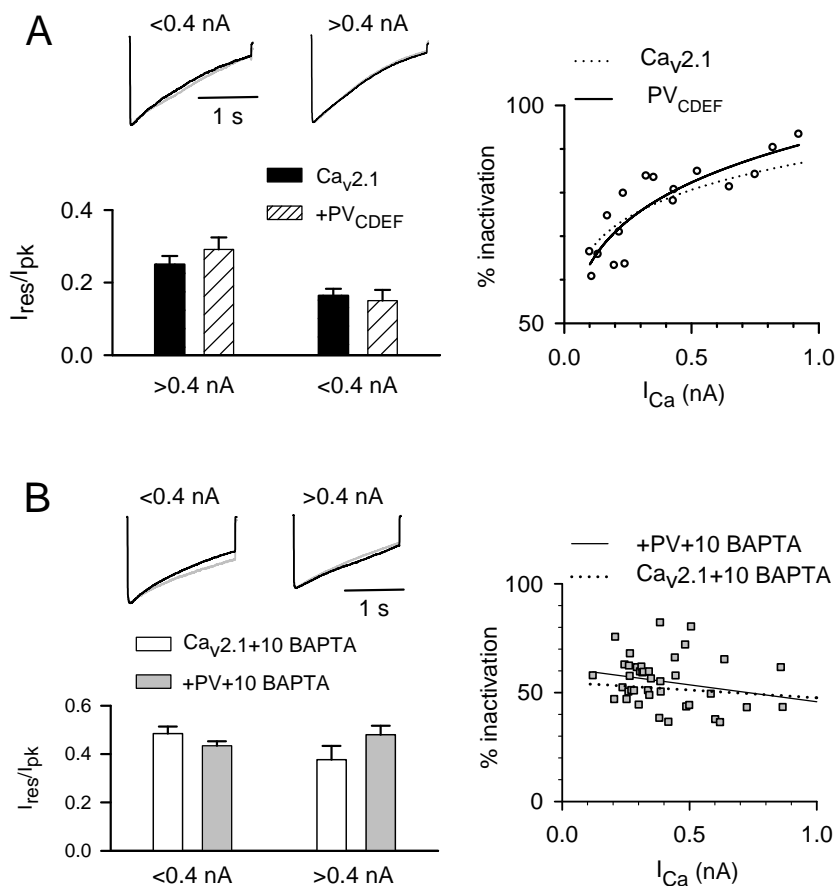


Figure 2.5. Effects of PV require Ca^{2+} -binding to PV and are specific for CDI. *A,B, left panels*, I_{res}/I_{pk} was determined as in Fig. 2.1 for I_{Ca} less than or greater than 0.4 nA. Traces above show normalized I_{Ca} in cells transfected alone (black), cotransfected with PV_{CDEF} (hatched, *A*), or cotransfected with PV (grey, *B*). *Right*, relationship between % inactivation and I_{Ca} amplitude for cells transfected with $Ca_v2.1+PV_{CDEF}$ (circles, *A*) or $Ca_v2.1+PV$ (squares, *B*). Dotted line represents data replotted from Fig. 2.1C. Smooth line shows fit from nonlinear (*A*) and linear (*B*) regression.

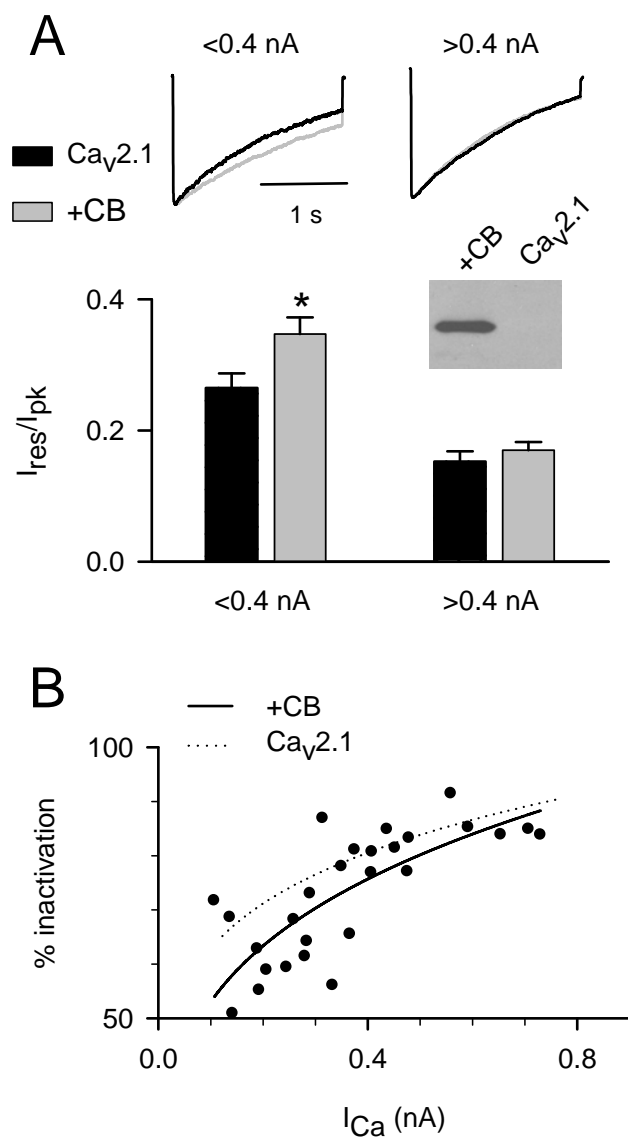
Figure 2.6

Figure 2.6. CB inhibits inactivation of small-amplitude I_{Ca} . *A*, I_{res}/I_{pk} was determined as in Fig. 2.1 for cells transfected with $Ca_v2.1$ alone (black bars) or cotransfected with CB (grey bars). Current traces show I_{Ca} from cells cotransfected with CB (grey traces) normalized to I_{Ca} from cells transfected with $Ca_v2.1$ alone (black traces) for $I_{Ca} < \text{or} > 0.4$ nA. *, $p < 0.05$. *Inset*, Western blot shows expression of CB in cells cotransfected with CB and $Ca_v2.1$ but not in cells transfected with $Ca_v2.1$ alone. *B*, Current-dependence of I_{Ca}

inactivation. Individual data points were plotted and fit (smooth line) as in Fig. 2.3B.

Curve-fit of data from cells transfected with $Ca_v2.1$ alone was replotted from Fig. 2.1C (dotted line).

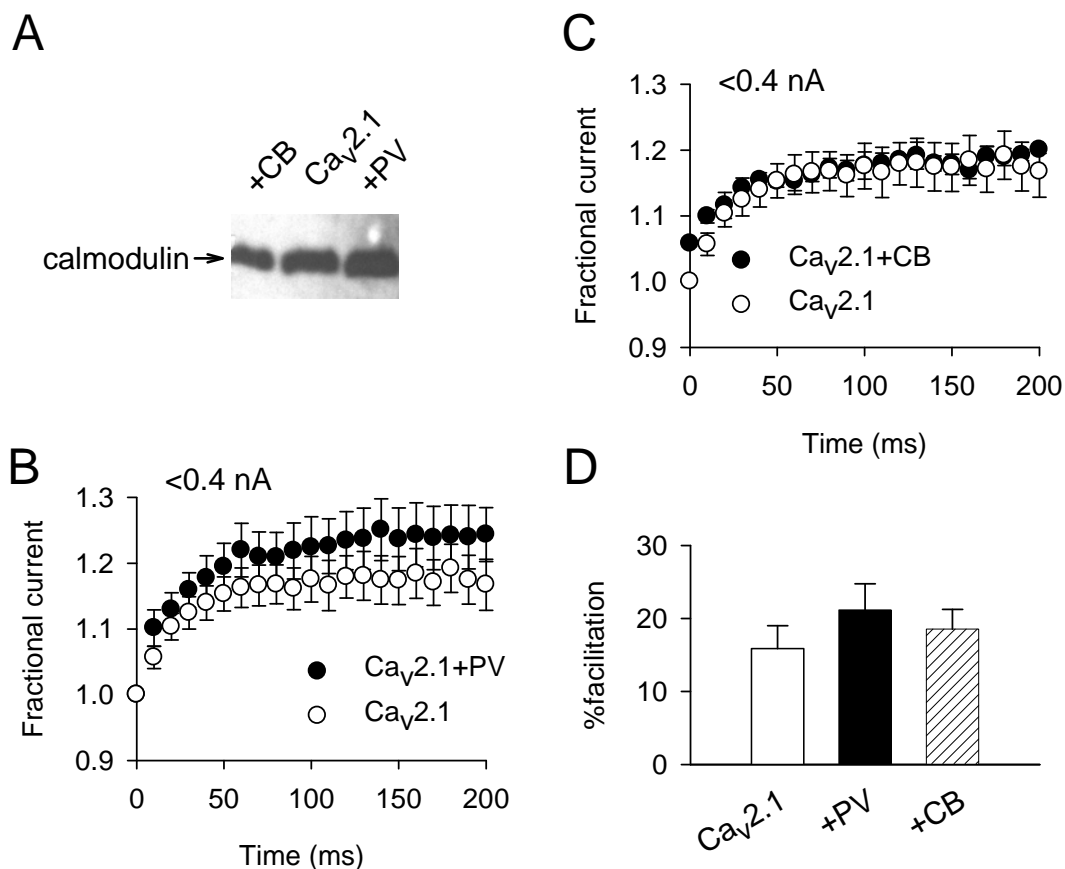
Figure 2.7

Figure 2.7. PV and CB do not influence levels of calmodulin or Ca²⁺-dependent facilitation of Ca_v2.1. *A*, Western blot probed with calmodulin antibody shows that calmodulin is expressed equally well in cells transfected with Ca_v2.1 alone or cotransfected with PV or CB. *B*, Repetitive voltage pulses were applied to cells transfected with Ca_v2.1 alone (○) or cotransfected with PV (●) as in Fig. 2.2B. Results are shown for the first 200 ms in cells with $I_{Ca} < 0.4\text{ nA}$. *C*, Same as in *B*, except cells were transfected with Ca_v2.1 alone (○) or cotransfected with CB (●). *D*, The % facilitation for cells transfected with Ca_v2.1 alone (white bar) or cotransfected with PV

(black bar) or CB (hatched bar) was determined as: average fractional current for the first 200 ms*100.

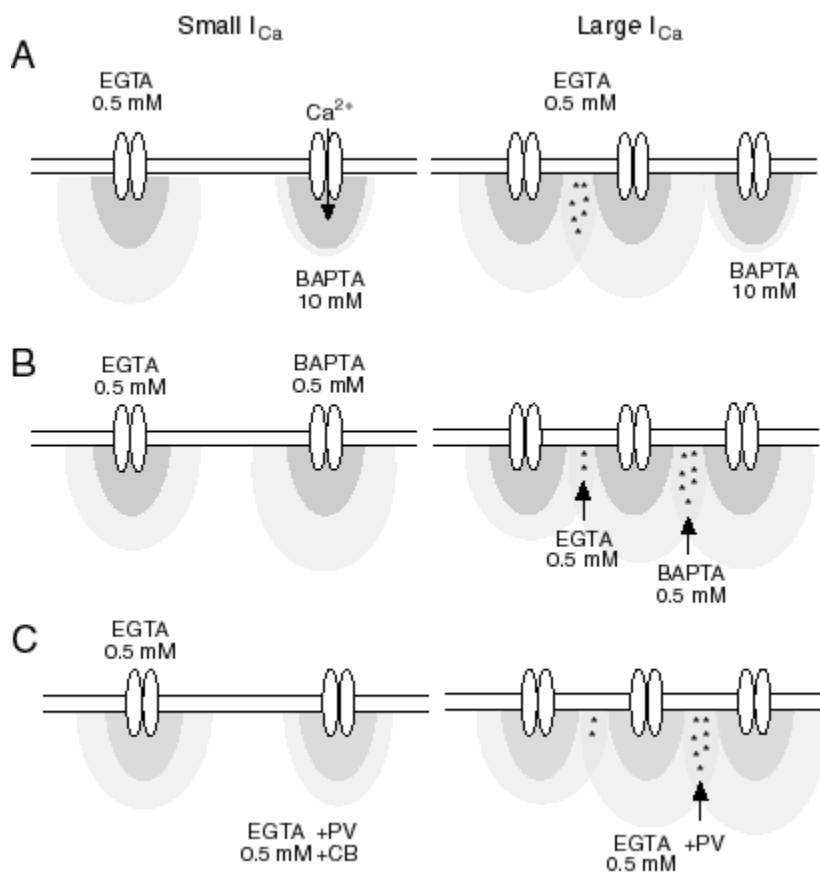
Figure 2.8

Figure 2.8. Model for differential regulation of CDI by Ca^{2+} buffers. Ca^{2+} microdomains associated with individual $\text{Ca}_v2.1$ channels are considered as a rapidly accumulating BAPTA-insensitive compartment near the pore (dark grey), which diffuses into a more slowly filling pool away from the pore (light grey), which supports CDI and can be buffered Ca^{2+} chelators. *A*, Large I_{Ca} (right) shows more CDI than small I_{Ca} (left) due to overlap of Ca^{2+} microdomains (asterisks). High BAPTA (10 mM) suppresses Ca^{2+} and CDI for small and large I_{Ca} . *B*, Limiting concentrations (0.5 mM) of BAPTA cause more CDI due to less efficient Ca^{2+} buffering than EGTA for small and large I_{Ca} . *C*, PV and

CB inhibit Ca^{2+} microdomains when channel density is low (left), but Ca^{2+} unbinding from PV may increase Ca^{2+} supporting CDI when channel density is high (right).

Chapter 3: Caffeine increases Ca^{2+} -dependent inactivation of $\text{Ca}_v2.1$ (P/Q-type) Ca^{2+} channels

Abstract

$\text{Ca}_v2.1$ (P/Q-type) Ca^{2+} channels are major routes of Ca^{2+} entry and undergo Ca^{2+} -dependent inactivation (CDI) mediated by the Ca^{2+} -binding protein calmodulin (CaM). We have shown previously that CDI of $\text{Ca}_v2.1$ is modulated by Ca^{2+} buffers, which supports the hypothesis that CDI depends on global, rather local, elevations in Ca^{2+} relative to individual $\text{Ca}_v2.1$ channels. Because the cytoplasmic Ca^{2+} concentration is also affected by Ca^{2+} release from intracellular stores, we tested if caffeine, which stimulates intracellular Ca^{2+} release, would enhance CDI of $\text{Ca}_v2.1$. In whole-cell patch clamp recordings of HEK 293T cells transfected with cDNAs encoding $\text{Ca}_v2.1$ subunits (rbA , β_{2A} , $\alpha_2\delta$), extracellular caffeine (1 mM) with minimal intracellular Ca^{2+} buffering (0.5 mM EGTA) significantly increased inactivation of $\text{Ca}_v2.1$ Ca^{2+} currents (I_{Ca} , >50%, $p < 0.01$, $n=6$). Caffeine did not affect I_{Ca} inactivation when EGTA was increased (10 mM), indicating the importance of cytosolic Ca^{2+} for this effect of caffeine. Addition of the ryanodine receptor antagonist ruthenium red (100 μM) and/or the IP_3 receptor antagonist heparin (5 mg/ml) to the recording pipette also abolished the effect of caffeine on I_{Ca} inactivation. These results suggest that Ca^{2+} release from intracellular stores may limit Ca^{2+} influx into some excitable cells by augmenting CDI of $\text{Ca}_v2.1$.

Introduction

Transient increases in the cytoplasmic concentration of Ca^{2+} regulate neurotransmitter secretion, neuronal excitability, gene transcription, and other metabolic

functions. In most cells, Ca^{2+} entry into the cytoplasm comes mainly from two sources: voltage-gated Ca^{2+} channels in the plasma membrane, and Ca^{2+} release channels in the endoplasmic reticulum (ER). Ca^{2+} -induced Ca^{2+} release (CICR), originally demonstrated in muscle cells, occurs when Ca^{2+} entering through voltage-gated Ca^{2+} channels binds to inositol 1,4,5-trisphosphate receptors (IP_3 Rs) and ryanodine receptors (RyRs) in the ER membrane (Fabiato and Fabiato, 1975). Binding of Ca^{2+} supports opening of these Ca^{2+} permeable channels in a concentration-dependent manner, thus boosting the release of Ca^{2+} into the cytoplasm. In neurons, membrane depolarization can activate CICR (Llano et al., 1994; Peng, 1996; Narita et al., 1998), which can amplify Ca^{2+} signals leading to exocytosis at presynaptic terminals (Narita et al., 2000) and the induction of long-term depression (LTD) (Kohda et al., 1995).

Ca^{2+} ions can also initiate feedback regulation of voltage-gated (Ca_v) Ca^{2+} channels in the plasma membrane. This process is mediated by calmodulin (CaM) binding directly to the $\alpha_1 2.1$ subunit. For $\text{Ca}_v 2.1$ channels that mediate P/Q-type currents, Ca^{2+} -induced conformational change in the associated CaM causes an initial increase (Ca^{2+} -dependent facilitation (CDF)), followed by decrease (Ca^{2+} -dependent inactivation (CDI)) of Ca^{2+} current (I_{Ca}) (Lee et al., 1999; DeMaria et al., 2001). CDI of $\text{Ca}_v 2.1$ can be blocked by high intracellular concentrations of Ca^{2+} buffers such as EGTA and BAPTA (Lee et al., 2000; Kreiner and Lee, 2006), which are too slow to blunt rapid local increases in Ca^{2+} near the pore of individual channels. This result suggests that CDI is mediated by global Ca^{2+} supported by Ca^{2+} microdomains from multiple channels. Since these Ca^{2+} microdomains may also be influenced by IP_3 Rs and RYRs, Ca^{2+} influx through $\text{Ca}_v 2.1$ channels could promote CICR that then enhances CDI. To test this

hypothesis, we analyzed the effects of ryanodine and/or IP₃ receptor antagonists on Ca_v2.1 currents in transfected HEK 293T cells. Our findings suggest that CICR may contribute to the negative regulation of Ca_v2.1 by Ca²⁺, and may therefore provide additional levels of Ca²⁺ signaling regulation in neurons.

Materials and Methods

cDNAs. Ca_v2.1 subunits used in electrophysiological experiments were α₁2.1 (rbA isoform), β_{2a} and α₂δ (Starr et al., 1991; Perez-Reyes et al., 1992; Stea et al. 1994).

Cell culture and transfection. HEK 293T cells were maintained in Dulbecco's Modified Eagle's Medium supplemented with 10% fetal bovine serum at 37°C under 5% CO₂. Cells plated in 35 mm tissue culture dishes were grown to 65-80% confluency and transfected with GenePORTER transfection reagent (Gene Therapy Systems, Inc., San Diego, CA) according to the manufacturer's protocol with a 1:1 molar ratio of cDNAs for Ca²⁺ channel subunits (total 5 μg) and 0.7 μg of a CD8 expression plasmid for identification of transfected cells.

Electrophysiological recordings. At least 48 h after transfection, HEK 293T cells were incubated with CD8 antibody-coated microspheres (Dynal, Oslo, Norway) for identification of transfected cells. Ca²⁺ or Ba²⁺ currents were recorded in whole-cell patch-clamp recordings with a HEKA EPC-9 patch-clamp amplifier driven by PULSE software (HEKA Electronics, Lambrecht/Pfalz, Germany). Leak and capacitive transients were subtracted using a P/-4 protocol. Extracellular recording solutions contained (in

mM): 150 Tris, 1 MgCl₂, and 10 CaCl₂ or 10 BaCl₂. Intracellular recording solutions contained (in mM): 130 N-methyl-D-glucamine, 60 HEPES, 1 MgCl₂, 2 Mg-ATP, and EGTA (0.5 or 10 mM). The pH of extracellular and intracellular recording solutions was adjusted to 7.3 with methanesulfonic acid.

Drugs. Ca²⁺ release agonists, caffeine (1, 5, or 10 mM, Sigma) or IBMX (100 mM), were included in the extracellular solution as indicated. Ca²⁺ release antagonists, ruthenium red (100 mM) and/or heparin (5mg/ml), were included in the intracellular recording solution. All pharmacological agents were obtained from Sigma-Aldrich (St. Louis, MO).

Data analysis. All data were analyzed using custom written procedures in IGOR Pro software (Wavemetrics, Portland, OR). Averaged data represent the mean±SEM. Statistical differences in averaged inactivation (I_{res}/I_{pk}) was determined by paired t-test unless otherwise noted. *I-V* curves were fit with the function: $g(V - E)/\{1 + \exp[(V - V_{1/2})/k] + b\}$ where *g* is the maximum conductance, *V* is the test potential, *E* is the apparent reversal potential, *V*_{1/2} is the potential of half activation, *k* is the slope factor, and *b* is the baseline. Regression and statistical analyses were done with Sigma Plot (SPSS, Inc., Chicago, IL). Significant deviations of percent inactivation data from linearity were determined by Runs test. Data describing current-dependence of I_{Ca} inactivation were fit with a nonlinear regression equation, $y=ax^b$ where *y* is % inactivation, *x* is the current amplitude, and *a* and *b* are constants. F-tests were used for comparisons of nonlinear regression curves, with statistical significance considered as $p<0.05$.

Results

Caffeine modulates CDI of Cav2.1. To determine if Ca^{2+} release from intracellular stores influenced CDI of $\text{Ca}_v2.1$, we tested the effects of caffeine, which is a ryanodine receptor agonist. CDI was measured as the amplitude of I_{Ca} at the end of a 2 s voltage pulse normalized to the peak current amplitude ($I_{\text{res}}/I_{\text{peak}}$). With relatively low concentrations of EGTA in the intracellular recording solution (0.5 mM), caffeine caused significant increases in CDI at all concentrations ($p < 0.05$, Fig.3.1A). However, the effect of caffeine was not dose-dependent ($p = 0.12$, single factor ANOVA on difference in $I_{\text{res}}/I_{\text{peak}}$ before and after the addition of caffeine, Fig.3.1A). Exponential fits of current traces showed that caffeine significantly accelerated the rate of inactivation ($\tau_{\text{fast}} = 0.87 \pm 0.11$ and 0.50 ± 0.09 , $\tau_{\text{slow}} = 1.23 \pm 0.15$ and 0.57 ± 0.07 , before and after caffeine, respectively, $p < 0.05$). However, when EGTA in the intracellular recording solution was raised to 10 mM, this effect of caffeine on CDI was prevented ($p = 0.20$, Fig.3.1A). This suggests that caffeine stimulation of CDI requires elevations in intracellular Ca^{2+} due to Ca^{2+} influx and/or release from intracellular stores.

Increased CDI in response to caffeine was readily apparent during repetitive depolarizations (Figs. 3.1B and 3.1C). Fractional current was defined as the amplitude of test currents normalized to the amplitude of the first current in a train. As we have shown previously (Kreiner and Lee, 2006), CDI was greater in cells exhibiting larger (> 0.4 nA) currents. CDI for repetitive pulses was calculated as the average fractional current of the last 5 pulses normalized to the peak fractional current in the train. Caffeine significantly increased CDI for large (> 0.4 nA), but not small (< 0.4 nA) I_{Ca} (7% increase in

inactivation after caffeine application for $I_{Ca} < 0.4$ nA, $p = 0.16$; and 17% increase in inactivation after caffeine application for $I_{Ca} > 0.4$ nA, $p < 0.05$).

Since CDI increases with the amplitude of I_{Ca} , the effect of caffeine could be due to nonspecific enhancement of I_{Ca} amplitude or voltage-dependent activation. Therefore, we characterized the current-voltage (I - V) relationship before and after caffeine. For test pulses of -50 to +90 mV, caffeine (10 mM) significantly increased I_{Ca} amplitude ($p < 0.05$, Fig. 3.1C). In addition, caffeine caused $Ca_v2.1$ channels to activate at more negative voltages ($V_{1/2} = +6.0$ mV, control and +2.6 mV, for +10 mM caffeine; $p < 0.05$, Fig. 3.1D). The relationship between I_{Ca} amplitude and CDI was shown by plotting the % inactivation ($((1 - I_{res}/I_{peak}) * 100)$) against the peak current amplitude (Fig. 3.1E). Consistent with our previous results (Fig. 2.1C, top), inactivation increased nonlinearly with I_{Ca} amplitude. If caffeine caused a nonspecific increase in I_{Ca} amplitude, we would not expect a change in the relationship between I_{Ca} amplitude and CDI, but rather a shift in the distribution of I_{Ca} amplitudes to higher values compared to in the absence of caffeine. However, caffeine caused a significant upward translation and more shallow dependence of inactivation on I_{Ca} amplitude ($p < 0.05$, F-test, Fig. 3.1E, gray line). Inactivation was generally as great for small currents as for large currents with caffeine, suggesting that the effect of caffeine is not solely due to an increase in I_{Ca} amplitude. These observations suggest complex effects of caffeine in increasing voltage-dependent activation of $Ca_v2.1$ and inhibiting the current dependence of CDI.

To determine if caffeine modulates CDF, we measured the fractional current (described above) during the first 200 ms of repetitive voltage steps for the application of 5 mM caffeine with increased intracellular EGTA (10 mM) (Fig. 3.2A). Since 10 mM

EGTA strongly depresses CDI of $\text{Ca}_v2.1$ (Lee et al., 2000), this approach should allow isolation of CDF in the absence of CDI. The amount of facilitation was determined during 200 ms of repetitive depolarizations as: $(\text{average fractional current} - 1) * 100$. Under these conditions, caffeine (5 mM) did not produce a significant change in CDF ($p = 0.75$, Fig.3.2B). These results suggest that caffeine does not influence the local Ca^{2+} levels that support CDF of $\text{Ca}_v2.1$.

Blockers of Ca^{2+} release channels prevent caffeine-induced enhancement of CDI.

To test if the actions of caffeine on CDI were due to actions on Ca^{2+} release channels, we included IP_3 and ryanodine receptor antagonists, heparin (5 mg/ml) and ruthenium red (100 μM), respectively, in the recording pipette solution. Under these conditions, CDI was not significantly increased by caffeine (Fig.3.3; $p = 0.52$). Including heparin and ruthenium red in the recording pipette did not influence CDI independent of caffeine ($p=0.62$, two sample t-test, Fig 3.3). To determine if the caffeine-induced increase in CDI was mediated by IP_3Rs or RyRs , we used the same experimental protocol with either heparin (5 mg/ml) or ruthenium red (100 μM) in the recording pipette. Unexpectedly, both heparin and ruthenium red alone prevented the actions of caffeine (Fig. 3.3). These results suggest that the effects of caffeine may result from Ca^{2+} release from either IP_3Rs or RyRs .

To confirm that heparin and ruthenium red did not affect voltage-dependent activation of $\text{Ca}_v2.1$, $I-V$ curves were generated before and after the application of caffeine (1 mM) (Fig. 3.4). In contrast to the results obtained with 10 mM caffeine (Fig. 3.1D), the lower dose of caffeine did not significantly increase current amplitude or change the voltage dependence of $\text{Ca}_v2.1$ activation ($p>0.05$; Fig.3.4). Heparin and/or

ruthenium red did not affect the parameters of the *I-V* curve either in the presence or absence of caffeine (Fig. 3.4B-D). These results suggest that effects of heparin and ruthenium red on blocking caffeine-mediated enhancement of CDI do not involve changes in voltage-dependent activation.

IBMX enhances CDI. In addition to its actions on ryanodine receptors, caffeine is also a potent inhibitor of phosphodiesterases involved in the breakdown of cAMP. If the effects of caffeine on $\text{Ca}_v2.1$ were due to alterations in cAMP levels rather than on Ca^{2+} release, they should be reproduced by other phosphodiesterase inhibitors. To test this, we compared I_{Ca} inactivation in the presence and absence of 3-isobutyl-1-methylxanthine (IBMX), a phosphodiesterase inhibitor. Unexpectedly, IBMX significantly increased CDI ($p < 0.05$, paired t-test, Fig 3.5A). *I-V* curves did not indicate any significant shift in half maximal activation, peak amplitude, or peak location caused by the addition of IBMX (Fig. 3.5B). In addition, repetitive voltage pulse protocols demonstrated that maximum fractional I_{Ca} was not significantly decreased after the addition of 100 μM IBMX ($p = 0.29$, Fig. 3.5C), indicating IBMX causes no change in facilitation. These results suggest caffeine-induced enhancement of CDI may be partially mediated through phosphodiesterase inhibition.

Discussion

Mechanisms of action of caffeine. Our results show that caffeine enhances CDI but not CDF of $\text{Ca}_v2.1$ in transfected HEK 293T cells. The possibility that this effect of caffeine is mediated in part by Ca^{2+} release pathways is supported by the blockade of caffeine's effects by heparin and ruthenium red. However, the ability of IBMX to

partially mimic the effects of caffeine on CDI suggests a potential role for phosphodiesterase inhibition in the underlying mechanism by which caffeine modulates $Ca_v2.1$.

The block of caffeine's effects by either heparin or ruthenium red (Fig. 3.3) was unexpected since caffeine activates RYRs but not IP_3Rs . However, a previous study showed that caffeine could deplete IP_3R -sensitive Ca^{2+} stores, leading to capacitative Ca^{2+} entry in HEK 293 cells (Luo et al., 2005). This same study showed that caffeine could also activate Ca^{2+} release from RYRs and that RYRs are detectable by immunocytochemistry in HEK 293 cells. These results were specific to early passage HEK 293 cells, which is relevant for our studies since we do not use these cells for more than 10-13 passages due to reductions in transfection efficiency with greater passage numbers. By activating RYRs, caffeine could raise Ca^{2+} levels which positively regulate IP_3Rs under basal levels of IP_3 . This would explain the efficiency of heparin in blocking the effects of caffeine. Further studies using IP_3R agonists would help address this possibility.

Caffeine and IBMX have the effects of raising cAMP levels due to their actions as phosphodiesterase inhibitors. Increased cAMP could activate cAMP-dependent protein kinase (PKA) which is known to phosphorylate $\alpha_12.1$ (Sakurai et al., 1995). While direct facilitation of $Ca_v2.1$ by PKA has not been demonstrated, PKA activators can prevent ethanol-induced inhibition of $Ca_v2.1$ (Solem et al., 1997). In addition G-protein coupled receptor-dependent increases in cAMP can cause facilitation of neurotransmitter release through activation of presynaptic $Ca_v2.1$ channels (Arias-Montano et al., 2007). PKA positively regulates ryanodine receptors (Reiken et al., 2003) and type I IP_3 receptors

(Nakade et al., 1994), which could increase Ca^{2+} levels that support CDI of $\text{Ca}_v2.1$.

Studies using forskolin and other activators of cAMP-dependent pathways are required to test the involvement of PKA in CDI. A schematic representation of the possible targets of caffeine in the regulation of CDI is presented in Fig. 3.6.

Future directions. A major assumption in our studies is that caffeine is promoting Ca^{2+} release by RYRs. This mechanism is supported by previous studies (Sitsapesan and Williams, 1990; Kano et al., 1995; Hernández Cruz et al., 1995; Kong et al., 2008). However, future efforts can use the ratiometric Ca^{2+} indicator, fura-2, to quantify the change in Ca^{2+} concentration in response to addition of caffeine. The ability of heparin and ruthenium red to suppress Ca^{2+} signals caused by caffeine would confirm that caffeine caused Ca^{2+} release via activation of RYRs and IP_3Rs . Inhibitors of PKA such as H-89 or cAMP agonists, such as 8-bromo-cyclic AMP could be used to determine if caffeine acted via the cAMP pathway to promote Ca^{2+} release that then increased in CDI.

Functional implications of the effects of caffeine on $\text{Ca}_v2.1$. The effects of caffeine on CDI were significant but rather small in magnitude, raising the question as to whether it would be significant enough to impact neuronal $\text{Ca}_v2.1$ function. It is possible that the effect of caffeine may underestimate the modulation of $\text{Ca}_v2.1$ by intracellular Ca^{2+} in neurons due to difference in the subcellular morphology of neurons and HEK 293T cells. For example, in Purkinje neurons the ER is close enough to the plasma membrane to produce overlapping Ca^{2+} microdomains between Ca^{2+} influx and Ca^{2+} release pathways (Martone et al., 1993). This could significantly amplify the contribution of RyR- or IP_3R -mediated Ca^{2+} release to Ca^{2+} -dependent regulation of plasma membrane $\text{Ca}_v2.1$ channels. Our results suggest that Ca^{2+} release from intracellular stores

may terminate $\text{Ca}_v2.1$ -mediated Ca^{2+} entry by increasing CDI. Enhanced CDI of $\text{Ca}_v2.1$ could have a number of neurophysiological consequences. Due to the importance of $\text{Ca}_v2.1$ in presynaptic neurotransmitter release, increased CDI could cause synaptic depression as has been reported at some synapses (Uchitel et al., 1992; Mintz et al., 1995). In addition, enhanced CDI of $\text{Ca}_v2.1$ may curtail activation of Ca^{2+} -activated (K_{Ca}) K^+ channels, which is tightly coupled to $\text{Ca}_v2.1$ Ca^{2+} influx in cerebellar Purkinje neurons (Womack et al., 2004). K_{Ca} channels mediate the afterhyperpolarization that regulates spontaneous firing (pacemaking) in Purkinje neurons (Edgerton and Reinhart, 2003). Decreased K_{Ca} channel activity could result in a reduced afterhyperpolarization and lead to faster firing (Sah and McLachlan, 1992). Due to the widespread distribution of $\text{Ca}_v2.1$ channels in the nervous system (Llinas et al., 1992; Craig et al., 1998), the interplay between Ca^{2+} release and CDI of $\text{Ca}_v2.1$ may play a fundamental role in regulating synaptic transmission and neuronal excitability.

Figure 3.1

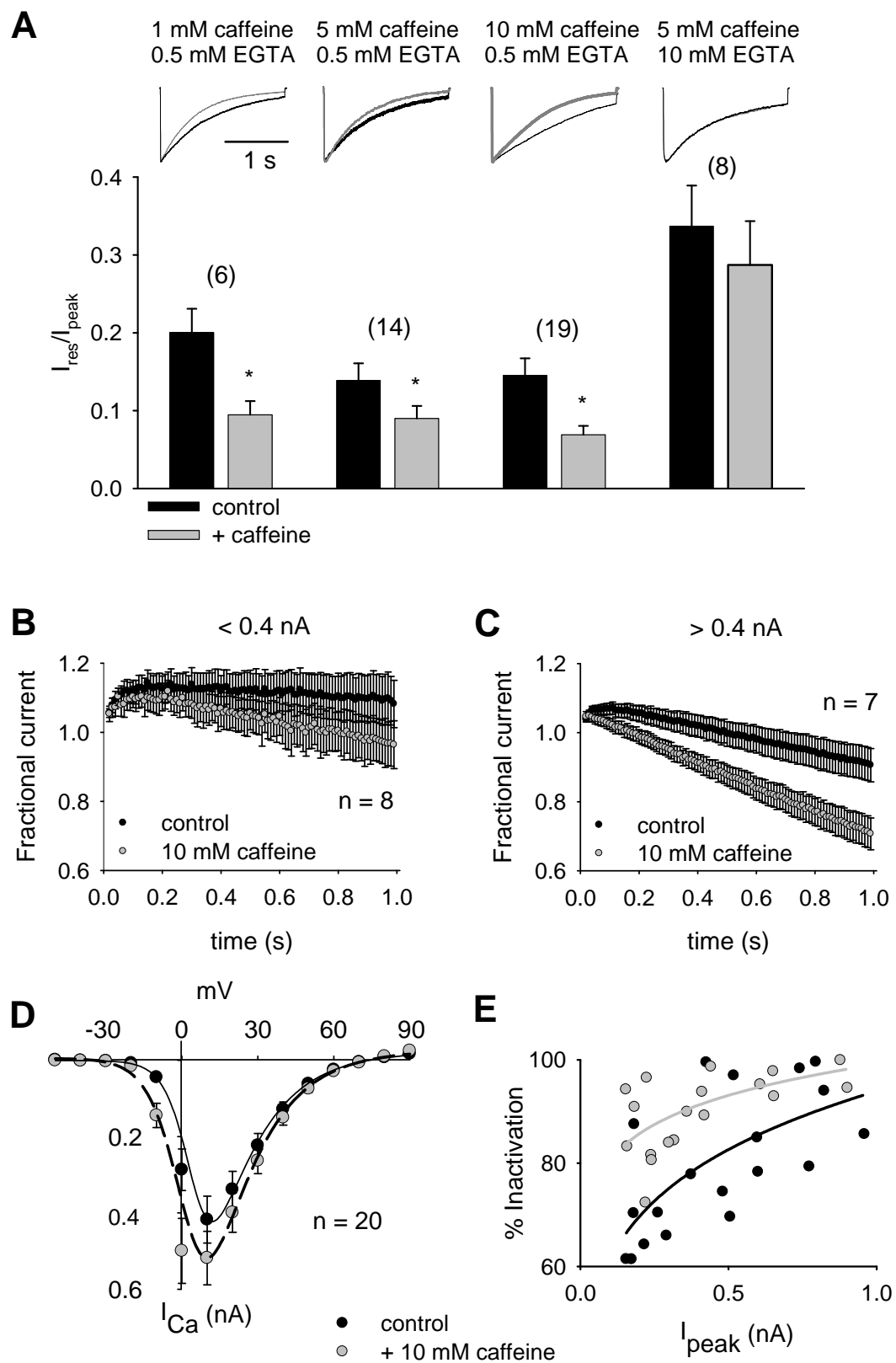


Figure 3.1 Caffeine enhances CDI. A. I_{Ca} was evoked by 2-s pulses from -80 to +10 mV. I_{res}/I_{peak} is residual current amplitude normalized to the peak current amplitude. Bars represent mean \pm SEM; parentheses indicate numbers of cells. Current traces represent normalized I_{Ca} before (black) and after (gray) bath application of caffeine. Extracellular solution: 10 mM Ca^{2+} . Intracellular solution 0.5 or 10 mM EGTA, as indicated. B, C. Currents were evoked with 5 ms depolarizations (-80 to +10 mV) at a frequency of 100 Hz. Fractional current is test current amplitude normalized to that for the first pulse in the train and plotted against time for I_{Ca} for currents less than (B) or greater than (C) 0.4 nA. D. I - V curves for $Ca_v2.1$ before (black symbols) or after application of 10 mM caffeine (gray symbols). E. For data in A, % inactivation $\{(1-I_{res}/I_{peak})*100\}$ is plotted against peak current amplitude for I_{Ca} . Lines represent fits from nonlinear regression for values obtained before (black) and after (gray) bath application of 10 mM caffeine.

Figure 3.2

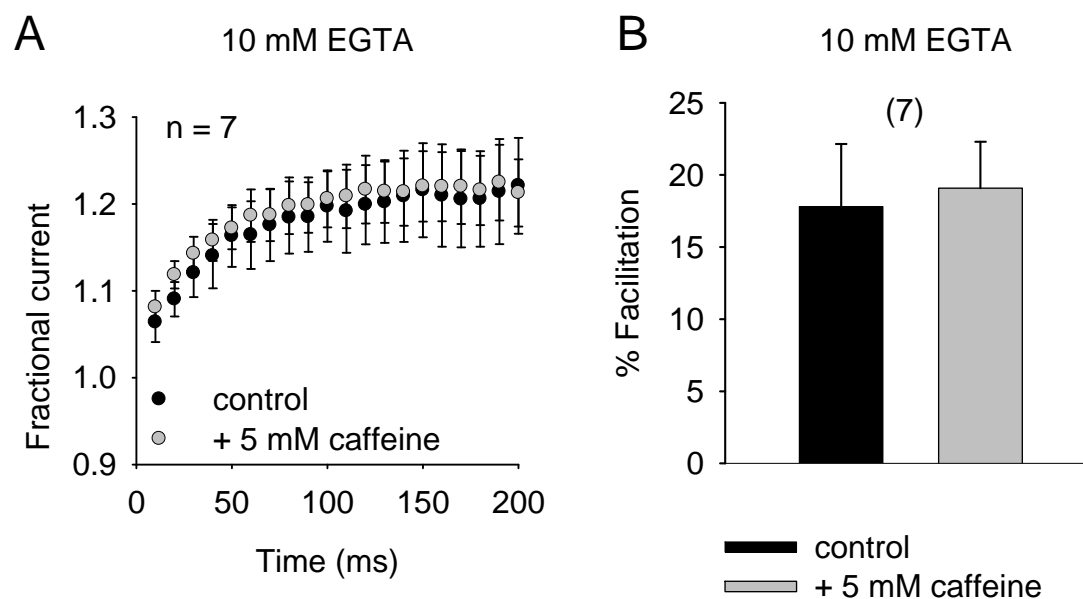
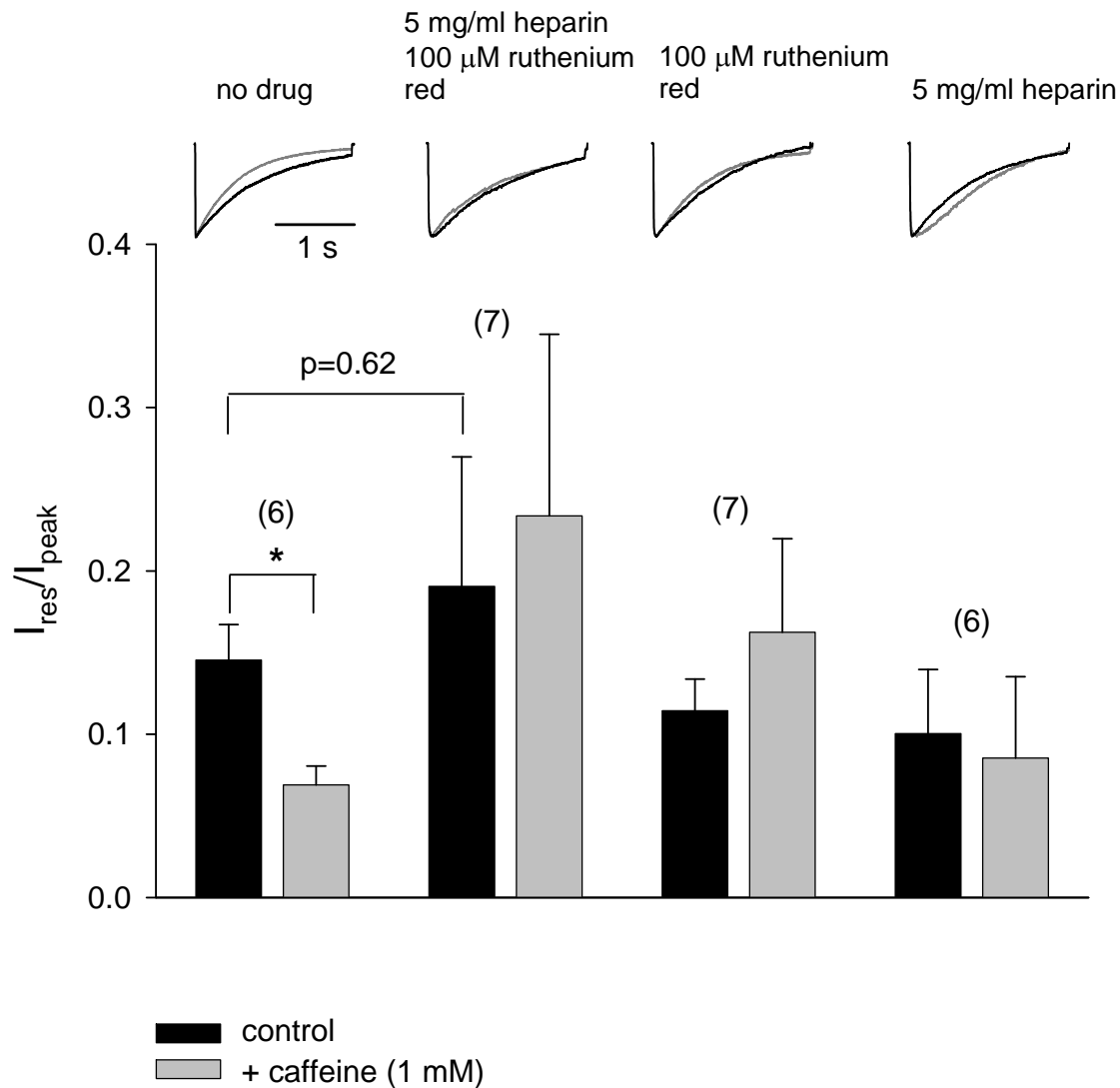


Figure 3.2 Effects of caffeine on CDF. A. I_{Ca} was evoked with 100 Hz voltage pulse protocol before (black symbols) or after (gray symbols) addition of caffeine (5 mM). Symbols represent mean \pm SEM. Intracellular solution contained 10 mM EGTA. B The % facilitation for cells before (black bars) or after (gray bars) application of caffeine was determined as: (average fractional current for the first 200 ms - 1)*100. Bars represent mean \pm SEM; parentheses indicate numbers of cells.

Figure 3.3**Figure 3.3** Blocking intracellular Ca²⁺ release blocks the effect of caffeine on CDI.

I_{res}/I_{peak} was measured for Ca_v2.1 transfected cells without or with 5 mg/ml heparin and/or 100 μ M ruthenium red in the intracellular solution. Measurements were performed before (black bars) or after (gray bars) the addition of 1 mM caffeine. Bars represent mean \pm SEM; parentheses indicate numbers of cells. Traces represent I_{Ca} before (black) or after (gray) application of 1 mM caffeine.

Figure 3.4

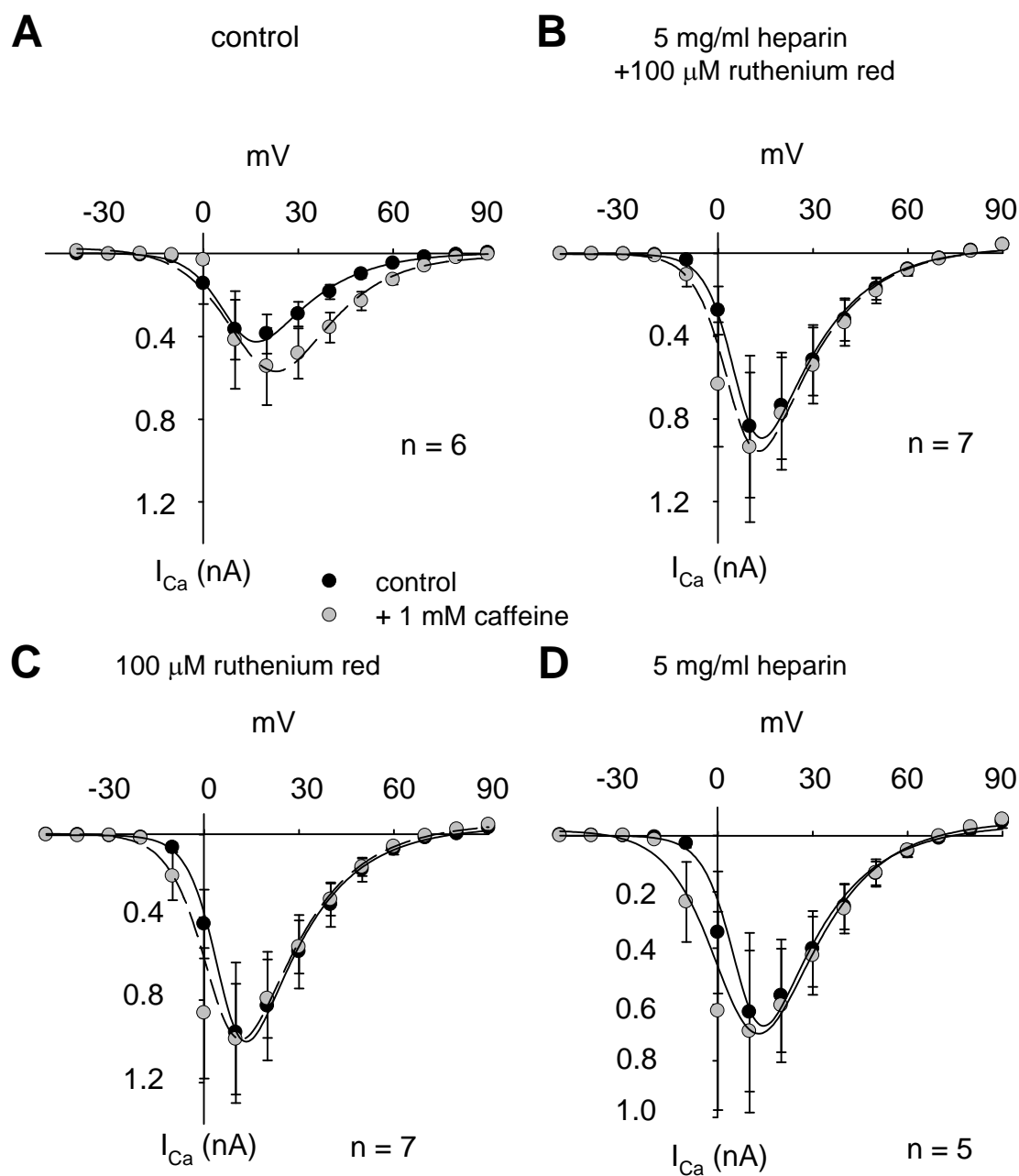


Figure 3.4 *I-V* curves in the presence and absence of intracellular Ca^{2+} antagonists. A. *I-V* curve for $Ca_v2.1$ before (black symbols) or after application of 1 mM caffeine (gray symbols) for (A) control condition or (B) with 5mg/ml heparin and 100 μ M ruthenium red or (C) 5mg/ml heparin only or (D) 100 μ M ruthenium red only.

Figure 3.5

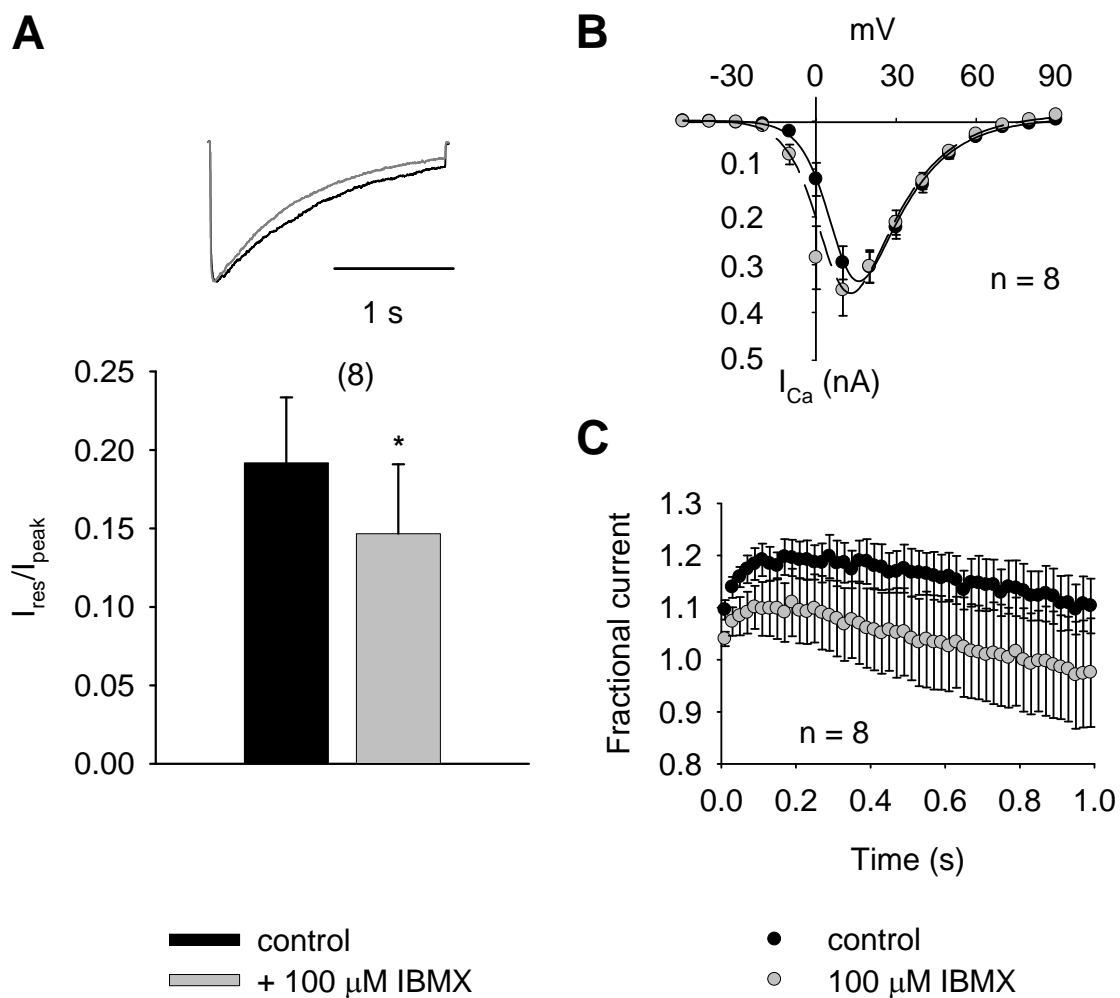


Figure 3.5 IBMX mimics the effect of caffeine on CDI. A. I_{res}/I_{peak} and representative traces for cells before (black) or after (gray) bath application of 100 mM IBMX. B. $I-V$ curves for $Ca_v2.1$ before (black symbols) or after application of 100 mM IBMX (gray symbols). C. I_{Ca} was evoked with 100 Hz voltage pulse protocol before (black symbols) or after (gray symbols) addition of 100 mM IBMX.

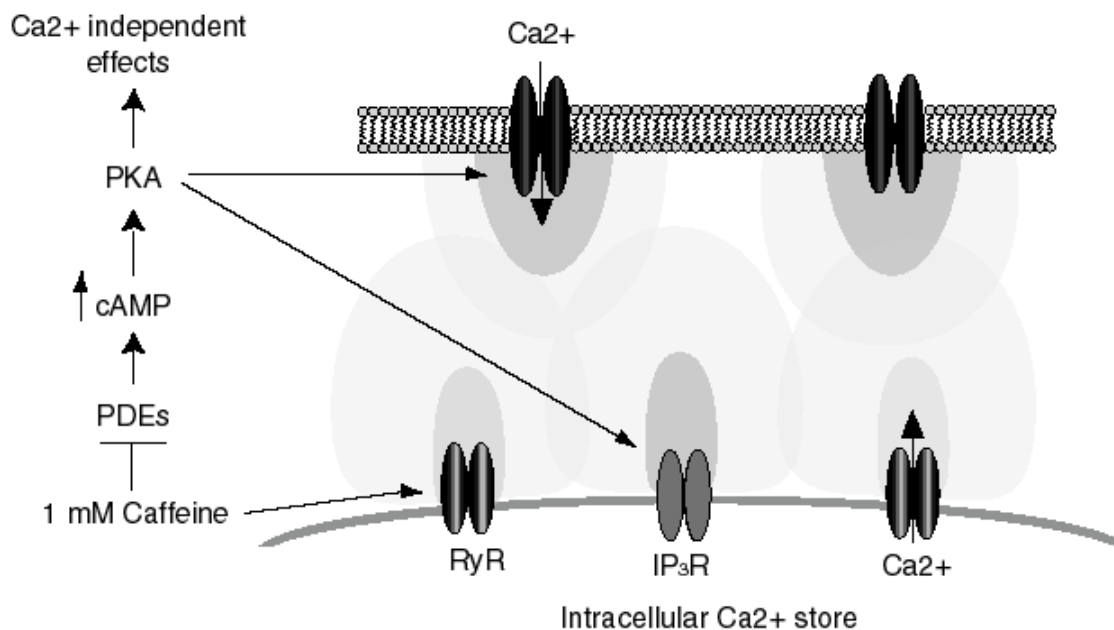
Figure 3.6

Figure 3.6 Schematic representation of the effect of caffeine on pathways that could lead to increased CDI. Gray areas represent Ca²⁺ microdomains that form around the pores of voltage-gated and Ca²⁺ release channels. Mechanisms that cause caffeine influx into the cytoplasm where the plasma membrane and ER are closely associated will cause overlap of these microdomains leading to increased global Ca²⁺ concentration and increased CDI. Other possible targets of caffeine are also included. Arrows indicate activation of a pathway, perpendicular lines indicate inhibition.

Chapter 4: Altered Ca²⁺-feedback to Ca_v2.1 Ca²⁺ channels in Purkinje neurons lacking parvalbumin and calbindin

Abstract

Ca_v2.1 (P/Q-type) Ca²⁺ channels regulate Ca²⁺ signaling and spontaneous firing in cerebellar Purkinje neurons. These channels undergo a dual feedback regulation by incoming Ca²⁺ ions, Ca²⁺-dependent facilitation and inactivation, which is mediated by calmodulin binding to the Ca_v2.1 α₁-subunit. We showed previously that the Ca²⁺ binding proteins parvalbumin (PV) and calbindin D-28k (CB), which are highly expressed in Purkinje neurons, significantly impact Ca²⁺-dependent inactivation, but not facilitation, of Ca_v2.1 in transfected HEK 293T cells. PV and CB may buffer global Ca²⁺ levels that support Ca²⁺-dependent inactivation, but not local Ca²⁺ signals that cause facilitation of Ca_v2.1. We tested this hypothesis in whole-cell patch-clamp recordings of acutely dissociated Purkinje neurons from wild-type (WT) mice and those lacking PV and CB (PV^{-/-}/CB^{-/-}). Ca²⁺ and voltage-dependent inactivation of Ca_v2.1 currents was measured using Ca²⁺ and Ba²⁺, respectively, as the permeant ion. Compared to WT neurons, inactivation of Ca²⁺ currents (I_{Ca}), but also Ba²⁺ currents (I_{Ba}), was significantly greater in PV^{-/-}/CB^{-/-} neurons (~34%, p<0.05, for I_{Ca}; ~42%, p<0.05, for I_{Ba}). Moreover, during trains of action potential waveforms, Ca²⁺-dependent facilitation was significantly less pronounced (~49% reduction, p<0.05) in PV^{-/-}/CB^{-/-} than in WT neurons. These unexpected differences in Ca_v2.1 properties could result from alterations in Ca_v2.1 subunit composition, since the auxiliary Ca_vβ_{2a} subunit confers less voltage-dependent inactivation and greater Ca²⁺-dependent facilitation for Ca_v2.1 than other Ca_vβ subunits.

Consistent with this possibility, $\text{Ca}_v\beta_2$ was detected in a smaller percentage of $\text{PV}^{-/-}/\text{CB}^{-/-}$ mice (45%) compared to WT mice (75%) by single-cell RT-PCR. A $\text{Ca}_v2.1 \alpha_1$ splice variant (EF37b) shown previously to be deficient in Ca^{2+} -dependent facilitation, was shown to be downregulated in $\text{PV}^{-/-}/\text{CB}^{-/-}$ Purkinje neurons, indicating the possibility that expression of this variant caused the lack of facilitation in $\text{PV}^{-/-}/\text{CB}^{-/-}$ Purkinje neurons. Increased inactivation of $\text{Ca}_v2.1$ due to downregulation of $\text{Ca}_v\beta_2$ and decreased facilitation due to an alternate mechanism may limit Ca^{2+} influx in the absence of Ca^{2+} buffering proteins in $\text{PV}^{-/-}/\text{CB}^{-/-}$ Purkinje neurons. Our findings highlight the significance of $\text{Ca}_v\beta_2$ as a key determinant for Ca^{2+} -dependent inactivation of $\text{Ca}_v2.1$ in neurons and suggest a mechanism that may contribute to abnormal Purkinje cell firing rate and rhythmicity shown previously in $\text{PV}^{-/-}/\text{CB}^{-/-}$ mice.

Introduction

Purkinje neurons function as the sole output neuron of the cerebellum and are essential for motor coordination and learning (Ito, 1984). Ca^{2+} modulates several key processes in these neurons including dendritic spiking (Llinas and Nicholson, 1971; Llinas and Hess, 1976), membrane excitability (Hounsgaard and Midtgaard, 1988), and long term depression (LTD) at spines (Sakurai, 1990).

$\text{Ca}_v2.1$ (P/Q-type) Ca channels mediate ~90% of the Ca^{2+} current in the Purkinje neuron soma (Regan, 1991; Mintz et al., 1992; McDonough et al., 1997). Modulation of Ca^{2+} influx through $\text{Ca}_v2.1$ is achieved by a direct interaction of Ca^{2+} bound calmodulin (CaM) with the α_1 subunit of the channel (Lee et al., 1999). This interaction causes $\text{Ca}_v2.1$ channels to undergo a dual feedback regulation by Ca^{2+} consisting of an initial

facilitation (CDF) followed by inactivation (CDI) of the Ca^{2+} current (Lee et al., 2000; DeMaria et al., 2001). CDI of $\text{Ca}_v2.1$ is mediated by a Ca^{2+} microdomain influenced by neighboring open channels, while facilitation is due to a Ca^{2+} nanodomain supported by Ca^{2+} influx through individual channels (Lee et al., 2000; DeMaria et al., 2001; Soong et al., 2002; Liang et al., 2003; Dick et al., 2008). We have previously shown that the Ca^{2+} buffering proteins PV and CB modulate CDI of $\text{Ca}_v2.1$ in transfected HEK 293T cells (Kreiner and Lee, 2006). Purkinje neurons express high concentrations (100-200 μM) of PV and CB (Plogmann and Celio, 1993; Kosaka et al., 1993; Fierro and Llano, 1996; Maeda et al., 1999; Bastianelli, 2003), which may modulate Ca^{2+} /CaM mediated regulation of $\text{Ca}_v2.1$.

To test this hypothesis, we compared CDI and other $\text{Ca}_v2.1$ properties in whole-cell patch-clamp recordings of acutely dissociated Purkinje neurons from WT and $\text{PV}^{-/-}/\text{CB}^{-/-}$ mice. Compared to WT neurons, $\text{Ca}_v2.1$ currents in $\text{PV}^{-/-}/\text{CB}^{-/-}$ Purkinje neurons not only showed a significant increase in CDI but also in voltage-dependent inactivation (VDI). This was accompanied by a reduction in the expression of the $\text{Ca}_v\beta_2$ subunit in $\text{PV}^{-/-}/\text{CB}^{-/-}$ Purkinje neurons, which normally confers slow CDI and VDI to $\text{Ca}_v2.1$. Our findings highlight the importance of Ca^{2+} buffering proteins in the regulation of $\text{Ca}_v2.1$ properties, and suggest a compensatory mechanism by which Ca^{2+} homeostasis may be achieved in the absence PV and CB.

Materials and Methods

cDNA expression constructs. Ca_v2.1 subunits used in electrophysiological experiments were $\alpha_{12.1}$ (rbA isoform), β_{2a} , β_4 and $\alpha_2\delta$ (Starr et al., 1991; Perez-Reyes et al., 1992; Castellano et al., 1993).

Cell culture and transfection. HEK 293T cells were maintained in Dulbecco's Modified Eagle's Medium supplemented with 10% fetal bovine serum at 37°C under 5% CO₂. Cells plated in 35 mm tissue culture dishes were grown to 65-80% confluency and transfected with GenePORTER transfection reagent (Gene Therapy Systems, Inc., San Diego, CA) according to the manufacturer's protocol with a 1:1 molar ratio of cDNAs for Ca²⁺ channel subunits (total 5 μ g) and 0.7 μ g of a CD8 expression plasmid for identification of transfected cells. At least 48 hours after transfection, 293T cells were incubated with CD8 antibody-coated microspheres (Dynal, Oslo, Norway) for identification of transfected cells during whole-cell recording.

Mice. The development and characterization of PV^{-/-}/CB^{-/-} knockout mice was described previously (Vecellio et al., 2000). Briefly, PV deficient (PV^{-/-}, (Schwaller et al., 1999)) and CB deficient (CB^{-/-}, (Airaksinen et al., 1997)) mice, generated on a mixed Sv129 X C57Bl/6 genetic background were used to breed double knockout mice.

Purkinje cell dissociation. All animal procedures fully complied with the National Institutes of Health guidelines on animal care and use and were conducted under a protocol approved by Emory IACUC. PV and CB double knockout mice (PV^{-/-}/CB^{-/-}, (Vecellio et al., 2000)), or as controls, Sv129 X C57/BL6 mice (WT) ranging in age from

14-21 days old were anaesthetized with isoflurane. After decapitation, sagittal cerebellar slices (400 μm) were cut and incubated in Tyrodes solution (in mM: 150 NaCl, 4 KCl, 2 CaCl₂, 2 MgCl₂, 10 HEPES, 10 Glucose, adjusted to pH 7.4 with NaOH) at 34° C for 30 min. before allowing them to cool to room temperature. Immediately prior to recording, slices were incubated in 1 mg/ml papain (Worthington, Lakewood NJ) dissolved in dissociation solution (in mM: 82 Na₂SO₄, 30 K₂SO₄, 5 MgCl₂, 10 HEPES, 10 Glucose, adjusted to pH 7.4 with NaOH) for 10 min. Slices were then washed in Tyrodes solution and placed in a fresh tube containing 1 ml Tyrodes solution and dissociated by gentle trituration through a series of fire-polished pipettes. Supernatant containing dissociated cells was placed on poly-L-lysine coated cover slips for whole-cell recording.

Electrophysiological recordings. Ca²⁺ or Ba²⁺ currents were recorded in transfected 293T cells and Purkinje neurons in whole-cell patch-clamp configuration with a HEKA EPC-9 patch-clamp amplifier driven by PULSE software (HEKA Electronics, Lambrecht/Pfalz, Germany). Leak and capacitive transients were subtracted using a P/-4 protocol.

Extracellular recording solutions for 293T cells contained (in mM): 150 Tris, 1 MgCl₂, and 10 CaCl₂ or 10 BaCl₂. Intracellular recording solutions contained (in mM): 130 N-methyl-D-glucamine, 60 HEPES, 1 MgCl₂, 2 Mg-ATP, and 0.5 EGTA. The pH of extracellular and intracellular recording solutions was adjusted to 7.3 with methanesulfonic acid. Extracellular recording solutions for voltage clamp recordings of Purkinje neurons contained (in mM): 155 TEA-Cl, 10 HEPES, 1 EGTA, and 10 CaCl₂ or 2 BaCl₂, adjusted to pH 7.4 with TEA-OH. Prior to recording, 1 μM TTX and 5 μM nimodipine were bath applied to block Na⁺ and L-type Ca²⁺ currents, respectively.

Intracellular solutions contained (in mM): 140 Cs Methanesulfonate, 4 MgCl₂, 0.5 EGTA, 9 HEPES, 14 Creatine phosphate (tris salt), 4 Mg-ATP, 0.3 Tris-GTP, adjusted to pH 7.4 with CsOH. Voltage protocols were adjusted as noted to compensate for a shift in the activation curve of -10 mV when extracellular Ba²⁺ was used.

Construction of action potential waveform stimuli. An action potential waveform was constructed by averaging recordings of spontaneous action potentials in dissociated wild-type Purkinje neurons. The action potential stimulus was applied from a holding potential of -60 mV and consisted of a waveform with a half-width of 0.75 ms and peak amplitude of +27 mV for Purkinje neuron recordings or was scaled to peak at +55 mV for transfected HEK 293T cell recordings. Waveforms were applied for 1 s at frequencies of 200, 100, 50, 20 or 10 Hz.

Synthesis of cDNA. Total RNA was isolated from cerebellar tissue in wild-type and PV^{-/-}/CB^{-/-} mice by incubation in 1 ml trizol (Invitrogen, Carlsbad, CA) for 5 min. Chloroform (0.2 ml) was added and tissue was shaken, then allowed to stand for 2-3 min. The mixture was then centrifuged at 12,000 x g for 15 min. at 4°C, and the supernatant was placed in a fresh tube. Isopropanol (0.5 ml) was added to the tube and allowed to stand for 10 min. before centrifugation at 12,000 x g for 10 min. at 4°C. The pellet was washed with 75% ethanol and dissolved before another spin at 7,500 x g for 5 min. at 4°C. The supernatant was removed and the pellet allowed to air dry before it was dissolved in RNase free H₂O. cDNA was then reverse transcribed by combining 2 µg RNA with the following reagents: 5 µM random hexamers (Fermentas), 0.5 mM dNTPs, 0.1 mM DTT, 5X first

strand buffer, RNaseout, and Superscript II (Invitrogen, Carlsbad, CA) and incubated at 42°C for 50 min. Synthesis of cDNA from single cells was accomplished by harvesting the entire neuron via negative pressure on the recording pipette. The tip of the pipette was then pressurized to expel contents and broken into a tube containing the same reagents described above and incubated at 40°C overnight.

RT-PCR. For all sets of primers the PCR reactions were performed using a Mastercycler (Eppendorf) programmed as follows: 1 cycle of 94°C for 2 min; followed by 40 cycles of 94°C for 20 s, 55°C for 30 s, and 68°C for 1 min; followed by a final 5 min extension at 68°C. Products were run on 1% agarose gels prestained with ethidium bromide. The negative controls included filled recording electrodes not used for whole-cell recording. The PCR primer sequences and their predicted PCR product sizes were as follows:

5'AGGCACGAAAGAAGGCTGGAT (forward) and
 5'TCCCACACATTTTGATTCCCTG (reverse); calbindin (432 bp)
 5'ATGGCTGGCCCGCAGCAGCAG (forward) and
 5'TAACATGGGGGGCTCACTGC (reverse); calretinin (816 bp)
 5'GTGGGCCGCTCTAGGCACCAA (forward) and
 5'CTCTTTGATGTCACGCACGATTTC (reverse); β -actin (539 bp)
 5'ATCCCTATGGAGGTCTTCGA (forward) and
 5'CTTTCTCGAGCTGGGCTAAG (reverse); $\text{Ca}_v\beta 1$ (235 bp)
 5'AACCAGCTGGAGGACGCTTG (forward) and
 5'CATACCGGTCCACATGTTCA (reverse); $\text{Ca}_v\beta 2$ (412 bp)
 5'GCGAGAAGTGGAGAGTCAGG (forward) and

5'AAGGCGATTGCTCCGCCTTC (reverse); Ca_vβ3 (270 bp)

5'TCTCACCATATCCCACAGCA (forward) and

5'CAAAGCCTATGTCTGGGAGTC (reverse); Ca_vβ4 (296 bp)

5'CGCGTACTTCTACTTTGTC; (forward) EF

5'TATTACTCGCAATAAACTG; (reverse) EFa (220 bp)

5'CATGTGTCTCAGCATCTGA; (reverse) EFb (220 bp)

Quantitative PCR. Pools of 5-10 Purkinje neurons were isolated and subject to reverse transcription as described for endpoint PCR. Oligonucleotide primers were designed to amplify 100 bp fragments of the mouse sequences for Ca_vβ2a, α₁2.1 (EFa and EFb variants of exon 37), and GAPDH. Amplification of a single band was confirmed initially by endpoint PCR and gel electrophoresis. Quantitative PCR was performed according to manufacturer's protocols with the Finnzymes DyNAmo HS SYBR Green qPCR kit and a BioRad iCycler real-time PCR machine. Reverse transcription (RT) reactions (2 μl) were added to reactions containing forward and reverse primers (1 μl each of 100 μM stock), 2x master mix (10 μl), and water for a final volume of 20 μl. Thermocycling conditions were 95 °C (15 min "hot start") followed by 40 cycles of: 94 °C (20 s), 60 °C (30 s), 72 °C (30 s). Melt curve analysis revealed a single peak in SYBR green fluorescence, indicating amplification of a single product for each primer set. The efficiency of amplification was measured as the slope of the relationship between cycle threshold (C(t)) and dilution of the RT reaction, which was found to be ~100% for each primer set. Relative change in Ca_vβ2a, α₁2.1 (EFa and EFb variants of exon 37) in WT compared to PV/CB^{-/-} neurons was determined as:

$$\Delta C(t)PV/CB^{-/-} = C(t)\beta_{2a}(PV/CB^{-/-}) - C(t)GAPDH(PV/CB^{-/-})$$

$$\Delta C(t)WT = C(t)\beta_{2a}(WT) - C(t)GAPDH(WT)$$

$$\Delta\Delta C(t) = \Delta C(t)PV/CB^{-/-} - \Delta C(t)WT$$

Primers used for quantitative PCR were as follows:

GTTCTGCCACCTCTTCATGC (forward) and

CTGCCGCTCAGCTTCTCTAC (reverse); β_{2a} (220 bp)

TGAATACGTGCGTGTCTGG (forward) and

GCAAGCAACCCTATGAGGAC (reverse); EF37a (150 bp)

ACAACTTCGAGTACCTCACC (forward) and

GGGACATGTGTCTCAGCATC (reverse); EF37b (120 bp)

CCTCTGGAAAGCTGTGGCGTGATGG (forward) and

AGATCCACGACGGACACATT (reverse); GAPDH (243 bp)

Data analysis. All data were analyzed using custom written procedures in IGOR Pro software (Wavemetrics, Portland, OR). Averaged data represent mean \pm SEM. Statistical differences in average inactivation (I_{res}/I_{peak}) between groups were determined by Student's t-test. *I-V* curves were fit with the function: $g(V-E)/\{1+\exp[(V-V_{1/2})/k]+b\}$ where g is the maximum conductance, V is the test potential, E is the apparent reversal potential, $V_{1/2}$ is the potential of half-activation, k is the slope factor, and b is the baseline. Significant differences between *I-V* curve values were determined with two-way repeated measure ANOVA.

Results

Characterization of Ca_v2.1 currents in Purkinje neurons. To isolate currents carried by voltage-gated Ca²⁺ channels in acutely dissociated mouse Purkinje neurons, whole-cell patch clamp recordings were conducted with 10 mM extracellular Ca²⁺ and with blockers of voltage-gated Na⁺ and K⁺ channels. Depolarizing steps were made from a holding voltage of -60 mV to minimize contribution of low-voltage activated T-type currents in these cells (Raman and Bean, 1999). Under these conditions, we observed large inward currents (>1 nA) consistent in activation and inactivation kinetics to the P/Q-type current carried by Ca_v2.1 channels that was described in previous studies (Usowicz et al., 1992; Raman and Bean, 1999). The ability of relatively low concentrations of ω-agatoxin IVA to block most of the inward Ca²⁺ current further supports the identity of this current as P/Q-type (Fig. 4.1A) (Mintz et al., 1992).

To characterize CDF and CDI of the native P/Q-type current in these cells, we developed an action potential waveform stimulus protocol based on the properties of action potentials measured in current clamp recordings (Fig. 4.1B). At a frequency of 200 Hz, these waveforms produced a robust initial facilitation (~27% peak facilitation) followed by a progressive inactivation of Ca²⁺ current (I_{Ca}) (fractional current decayed to 80% of the maximal value in 1 s, Fig. 4.1C). With the same protocol, Ba²⁺ currents (I_{Ba}) showed less facilitation (~2%) and similar inactivation (75% of the maximal value) as I_{Ca} (Fig. 4.1D). The small amount of facilitation shown by I_{Ba} may result from relief of G-protein inhibition, which has been shown to cause facilitation of Ca_v2 channels during AP waveforms in neurons (Park and Dunlap, 1998; Brody and Yue, 2000; Diverse-Pierluissi et al., 2000; Zhou et al., 2003). I_{Ca} and I_{Ba} during AP stimuli of different frequencies were further compared in plots of fractional current (amplitude of test current normalized to

the first in the train) against time (Fig.4.2). In general, facilitation of both I_{Ca} and I_{Ba} was greater with higher frequency stimulation (maximum fractional current for I_{Ca} 200 Hz = 1.29 ± 0.03 , 100 Hz = 1.17 ± 0.02 , and 50 Hz = 1.11 ± 0.01 , for I_{Ba} 200 Hz = 1.04 ± 0.02 , 100 Hz = 1.03 ± 0.02 , and 50 Hz = 1.02 ± 0.01 , Fig. 4.2A-C). However, facilitation was significantly greater for I_{Ca} than for I_{Ba} at all frequencies tested ($p < 0.05$), which is consistent with our previous observations of CDF of $Ca_v2.1$ in transfected HEK293T cells (Kreiner and Lee, 2006).

I_{Ba} inactivation was generally greater in Purkinje neurons than for recombinant $Ca_v2.1$ in transfected cells perhaps due to the presence of factors such as multiple $Ca_v\beta$ subunits, particularly the β_3 and β_4 subunits (Richards et al., 2007), which can significantly increase voltage-dependent inactivation of I_{Ba} through $Ca_v2.1$ channels. For this reason, CDI (increased inactivation of I_{Ca} relative to I_{Ba}) was not readily apparent during the AP trains. However, during sustained depolarizations (2-s), inactivation of I_{Ca} was significantly greater than for I_{Ba} ($p < 0.05$, Fig. 4.2D). Collectively, these results demonstrate that the P/Q-type current in Purkinje neurons shows CDF and CDI that are generally similar to that described for $Ca_v2.1$ in transfected cells.

We next evaluated the role of Ca^{2+} buffering proteins by comparing $Ca_v2.1$ properties in WT and $PV^{-/-}/CB^{-/-}$ Purkinje neurons. We first characterized the general features of $Ca_v2.1$ activation. Current-voltage ($I-V$) relationships and cell capacitance values were not significantly different in WT and $PV^{-/-}/CB^{-/-}$ Purkinje neurons (Table 4.1).

To confirm that $Ca_v2.1$ accounts for most of the whole-cell I_{Ca} in $PV^{-/-}/CB^{-/-}$ neurons, we examined the sensitivity of Ca^{2+} currents to ω -Agatoxin IVA (500 nM).

Example traces representing a series of depolarizing steps given before and after the application of ω -Agatoxin IVA (500 nM) show that I_{Ca} was almost completely blocked in both WT and $PV^{-/-}/CB^{-/-}$ Purkinje neurons (Fig. 4.3A). As shown in Fig. 4.3B, ω -Agatoxin IVA caused significant block of I_{Ca} in WT and $PV^{-/-}/CB^{-/-}$ Purkinje neurons (90% in wild-type and 85% in $PV^{-/-}/CB^{-/-}$). There was no significant difference in the extent of ω -Agatoxin IVA block of the whole-cell I_{Ca} between WT and $PV^{-/-}/CB^{-/-}$ Purkinje neurons ($p=0.395$). These results show that I_{Ca} is mediated predominantly by $Ca_v2.1$ in both WT and $PV^{-/-}/CB^{-/-}$ Purkinje neurons.

Differences in inactivation and facilitation of $Ca_v2.1$ in WT and $PV^{-/-}/CB^{-/-}$ Purkinje neurons. Since EGTA depresses CDI, but not CDF of $Ca_v2.1$ in transfected cells (Lee et al., 2000), PV and CB may similarly influence $Ca_v2.1$ in Purkinje neurons. If so, then CDI but not CDF should be greater in Purkinje neurons from $PV^{-/-}/CB^{-/-}$ than WT mice. Consistent with this prediction, I_{Ca} showed stronger inactivation with 2-s depolarizations in $PV^{-/-}/CB^{-/-}$ than in WT neurons (79.8 \pm 1.7% inactivation in WT neurons and 85 \pm 1.3% inactivation in $PV^{-/-}/CB^{-/-}$ neurons, $p<0.05$; Fig. 4.4A). However, I_{Ba} also showed greater inactivation in $PV^{-/-}/CB^{-/-}$ than in WT neurons (53.9 \pm 3.6% inactivation in WT neurons and 66.3 \pm 4.2% inactivation in $PV^{-/-}/CB^{-/-}$ neurons, $p<0.05$, Fig. 4.4B). This result is unexpected if PV and CB were only acting to suppress CDI.

A possible explanation for these results is that there is a change in the expression of Ca_v β subunit isoforms in WT and $PV^{-/-}/CB^{-/-}$ Purkinje neurons. Of all 4 Ca_v β subunits (β_1 - β_4) that are expressed in Purkinje neurons, the β_{2a} subunit appears to be most prominent (Richards et al., 2007). $Ca_v2.1$ channels containing the $Ca_v\beta_{2a}$ subunit show

less inactivation of both I_{Ca} and I_{Ba} and, under some conditions, greater CDI and CDF than those channels containing the β_{1b} subunit (Lee et al., 2000). Therefore, downregulation of $Ca_v\beta_{2a}$ could account for the increased inactivation shown by I_{Ba} and I_{Ca} and decreased CDF in $PV^{-/-}/CB^{-/-}$ neurons. To test this, we first measured CDF in WT and $PV^{-/-}/CB^{-/-}$ Purkinje neurons during AP waveforms (Fig 4.5). As for WT neurons, facilitation of I_{Ca} was greater for higher frequency stimulation in $PV^{-/-}/CB^{-/-}$ neurons (Fig. 4.5A-F). While facilitation of I_{Ba} was not significantly different between WT and $PV^{-/-}/CB^{-/-}$ neurons for any of the stimulation frequencies, facilitation of I_{Ca} was significantly less in $PV^{-/-}/CB^{-/-}$ than WT neurons at frequencies of 200 and 100 Hz (Fig. 4.5G-H, Table 4.2). Taken together, these results demonstrate that $Ca_v2.1$ channels in $PV^{-/-}/CB^{-/-}$ neurons show alterations in gating that are consistent with decreased expression of the $Ca_v\beta_{2a}$ subunit.

Molecular distinctions between $Ca_v2.1$ in WT and $PV^{-/-}/CB^{-/-}$ Purkinje neurons. To test for differences in the $Ca_v\beta_2$ subunit between WT and $PV^{-/-}/CB^{-/-}$ neurons, we used RT-PCR analysis with primers specific for the different $Ca_v\beta$ subunits. We first validated our RT-PCR strategy by testing for amplification of specific mRNAs, CR is a Ca^{2+} buffering protein that is highly expressed in granule cells, but not Purkinje neurons. Consistent with this, we detected CR mRNA in whole cerebellar tissue, but not Purkinje neurons, indicating a lack of granule cell contamination in Purkinje neuron samples (Fig.4.6A). CB was amplified in whole cerebellar tissue and WT Purkinje neurons, but not in $PV^{-/-}/CB^{-/-}$ Purkinje neurons, verifying that CB mRNA is not expressed in $PV^{-/-}/CB^{-/-}$ mice. No amplicons were produced when using the extracellular solution alone as a

negative control. Consistent with previous work, all four $\text{Ca}_v\beta$ subunits were detected in whole cerebellum from WT and $\text{PV}^{-/-}/\text{CB}^{-/-}$ mice (Volsen et al., 1997; Richards et al., 2007) (Fig. 4.6B). To restrict analysis to Purkinje neurons, we made cDNA from acutely isolated Purkinje neurons, which were then used as input for the PCR reaction. In these experiments, $\text{Ca}_v\beta_1$, $\text{Ca}_v\beta_3$ and $\text{Ca}_v\beta_4$, were detected, but the $\text{Ca}_v\beta_2$ was clearly lacking in samples from $\text{PV}^{-/-}/\text{CB}^{-/-}$ mice (Fig. 4.6C). These results were obtained from pools of at least 5 neurons taken from 2 WT and $\text{PV}^{-/-}/\text{CB}^{-/-}$ mice. To verify these results in neurons that were used for electrophysiological recordings, we isolated the neurons after recording and performed single cell RT-PCR using primers specific to $\text{Ca}_v\beta_2$. With this approach, we detected $\text{Ca}_v\beta_2$ in a significantly smaller fraction of $\text{PV}^{-/-}/\text{CB}^{-/-}$ compared to WT neurons ($p < 0.05$, Fig. 4.6C). Of the β_2 splice variants expressed in Purkinje neurons (β_{2a-d}), β_{2a} is by far the most prominent (Richards et al., 2007). Since these experiments used primers that were designed to amplify a sequence common to all $\text{Ca}_v\beta_2$ splice variants, we verified that the β_{2a} splice variant expression was down regulated in $\text{PV}^{-/-}/\text{CB}^{-/-}$ Purkinje neurons by using quantitative PCR with β_{2a} specific primers. Relative quantification with GAPDH used as a reference molecule showed that $\text{PV}/\text{CB}^{-/-}$ Purkinje neurons (5-10 neurons per sample) express $52.7 \pm 8\%$ of β_{2a} mRNA compared to WT Purkinje neurons ($n = 5$). These results support our hypothesis that decreased β_{2a} expression could lead to the change in $\text{Ca}_v2.1$ properties in $\text{PV}^{-/-}/\text{CB}^{-/-}$ neurons.

However, alternative splicing of the $\alpha_{1.2.1}$ subunit has also been shown to cause changes in CDI and CDF (Stea et al., 1994; Bourinet et al., 1999; Soong et al., 2002). The EF-hand domain is a putative Ca^{2+} -binding motif, mutations in which alter CDI and VDI of Ca_v channels (Zuhlke and Reuter, 1998; Bernatchez et al., 1998; Peterson et al., 2000).

For $\alpha_12.1$, alternative splicing of exon 37 produces EF-hand variants (EF37a and EF37b, Fig. 4.7A), with altered CDF (Chaudhuri et al., 2004; Chaudhuri et al., 2005; Chaudhuri et al., 2007). The EF37b splice variant is preferentially expressed early in development and produces $\text{Ca}_v2.1$ channels that do not undergo CDF. Upregulation of the EF37a splice variant occurs during postnatal week 2 in rats, and is associated with $\text{Ca}_v2.1$ channels that show strong CDF (Chaudhuri et al., 2005). Therefore, the presence of EF37b or lack of EF37a could account for the decreased CDF of $\text{Ca}_v2.1$ in $\text{PV}^{-/-}/\text{CB}^{-/-}$ neurons. We tested this possibility with an RT-PCR strategy used previously (Chaudhuri et al., 2005). Both EF37a and EF37b were detected in whole cerebellum and Purkinje neurons from WT and $\text{PV}^{-/-}/\text{CB}^{-/-}$ mice (Figure 4.7B). By single-cell RT-PCR, we detected EF37a and EF37b in a similar fraction of WT and $\text{PV}^{-/-}/\text{CB}^{-/-}$ neurons (not shown). However, quantitative PCR on samples of 5-10 Purkinje neurons indicated that the EF37a splice variant is down regulated in $\text{PV}^{-/-}/\text{CB}^{-/-}$ Purkinje neurons (49.3% of WT levels, $n = 2$) and the EF37b splice variant is up regulated in $\text{PV}^{-/-}/\text{CB}^{-/-}$ neurons (138.7% of WT levels, $n = 2$), with GAPDH used as a reference molecule. Therefore, our results support a role for differential $\alpha_12.1$ splice variant expression in the mechanism underlying differences in facilitation of $\text{Ca}_v2.1$ in WT and $\text{PV}^{-/-}/\text{CB}^{-/-}$ neurons.

Because both $\text{Ca}_v\beta_{2a}$ and $\text{Ca}_v\beta_4$ are expressed in Purkinje neurons (Burgess et al., 1999; Richards et al., 2007), the properties of $\text{Ca}_v2.1$ in WT Purkinje neurons should result from a contribution of both subunits. A loss of $\text{Ca}_v\beta_{2a}$ expression in $\text{PV}^{-/-}/\text{CB}^{-/-}$ neurons should cause $\text{Ca}_v2.1$ to exhibit properties that are determined more strongly by the $\text{Ca}_v\beta_4$ subunit. To test this, we determined if the properties of $\text{Ca}_v2.1$ with $\text{Ca}_v\beta_{2a}$ or $\text{Ca}_v\beta_4$ in transfected HEK 293T cells were more similar to WT or $\text{PV}^{-/-}/\text{CB}^{-/-}$ neurons. We

used the same action potential waveform stimulus (200 Hz) that was used to analyze I_{Ca} and I_{Ba} in Purkinje neurons (Fig.4.5). Surprisingly, for I_{Ca} , similar levels of facilitation were seen for $Ca_v\beta_{2a}$ and $Ca_v\beta_4$ (Fig. 4.8A, max. fractional I_{Ca} = 1.35 ± 0.05 for $Ca_v\beta_{2a}$ and 1.28 ± 0.06 for $Ca_v\beta_4$, $p=0.42$). This was unexpected since repetitive square pulse (5-ms) depolarizations given at 100 Hz show significantly stronger facilitation of I_{Ca} with $Ca_v\beta_{2a}$ than $Ca_v\beta_4$ (not shown). However, consistent with results obtained with the square pulse stimuli, inactivation of both I_{Ca} and I_{Ba} was significantly increased during AP waveforms for $Ca_v\beta_4$ compared to $Ca_v\beta_{2a}$ (Fig.4.8A-B). This was particularly apparent during sustained depolarizations (Fig. 4.8C). Increased inactivation of I_{Ca} and I_{Ba} due to $Ca_v\beta_4$ are consistent with the behavior of $Ca_v2.1$ in PV^{-}/CB^{-} neurons (Fig.4.4, 4.5). However, the similar levels of facilitation of I_{Ca} seen with $Ca_v\beta_{2a}$ and $Ca_v\beta_4$ suggest that some other mechanism must account for the reduced CDF in PV^{-}/CB^{-} compared to WT neurons. We conclude that predominant expression of a β -subunit that confers fast inactivation, such as $Ca_v\beta_4$, is sufficient to produce the rapid inactivation but not decreased facilitation of $Ca_v2.1$ channels in PV^{-}/CB^{-} Purkinje neurons.

Discussion

Ca^{2+} -buffering proteins play an important role in modulating Ca^{2+} signaling and maintaining Ca^{2+} homeostasis in neurons. In the present study, we examined the contribution of PV and CB to the feedback regulation of $Ca_v2.1$ by Ca^{2+} in Purkinje neurons. We demonstrated that $Ca_v2.1$ channels in neurons lacking PV and CB not only differed with respect to CDI, but also showed a significant increase in VDI and a decrease in CDF. RT-PCR analysis confirmed a downregulation of the β_2 subunit in PV^{-}

/CB^{-/-} Purkinje neurons, which should result in increased inactivation of native Ca_v2.1 currents. These findings suggest a novel mechanism whereby PV and CB are required for maintaining normal Ca_v2.1 subunit composition, which could have important consequences for Purkinje cell physiology.

Feedback regulation of Ca_v2.1 is altered in the absence of PV and CB. Our initial intent was to determine if PV and CB regulated Ca_v2.1 channels by minimizing global Ca²⁺ that supported CDI. However, a formal test of this hypothesis was prevented since whole-cell patch clamp recordings showed that compared to in WT neurons, Ca_v2.1 channels in PV^{-/-}/CB^{-/-} neurons showed differences that suggested a major change in Ca_v2.1 subunit composition (Fig. 4.4B). Downregulation of the Ca_vβ₂ subunit may serve as a compensatory mechanism in PV^{-/-}/CB^{-/-} Purkinje neurons, which would limit Ca²⁺ influx through Ca_v2.1 by suppressing inactivation. Restricting voltage-gated Ca²⁺-entry in this way may help compensate for the lack of Ca²⁺ buffering in these neurons. In PV^{-/-}/CB^{-/-} neurons, a number of cellular alterations have been described, which would also help restore Ca²⁺ homeostasis in the absence of PV and CB. These include increases in mitochondrial volume (Chen et al., 2006) and the volume and density of dendritic spines (Vecellio et al., 2000). Our results are the first to demonstrate a molecular change in Ca_v2.1 channels as a consequence of loss of PV and CB expression. Decreased neuronal expression of PV and CB are associated with schizophrenia and epilepsy, respectively (Hashimoto et al., 2003; Carter et al., 2008). It would be interesting to determine if alterations in Ca_v2.1 properties, similar to that we observed in PV^{-/-}/CB^{-/-} neurons, represent a general mechanism to protect neurons against Ca²⁺ overloads in pathological conditions.

While factors regulating $\text{Ca}_v \beta_2$ expression have not been well-characterized, Ca^{2+} itself may play a role in maintaining normal $\text{Ca}_v2.1$ subunit expression. Evoked Ca^{2+} transients are larger in amplitude and decay more slowly in $\text{PV}^{-/-}/\text{CB}^{-/-}$ compared to WT Purkinje neurons (Chard et al., 1993; Schmidt et al., 2003b). This could lead to the activation of Ca^{2+} -dependent pathways that help turn down $\text{Ca}_v \beta_2$ expression. This possibility is supported by previous studies showing that the expression of a number of proteins, including CB itself (Gruol et al., 2005), depend on specific patterns of Ca^{2+} signaling in Purkinje neurons.

Based on the similar levels of CDF seen in $\text{Ca}_v2.1$ channels containing $\text{Ca}_v\beta_2$ or $\text{Ca}_v\beta_4$ in transfected cells (Fig. 4.8A-B), it is not likely that downregulation of $\text{Ca}_v\beta_2$ also leads to the reduced CDF in $\text{PV}^{-/-}/\text{CB}^{-/-}$ neurons (Fig. 4.6B-C). Since the $\text{Ca}_v2.1$ channels containing the EFb $\alpha_12.1$ splice variant show little CDF (Chaudhuri et al., 2004), increased expression of this variant could account for the lack of CDF in $\text{PV}^{-/-}/\text{CB}^{-/-}$ neurons. While our endpoint PCR analyses revealed the presence of the EFb variant in equal fractions of WT and $\text{PV}^{-/-}/\text{CB}^{-/-}$ neurons, quantitative PCR revealed differences in the levels of EFa and EFb in $\text{PV}^{-/-}/\text{CB}^{-/-}$ and WT neurons. Previous work showed that EFb is expressed mainly early in development at ages when PV and CB are nominally expressed in Purkinje neurons (Chaudhuri et al., 2005). It is interesting to speculate that the increased inactivation and decreased facilitation of $\text{Ca}_v2.1$ channels we observed in $\text{PV}^{-/-}/\text{CB}^{-/-}$ neurons represent a developmentally immature form of $\text{Ca}_v2.1$, which is important for producing modest Ca^{2+} signals at a time when Ca^{2+} buffering capacity is low.

Technical considerations. While our results show that the $\text{Ca}_v\beta_2$ mRNA is present in a smaller fraction of $\text{PV}^{-/-}/\text{CB}^{-/-}$ than WT neurons, our analysis does not necessarily indicate that there are differences $\text{Ca}_v\beta_2$ protein expression in the two groups. If specific $\text{Ca}_v\beta_2$ subunit antibodies were available, we could address this by western blotting Purkinje cell lysates for $\text{Ca}_v\beta_2$ in WT and $\text{PV}^{-/-}/\text{CB}^{-/-}$ neurons.

Our use of the whole-cell mode of the patch clamp method undoubtedly minimized the acute contributions of PV and CB to $\text{Ca}_v2.1$ CDI due to the dialysis of intracellular components into the recording pipette with this approach. Perforated patch recordings of WT neurons would overcome this problem and allow measurement of the influence of these proteins on CDI when compared with whole-cell recordings of WT neurons.

Physiological implications of altered Ca^{2+} feedback regulation. Purkinje neurons express two types of Ca^{2+} -activated K^+ channels (K_{Ca}), BK and SK, which mediate repolarization after an action potential and the amplitude of the afterhyperpolarization (AHP), respectively (Sah and McLachlan, 1992). $\text{Ca}_v2.1$ Ca^{2+} currents are tightly coupled to K_{Ca} channel activation, such that the net effect of $\text{Ca}_v2.1$ activation is an outward K_{Ca} -mediated K^+ current (Raman and Bean, 1999). Block of $\text{Ca}_v2.1$ channels prevents K_{Ca} activation, which eliminates the AHP and increases firing rate of Purkinje neurons (Edgerton and Reinhart, 2003; Womack et al., 2004). Alterations in firing have been characterized in $\text{PV}^{-/-}/\text{CB}^{-/-}$ mice *in vivo*. These consist of synchronous, rhythmic simple spike firing and increased complex spike duration, resulting in mono or dual frequency cerebellar oscillations seen in $\text{PV}^{-/-}/\text{CB}^{-/-}$ mice (Servais et al., 2005). Increased inactivation and decreased facilitation of $\text{Ca}_v2.1$ may contribute to reduced activation of

K_{Ca} , which could drive aberrant firing and the oscillatory activity in PV^{-}/CB^{-} Purkinje neurons. Reduced activation of K_{Ca} channels could alter the precision of spontaneous firing (pacemaking) in Purkinje neurons, which has been shown to produce ataxia in several $Ca_v2.1$ mutant mice strains (Walter et al., 2006), and may contribute to the impaired motor coordination observed in PV^{-}/CB^{-} mice (Airaksinen et al., 1997; Servais et al., 2005).

The present data emphasize the importance of Ca^{2+} buffers, not only in their ability to fine-tune Ca^{2+} signaling at the cellular level, but to dynamically regulate properties of $Ca_v2.1$ channels by modifying their subunit composition. Considering the widespread distribution of $Ca_v2.1$ and PV and CB throughout the nervous system, our results suggest a new mechanism by which Ca^{2+} buffering proteins may maintain the stability of neuronal networks.

Table 4.1. Membrane and Ca_v2.1 activation parameters in WT and PV^{-/-}/CB^{-/-} Purkinje neurons

	10 mM Ca ²⁺			2 mM Ba ²⁺		
	WT (n = 30)	KO (n = 24)	P-value	WT (n = 15)	KO (n = 13)	P-value
Cell capacitance (pF)	16.93 +0.57	17.63 +0.74	0.45	17.61 +0.71	17.38 +0.93	0.84
V _{1/2} (mV)	-19.30 +1.07	-16.16 +1.61	0.10	-25.42 +1.20	-27.33 +1.24	0.28
K	-4.19 +0.25	-3.94 +0.35	0.56	-3.96 +0.34	-4.52 +0.25	0.21
I _{max} (nA)	-1.31 +0.15	-2.01 +0.23	0.01*	-1.21 +0.17	-0.81 +0.13	0.09
I-V peak (mV)	-12.14 +1.05	-9.69 +1.72	0.21	-18.05 +1.36	-19.30 +1.24	0.51

Step depolarizations (50 ms) were used to generate *I-V* curves for WT and PV^{-/-}/CB^{-/-} Purkinje neurons in 10 mM Ca²⁺ and 2 mM Ba²⁺. *I-V* curves were fit with the function: $g(V-E)/\{1+\exp[(V-V_{1/2})/k] + b\}$ where *g* is the maximum conductance, *V* is the test potential, *E* is the apparent reversal potential, *V*_{1/2} is the potential of half-activation, *k* is the slope factor, and *b* is the baseline. Values represent mean ± SEM. Astericks indicate significant differences between WT and PV/CB neurons by Student's t-test.

Table 4.2: Facilitation (maximum fractional current) for Ca_v2.1 currents evoked by action potential waveforms

	ICa			IBa		
	WT (n = 13)	PV ^{-/-} /CB ^{-/-} (n = 14)	P value	WT (n = 12)	PV ^{-/-} /CB ^{-/-} (n = 10)	P value
200 Hz	1.29 ± 0.04	1.18 ± 0.02	0.01*	1.15 ± 0.03	1.07 ± 0.03	0.08
100 Hz	1.17 ± 0.02	1.13 ± 0.01	0.03*	1.10 ± 0.02	1.05 ± 0.01	0.11
50 Hz	1.11 ± 0.01	1.09 ± 0.01	0.18	1.03 ± 0.01	1.06 ± 0.01	0.11

Mean ± SEM for maximal facilitation (maximal fractional current) is shown for each stimulation frequency in Fig. 4.5. Astericks indicate significant differences between WT and PV^{-/-}/CB^{-/-} neurons by Student's t-test.

Figure 4.1

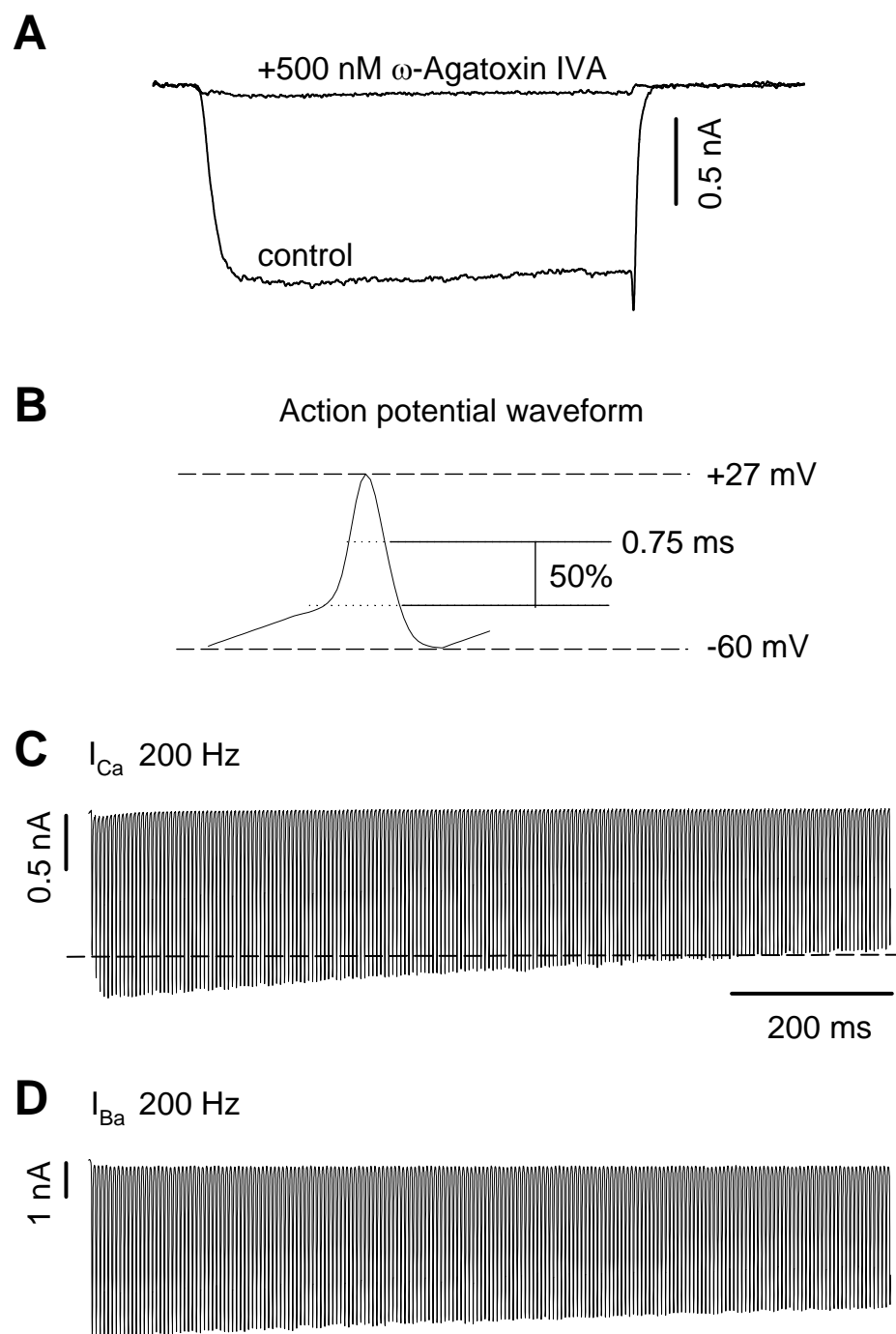


Figure 4.1: Facilitation and inactivation of $\text{Ca}_v2.1$ in wild-type (WT) Purkinje neurons.

A. I_{Ca} was evoked by 50 ms depolarization (-60 mV to -10 mV) in 10 mM extracellular Ca^{2+} solution before and after the addition of 500 nM ω -Agatoxin IVA. B. Voltage clamp protocols consisting of action potential waveforms were applied to acutely dissociated Purkinje neurons. Membrane resting potential was -60 mV. Action potential waveforms peaked at +27 mV with a half width of 0.75 ms. C. Current responses induced by 200 Hz action potential waveform train were recorded in the presence of 10 mM extracellular Ca^{2+} or D. 10 mM Ba^{2+} . Dotted lines correspond to the amplitude of the first action potential waveform in each train.

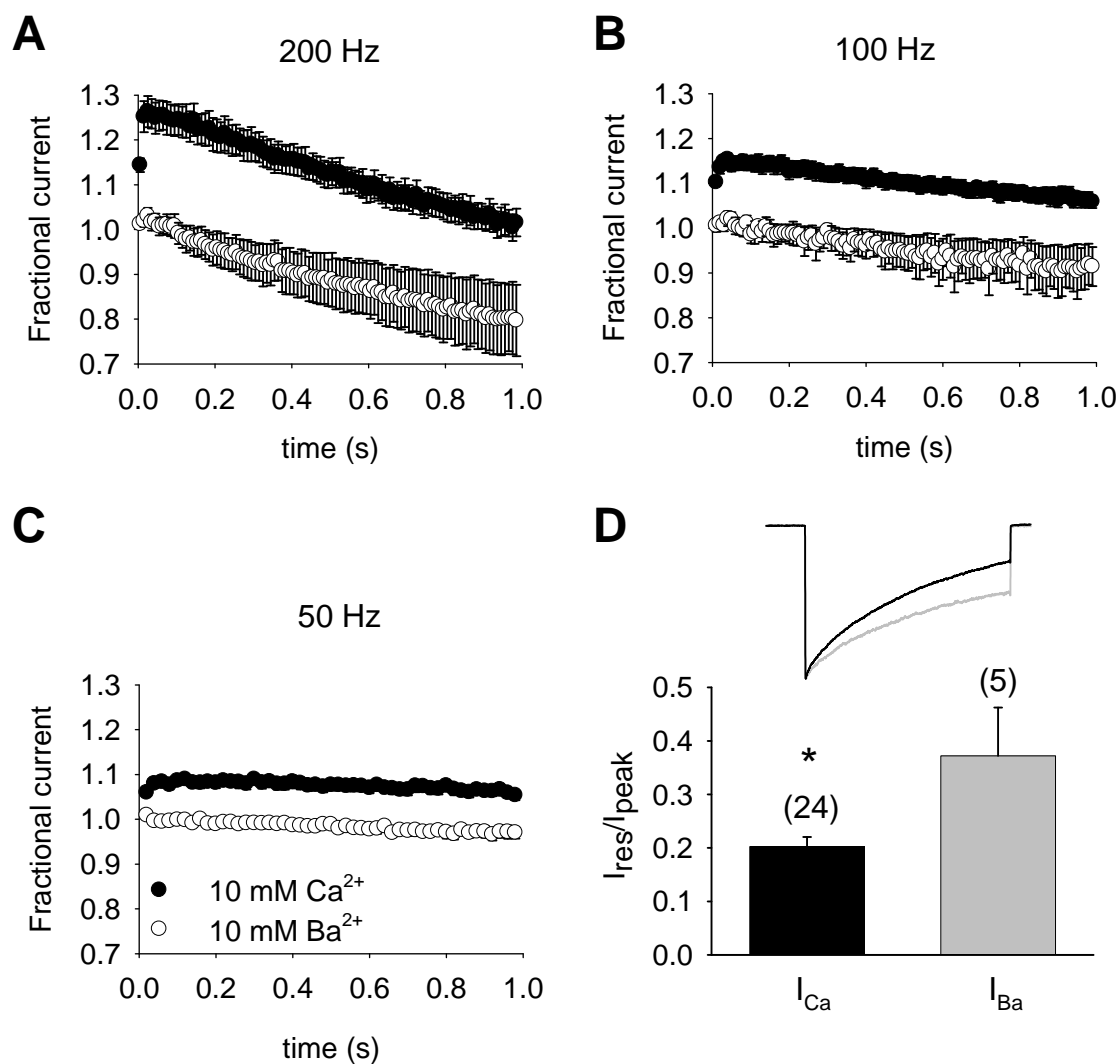
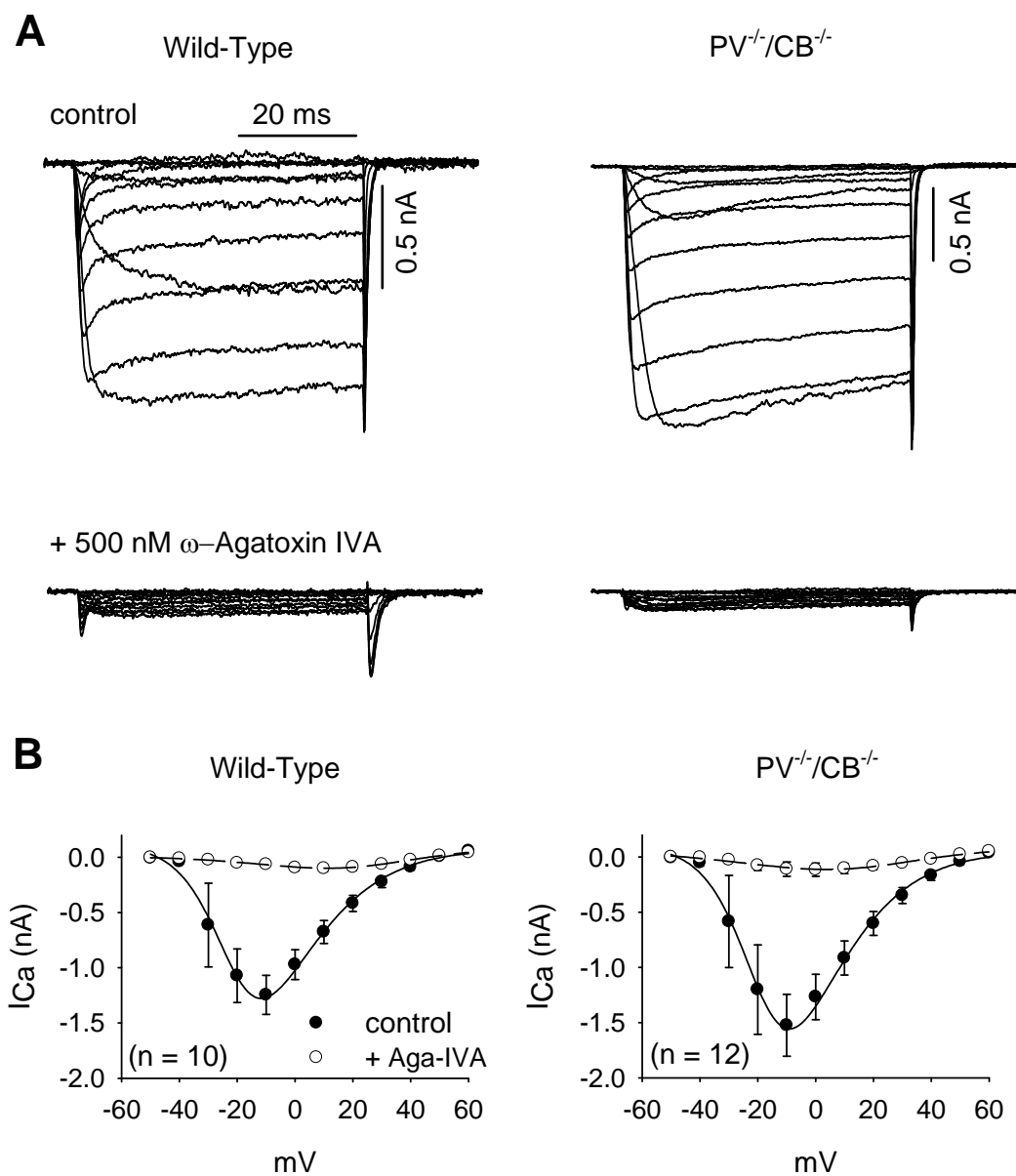
Figure 4.2

Figure 4.2: Facilitation and inactivation in WT Purkinje neurons in Ca^{2+} and Ba^{2+} . A. Average fractional current for waveforms applied as in Fig. 4.1 are shown for a frequency of 200 Hz. Current amplitudes are normalized to the amplitude of the first pulse in each train. Symbols represent average value \pm SEM for Purkinje cells in 10 mM Ca^{2+} (closed circles) or 10 mM Ba^{2+} (open circles) extracellular recording solution. B. Action potential waveforms applied as in (A) at a frequency of 100 Hz or C. 50 Hz. D. Traces (top) represent typical current responses to 2 s depolarizing pulses (-60 to 0 mV) for WT

Purkinje neurons in 10 mM Ca^{2+} (black lines) or 10 mM Ba^{2+} (gray lines) solution.

Average percent inactivation (bottom) was determined $((1 - I_{\text{res}}/I_{\text{peak}}) * 100)$ for I_{Ca} (black bars) I_{Ba} (grey bars). Bars represent mean \pm SEM; number of neurons in parentheses (*, $p < 0.05$).

Figure 4.3**Figure 4.3:** Characterization of $Ca_v2.1$ currents in WT and $PV^{-/-}/CB^{-/-}$ Purkinje neurons.

A. Examples of current responses to depolarizing steps from a holding potential of -60 mV for are shown for dissociated WT (left) and $PV^{-/-}/CB^{-/-}$ (right) Purkinje neurons before (top) and after (bottom) the application of $Ca_v2.1$ blocker ω -Agatoxin IVA (500 nM). B. Average current-voltage (I - V) relationships for currents recorded in WT and $PV^{-/-}$

$^{-}/CB^{-}/$ Purkinje neurons as in (A). Symbols correspond to average current values \pm SEM recorded in 10 mM extracellular Ca^{2+} without (closed circles) and with (open circles) 500 nM ω -agatoxin IVA.

Figure 4.4

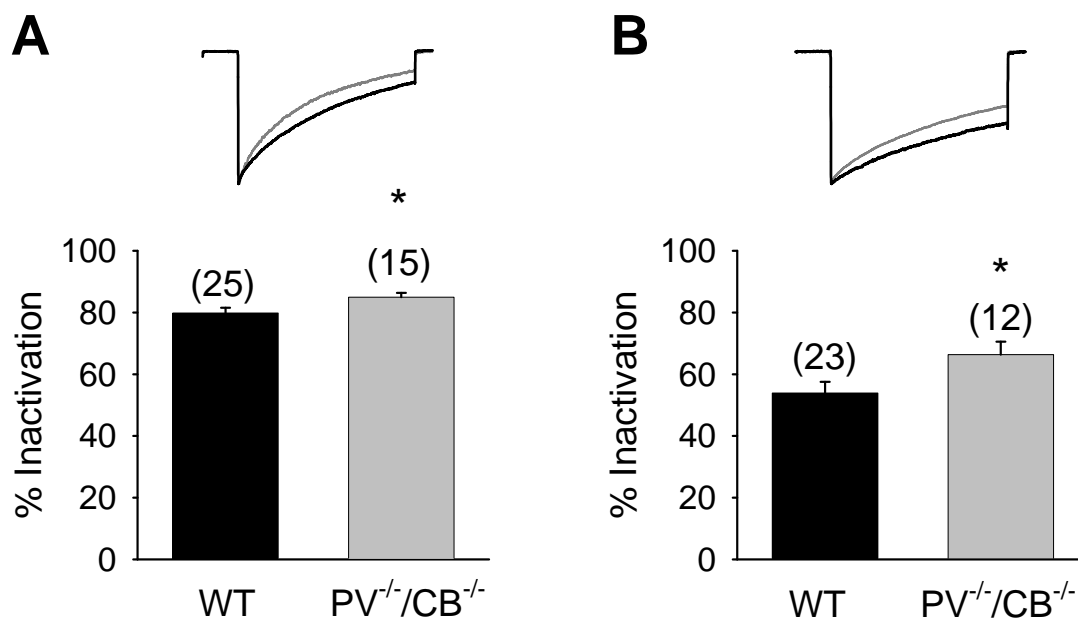


Figure 4.4: Increased inactivation in PV^{-/-}/CB^{-/-} Purkinje neurons. A. Traces (top) represent typical current responses to 2 s depolarizing pulses (-60 to 0 mV) for WT (black lines) and PV^{-/-}/CB^{-/-} (gray lines) Purkinje neurons. Average percent inactivation (bottom) was determined $((1 - I_{res}/I_{peak}) * 100)$ for WT (black bars) and PV^{-/-}/CB^{-/-} (grey bars) Purkinje neurons. Bars represent mean ± SEM; number of neurons in parentheses (*, p < 0.05). Recordings were obtained in 10 mM Ca²⁺ or B. 2 mM Ba²⁺ extracellular solution (2 s depolarizing pulses -60 to -10 mV).

Figure 4.5

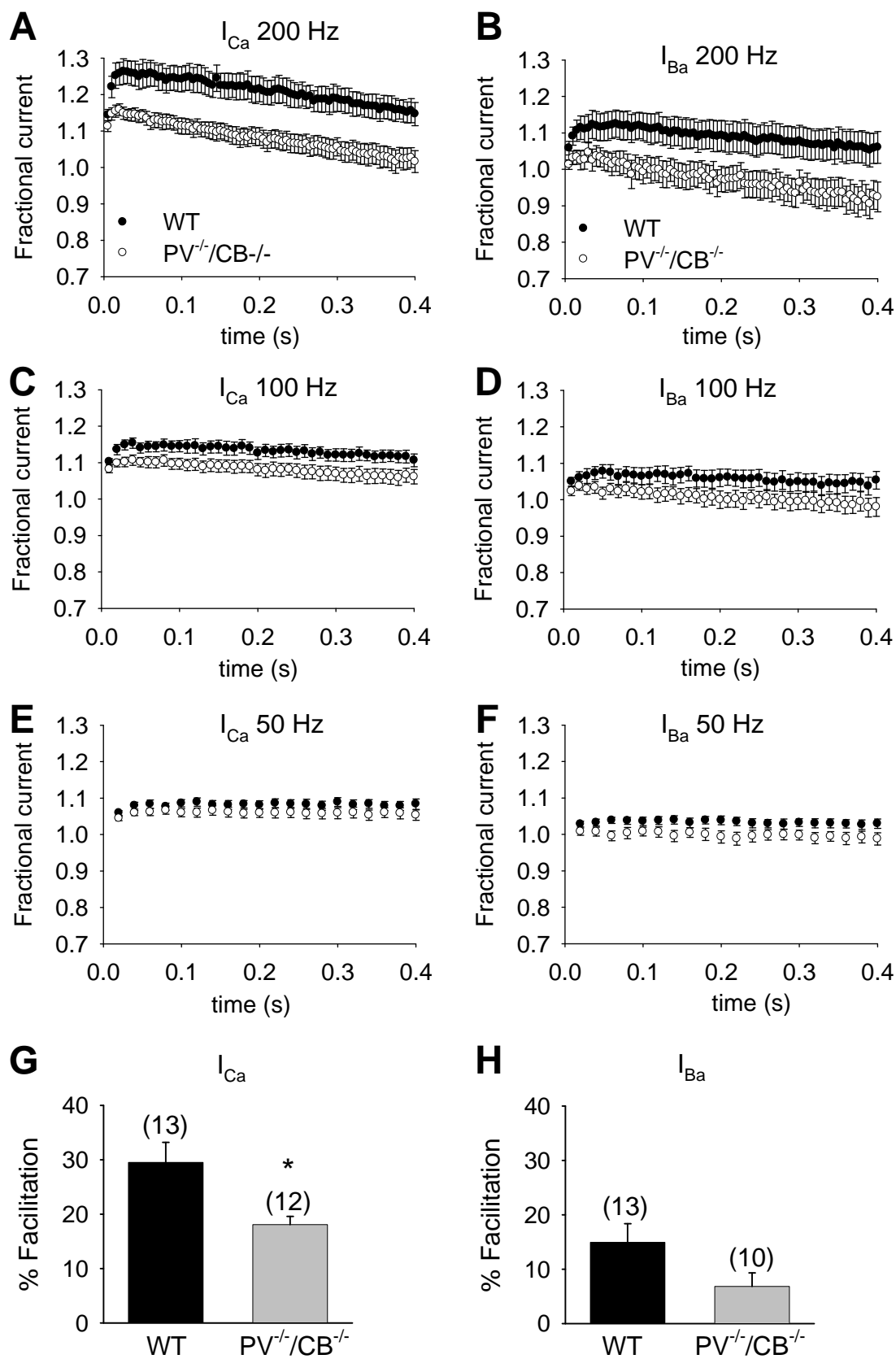


Figure 4.5: Comparison of responses to action potential waveforms in WT and PV^{-/-}/CB^{-/-} Purkinje neurons. A. Average fractional current for action potential waveforms applied at 200 Hz are shown for WT (closed circles) and PV^{-/-}/CB^{-/-} (open circles) neurons with 10 mM extracellular Ca²⁺. Current amplitudes are normalized to the amplitude of the first pulse in each train. Symbols represent average value \pm SEM. B. Action potential waveforms applied as in (A) in 2 mM Ba²⁺ extracellular recording solution. C,D. Action potential waveforms applied at 100 Hz in (C) 10 mM Ca²⁺ or (D) 2 mM Ba²⁺. E,F. Action potential waveforms applied at 50 Hz in (E) 10 mM Ca²⁺ or (F) 2 mM Ba²⁺. G. Percent facilitation was determined $((\text{maximal fractional current} - 1) * 100)$ for average fractional current of action potential waveforms applied in (A) for WT (black bars) and PV^{-/-}/CB^{-/-} (grey bars) Purkinje neurons. Bars represent mean \pm SEM; number of neurons in parentheses (*, p < 0.05). Recordings were obtained in 10 mM Ca²⁺ or H. 2 mM Ba²⁺ extracellular solution. Data from (B).

Figure 4.6

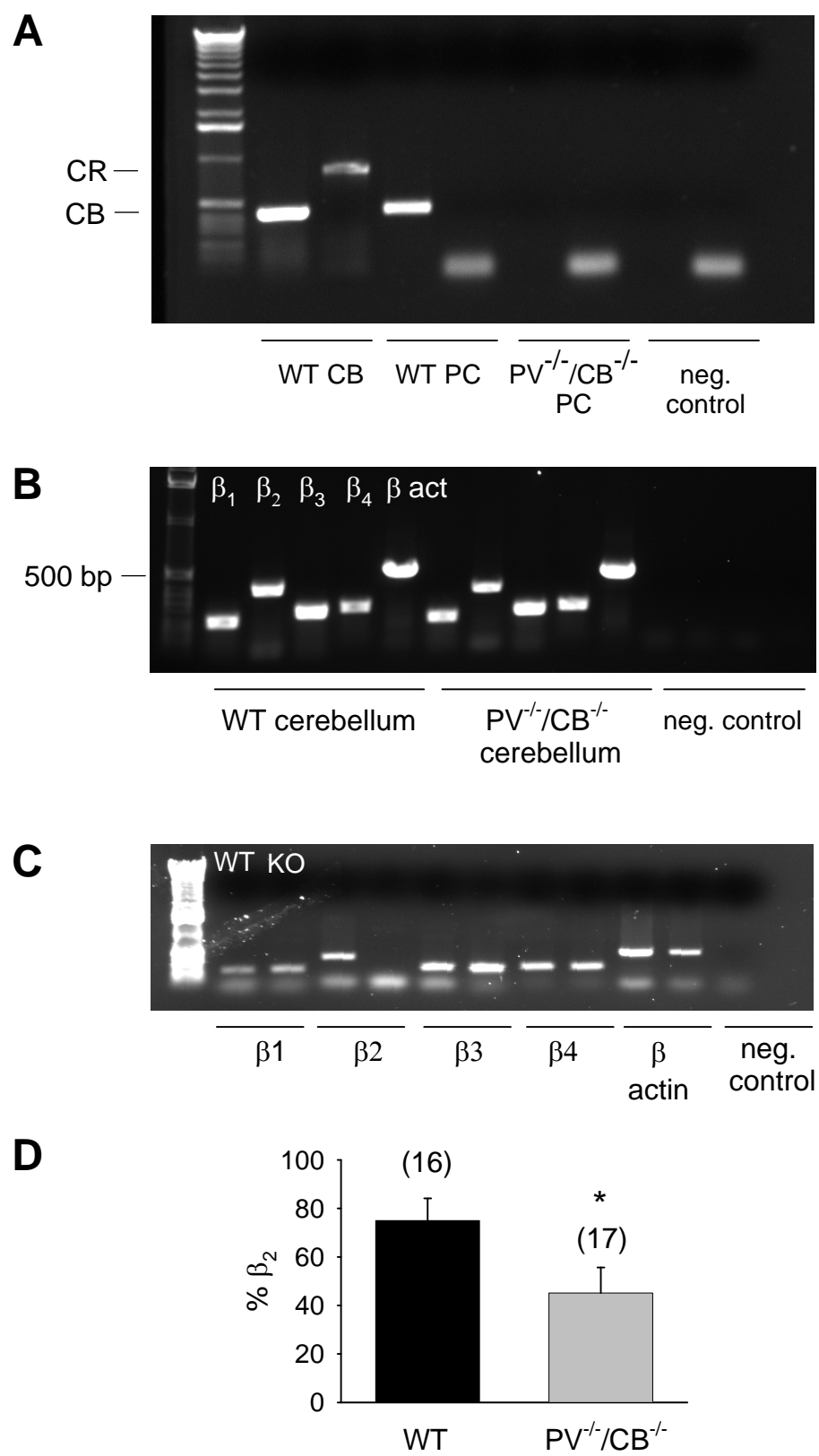
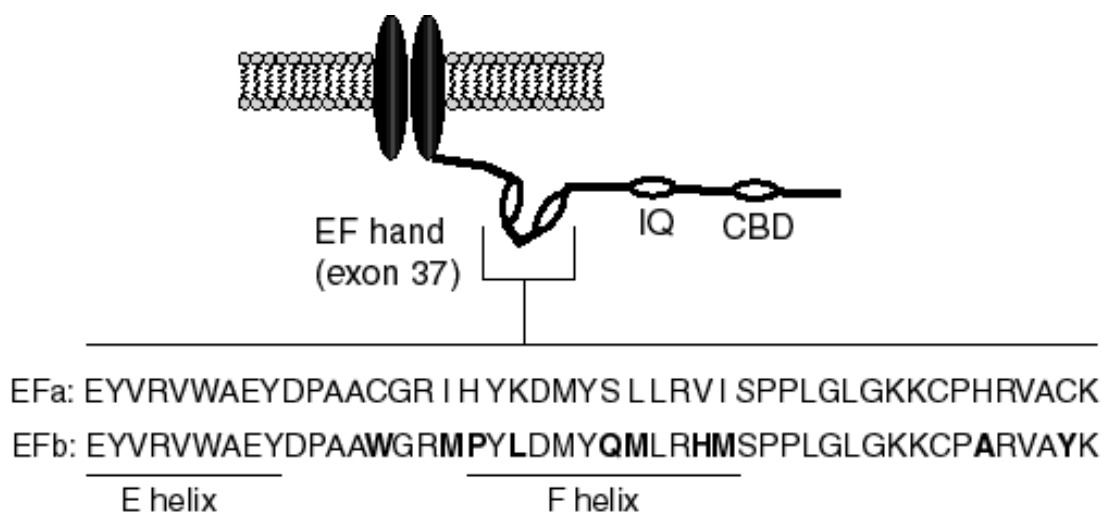


Figure 4.6: Comparison of $\text{Ca}_v\beta$ subunit expression in WT and $\text{PV}^{-/-}/\text{CB}^{-/-}$ neurons. A. RT-PCR analysis was performed on cerebellar tissue from WT mice (lanes 2 and 3), Purkinje neurons isolated from wild-type (lanes 4 and 5) or $\text{PV}^{-/-}/\text{CB}^{-/-}$ (lanes 6 and 7) mice, and a recording electrode where no cell was harvested (lanes 8 and 9). Primers specific to CB (432 bp, lanes 2, 4, 6 and 8) or CR (816 bp, lanes 3, 5, 7 and 9) were used. Ladder, extreme left. B. RT-PCR analysis was performed on cerebellar tissue from WT (lanes 2-6) and $\text{PV}^{-/-}/\text{CB}^{-/-}$ (lanes 7-11) mice or negative controls (lanes 12-15) using primers specific to $\text{Ca}_v\beta_1$ (235 bp, lanes 2, 7, and 12), $\text{Ca}_v\beta_2$ (412 bp, lanes 3, 8, and 13), $\text{Ca}_v\beta_3$ (270 bp, lanes 4, 9, and 14), $\text{Ca}_v\beta_4$ (296 bp, lanes 5, 10, and 15) and β -actin (539 bp, lanes 6 and 1). Ladder, extreme left. C. RT-PCR analysis was performed on Purkinje neurons isolated from wild-type (lanes 2, 4, 6, 8 and 10, from left) and $\text{PV}^{-/-}/\text{CB}^{-/-}$ (lanes 3, 5, 7, 9, and 11) mice. Primers specific to $\text{Ca}_v\beta_1$ (lanes 2 and 3), $\text{Ca}_v\beta_2$ (lanes 4 and 5), $\text{Ca}_v\beta_3$ (lanes 6 and 7) $\text{Ca}_v\beta_4$ (lanes 8 and 9) subunits and β -actin (lanes 10 and 11) were used. Ladder, extreme left. D. Single-cell RT-PCR analysis of isolated WT and $\text{PV}^{-/-}/\text{CB}^{-/-}$ Purkinje neurons was used to test for the presence of mRNA encoding $\text{Ca}_v\beta_2$. Bars represent average percent of β_2 expressing neurons per animal \pm SEM. Average values were compared for WT (black bar) and $\text{PV}^{-/-}/\text{CB}^{-/-}$ (grey bar) Purkinje neurons with an unpaired t-test. Sample sizes consisted of 1-3 neurons per animal, number of animals is shown in parenthesis (*, $p < 0.05$).

Figure 4.7

A



B

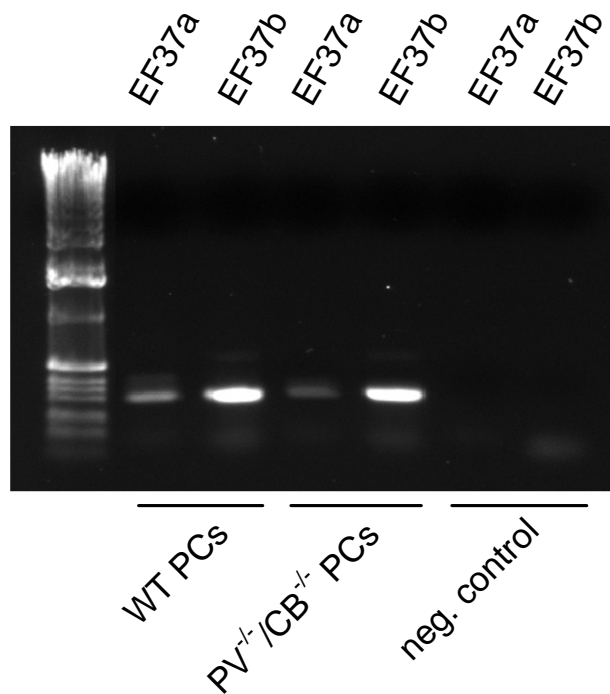


Figure 4.7: Comparison of Ca_v2.1 α1 splice variants in WT and PV^{+/-}/CB^{-/-} neurons. A.

Schematic diagram of Ca_v2.1 C-terminus showing the EF hand like region, IQ domain

and CBD. Amino acid sequence for two splice variants shown to produce facilitation of $Ca_v2.1$ (Chaudhuri et al., 2004), EF37a and EF37b, are shown below. Differences between EF37a and EF37b are in bold. B. RT-PCR analysis was performed using primers specific to EF37a (220 bp, lanes 2, 4 and 6, from left) or EF37b (220 bp, lanes 3, 5 and 7) splice variants in isolated WT (lanes 2 and 3), $PV^{-/-}/CB^{-/-}$ (lanes 4 and 5) Purkinje cells, or electrodes where no cell was harvested (negative control, lanes 6 and 7). Ladder, extreme left.

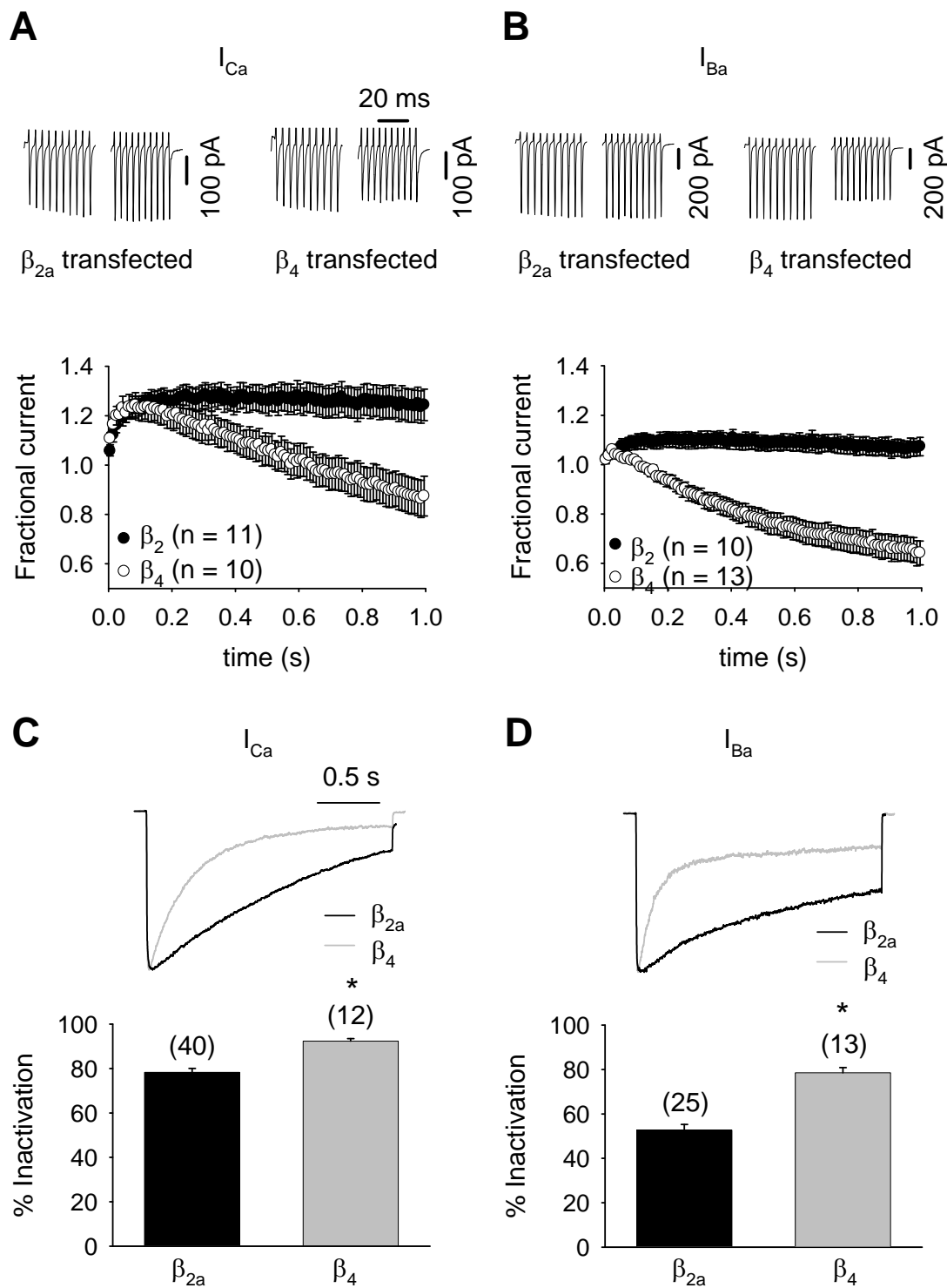


Figure 4.8: Characterization of $Ca_v2.1$ currents in 293T cells transfected with α_{1A} , $\alpha_2\delta$ and either β_{2a} or β_4 subunits. A. Voltage clamp protocols consisting of adjusted action potential waveforms (original action potential waveforms scaled to peak at +55 mV)

were applied at a frequency of 200 Hz to 293T cells transfected with α_{1A} , $\alpha_{2\delta}$ and β_{2a} or β_4 subunits in 10 mM extracellular Ca^{2+} . Current traces (top) show typical responses for the first and last 10 action potential waveforms for β_{2a} (left) or β_4 (right) transfected cells. Fractional current (bottom) is shown for average responses. Symbols correspond to average current values \pm SEM recorded in β_{2a} (closed circles) or β_4 (open circles) transfected cells. B. Average current values and example traces are shown as in (A) for 293T cells recorded in 10 mM Ba^{2+} extracellular solution. C. Traces (top) represent typical current responses to 2 s depolarizing pulses (-80 to +10 mV) for β_{2a} (black) and β_4 (gray) transfected cells. Percent inactivation (bottom) was determined $((1 - I_{\text{res}}/I_{\text{peak}}) * 100)$ for β_{2a} (black bars) and β_4 (gray bars) transfected cells. Bars represent mean \pm SEM; number of neurons in parentheses (*, $p < 0.05$). Recordings were obtained in (C) 10 mM Ca^{2+} or D. 10 mM Ba^{2+} extracellular solution. For I_{Ba} depolarizing pulses were -80 to 0 mV.

Chapter 5: Discussion

Ca^{2+} is used as a second messenger in a wide variety of physiological processes, and small changes in Ca^{2+} concentration can have a significant physiological impact. Therefore fine control of spatial and temporal patterns of Ca^{2+} signaling are critical for proper neuronal function. This dissertation project examined two factors that could modulate feedback regulation of $\text{Ca}_v2.1$: Ca^{2+} buffering proteins and Ca^{2+} release from intracellular stores. We hypothesized that these factors may influence $\text{Ca}^{2+}/\text{CaM}$ -dependent regulation of $\text{Ca}_v2.1$ by adjusting the Ca^{2+} available for binding to CaM. Our results suggest that Ca^{2+} -buffering proteins and Ca^{2+} release can alter Ca^{2+} -feedback regulation of $\text{Ca}_v2.1$ in unexpected ways, which may have physiological implications for neuronal Ca^{2+} signaling.

I_{Ca} and Ca^{2+} buffering proteins interact to regulate $\text{Ca}_v2.1$

CDI has traditionally been considered to be a process that is initiated by increases in global Ca^{2+} concentration in the vicinity of open Ca^{2+} channels. For $\text{Ca}_v2.1$, CDI is eliminated by high levels of intracellular Ca^{2+} buffering (Lee et al., 2000). In HEK 293T cells, we showed that the amount of CDI shows a non-linear dependence on the amplitude of I_{Ca} , with greater Ca^{2+} influx producing stronger CDI (Fig. 2.1). Our finding is consistent with the global Ca^{2+} hypothesis, since larger current amplitude means that more Ca^{2+} influx will occur, which will result in increased Ca^{2+} binding to CaM. These results are meaningful because they show that factors affecting $\text{Ca}_v2.1$ current density, such as disease causing mutations, will significantly affect negative feedback regulation of the channel by Ca^{2+} . For example, Soong et al. (2002) showed that splice variants of

the $\alpha_{12.1}$ subunit that inhibit $\text{Ca}_v2.1$ current densities, show limited CDI. Up- or down regulation of such splice variants may therefore provide a mechanism of controlling Ca^{2+} influx through open $\text{Ca}_v2.1$ channels.

An important feature of any Ca^{2+} chelator is the kinetics of Ca^{2+} binding. The affinity (K_d) and rate of Ca^{2+} binding (k_{on}) determine the speed and length of time that a Ca^{2+} ion will be bound. Our findings suggest that an equally important determinant of the actions of a Ca^{2+} buffer is the rate at which Ca^{2+} dissociates, determined by the off rate (k_{off}). In contrast to our original hypothesis, we found that PV differentially regulates CDI depending on I_{Ca} amplitude (Fig. 2.3 and 2.4), as evidenced by PV enhancing CDI in HEK 293T cells with large amplitude I_{Ca} . This unexpected result may indicate a role of Ca^{2+} buffering proteins in binding, shuttling, and unbinding Ca^{2+} within the microdomain that regulates feedback inhibition of $\text{Ca}_v2.1$. In addition, we found that EGTA and BAPTA, two exogenous Ca^{2+} buffers with very different Ca^{2+} buffering kinetics, differentially influence CDI (Fig. 2.2). Other studies have shown that buffers with different Ca^{2+} binding kinetics can differentially influence spatiotemporal patterns of Ca^{2+} signals. For example, (Dargan et al., 2004) showed that infusion of PV into *Xenopus* oocytes shortened IP_3 evoked Ca^{2+} signals and localized Ca^{2+} ions to discrete areas, while infusion of CR, a Ca^{2+} buffering protein with much faster Ca^{2+} binding kinetics, prolonged Ca^{2+} signals and produced a more uniform distribution of Ca^{2+} ions. Since CDI is strongly influenced by spatial and temporal distribution of Ca^{2+} signals, Ca^{2+} buffering proteins are likely to play an important role in regulating the function of $\text{Ca}_v2.1$.

Since binding kinetics of Ca^{2+} -buffering proteins play a fundamental role in determining the spatial and temporal pattern of Ca^{2+} signaling, the expression of specific

proteins in populations of neurons may be a method by which neurons can fine-tune Ca^{2+} -signaling to meet their specific needs. The size and morphology of a neuron may factor into which type of Ca^{2+} -buffering protein is expressed. For example, small fast-spiking GABAergic interneurons, such as cerebellar stellate and basket cells and hippocampal interneurons, typically express PV (Celio, 1990). This may indicate that PV performs a specific type of function in these neurons. CB is expressed in larger neurons, such as thalamic projection neurons and strionigral neurons, where its binding kinetics may make it more suited to handle larger Ca^{2+} influxes (Celio, 1990). For this reason, many different Ca^{2+} -buffering proteins may have evolved to handle specific needs of Ca^{2+} signaling in specific populations of neurons, which may be the reason that to date, at least 200 different Ca^{2+} -binding proteins have been identified in man (Schwaller et al., 2002).

At the single channel level, CDF results from the interaction of Ca^{2+} /CaM with $\text{Ca}_v2.1$ and represents an enhancement of the open probability of the channel (Chaudhuri et al., 2007). In $\text{PV}^{-/-}/\text{CB}^{-/-}$ mice, we observed a significant reduction in CDF compared to WT mice (Fig. 4.5). This decrease in facilitation may result from differential expression of a splice variant of the $\alpha 1$ subunit of the channel that is upregulated in $\text{PV}^{-/-}/\text{CB}^{-/-}$ mice. The effect of this decrease in facilitation results in smaller and shorter duration of Ca^{2+} influx into the channel in $\text{PV}^{-/-}/\text{CB}^{-/-}$ neurons. This response would make sense in neurons lacking PV and CB because it limits the amount of Ca^{2+} that can enter the cell, thus decreasing the risk of cell death due to Ca^{2+} excitotoxicity.

Since CDI depends on Ca^{2+} influx through more distal channels, it is not measurable at the single channel level. However, voltage-dependent mechanisms of

channel inactivation can be measured at single channels. Modulation of inactivation of $\text{Ca}_v2.1$ by different isoforms of the β subunit is achieved by a transition from a fast to a slower gating mode, where channels display longer mean closed times, greater latency to first opening and larger depolarizations are necessary to open the channel (Luvisetto et al., 2004). These transitions between fast and slow gating can occur when any β subunit is expressed, but the specific β subunit isoform regulates the relative occurrence of the fast and slow modes. In our experiments, we discovered a downregulation of the β_{2a} subunit, which promotes the slower gating mode, in $\text{PV}^{-}/\text{CB}^{-}$ Purkinje neurons (Fig. 4.6C-D). The downregulation of this subunit allows other β subunit isoforms to be predominantly expressed, which allows faster inactivation of the channel. Increasing the rate and amount of inactivation limits the amount of Ca^{2+} entering the channel, which results in a more moderate Ca^{2+} signal and may compensate for the lack of Ca^{2+} -buffering proteins.

While the role of Ca^{2+} influx through Ca_v1 channels in stimulating CREB-activated gene expression has been characterized (Murphy et al., 1991), an analogous role for $\text{Ca}_v2.1$ has not been extensively investigated. However, Ca^{2+} influx through $\text{Ca}_v2.1$ has been shown to regulate the expression of syntaxin-1A, a presynaptic protein involved in neurotransmitter release. Influx of Ca^{2+} through $\text{Ca}_v2.1$ initiates CICR, resulting in syntaxin-1A being expressed in an activity-dependent manner in transfected cells (Sutton et al., 1999). Alterations in the Ca^{2+} signal produced by $\text{Ca}_v2.1$ channels in PV/CB^{-} neurons may similarly cause changes in $\text{Ca}_v\beta$ subunit at the transcriptional level that help offset the Ca^{2+} buffering defect in these neurons.

Future studies might focus on correlating Ca^{2+} signaling with alterations in CDI in WT and $\text{PV}^{-/-}/\text{CB}^{-/-}$ Purkinje neurons. Imaging of Ca^{2+} signals with ratiometric Ca^{2+} indicators, such as fura-2, could be paired with physiological stimulation of Purkinje neurons to simultaneously quantify Ca^{2+} signals and CDI. This would allow characterization of differences in Ca^{2+} signaling between WT and $\text{PV}^{-/-}/\text{CB}^{-/-}$ Purkinje neurons, and help to define the role of Ca^{2+} buffering proteins in regulating Ca^{2+} signaling. In addition, the individual contribution of PV and CB to CDI could be characterized by similar investigations in $\text{PV}^{-/-}$ and $\text{CB}^{-/-}$ single knockout mice. The differences in Ca^{2+} buffering kinetics between these two proteins (Schmidt et al., 2003b), may underlie different consequences for $\text{Ca}_v2.1$ regulation.

Since the loss of PV and CB produces mice with impaired motor coordination (Airaksinen et al., 1997; Servais et al., 2005), it would be interesting to determine the mechanism by which altered Ca^{2+} buffering affects action potential firing properties. $\text{PV}^{-/-}/\text{CB}^{-/-}$ Purkinje neurons have been shown to fire faster *in vivo* (Servais et al., 2005). Since P/Q-type currents in these cells activate K_{Ca} channels (Womack et al., 2004), a possible link between enhanced CDI and faster firing due limited activation of K_{Ca} channels could be established. Spontaneous and/or evoked action potentials in WT and $\text{PV}^{-/-}/\text{CB}^{-/-}$ Purkinje neurons could be compared to determine if changes in Ca^{2+} buffering result in altered action potential parameters, such as the amplitude or duration of the AHP. This would provide further evidence for a mechanism by which CDI of $\text{Ca}_v2.1$ could influence motor output.

Factors that affect feedback regulation of $\text{Ca}_v2.1$ by CICR

In HEK 293T cells, the application of caffeine caused increased CDI, presumably by eliciting Ca^{2+} release from intracellular stores. However, with the ability of caffeine to act on multiple targets, we could not conclusively state that CICR contributes to CDI in HEK 293T cells. In neurons, CICR is an important contributor to Ca^{2+} signaling and may contribute to CDI of $\text{Ca}_v2.1$. This process could be influenced by several factors. First, the proximity of the endoplasmic reticulum to the plasma membrane will determine the speed and likelihood of CICR occurring. Since Ca^{2+} concentration decreases with increasing distance from the channel, IP_3Rs and RyRs have to be in close enough proximity that increases in Ca^{2+} concentration are sufficient to activate Ca^{2+} release. This condition is met in Purkinje neurons, where the endoplasmic reticulum extends into dendritic spines and can release Ca^{2+} upon stimulation of parallel fiber inputs to the spine (Martone et al., 1993).

Second, the amount of Ca^{2+} released from stores will determine the magnitude of CDI. Large amounts of Ca^{2+} release from stores, relative to the amount of Ca^{2+} entering through the plasma membranes would be sufficient to raise global Ca^{2+} concentration and initiate CDI. In Purkinje neurons, stimulation of climbing fibers produces much larger Ca^{2+} release from stores in comparison to the amount entering through $\text{Ca}_v2.1$ (Miyakawa et al., 1992). Additionally, IP_3Rs and RyRs are inhibited at high Ca^{2+} concentrations (0.1-1 mM for IP_3Rs and 1-10 mM for RyRs). Therefore large Ca^{2+} influxes (>10 mM) could cause a cessation of intracellular Ca^{2+} release which would subsequently limit feedback regulation of $\text{Ca}_v2.1$ (Finch et al., 1991; Bull and Marengo, 1993).

Third, relative expression levels of RyRs and IP_3Rs could influence how CDI is regulated in neurons. Since caffeine is mainly thought to exert its effect on RyRs by

lowering the threshold of activation (Hernández Cruz et al., 1995; Kong et al., 2008), differential expression of IP₃Rs and RyRs could have affected the amount of CDI detected in our experiments. Increased expression of RyRs would have resulted in greater amounts of Ca²⁺ release and thus greater CDI. Although blocking IP₃Rs eliminated the increase in CDI caused by caffeine (Fig 3.3), these effects are not thought to be a result of direct activation of the receptor (Luo et al., 2005), and therefore would likely produce a lesser effect on CDI. Since HEK cells are thought to express relatively high levels of IP₃Rs compared to RyRs, this could explain why CICR did not seem to contribute to CDI in control conditions (Fig. 3.3).

Fourth, Ca²⁺ sequestration by Ca²⁺ pumps and transporters can affect the rate of Ca²⁺ clearance and alter the global Ca²⁺ concentration that promotes CDI (Wanaverbecq et al., 2003). The expression of these pumps may differ in HEK293T cells and neurons. Since HEK293T cells do not endogenously express Ca²⁺ channels, these cells may not be well equipped to handle large Ca²⁺ influxes resulting in slower Ca²⁺ clearance. This buildup of Ca²⁺ would result in increased CDI in HEK293T cells. However, since the I_{res}/I_{peak} ratio is similar for HEK293T cells and Purkinje neurons (Figs 2.1 and 4.4A), it could be argued that either existing Ca²⁺ clearance mechanisms are sufficient to handle this increased Ca²⁺ influx in HEK293T cells, or a compensatory upregulation of Ca²⁺ pumps and transporters could occur in Ca_v2.1 transfected cells that allows these mechanisms to clear the additional Ca²⁺ (Patterson et al., 2007).

In Purkinje neurons, CICR has been well characterized and has been shown to be important for physiological processes such as induction of phasic firing (Li and Hatton, 1997). Whole cell voltage clamp analysis of dissociated Purkinje neurons could be

combined with Ca^{2+} imaging to analyze the effect of repetitive depolarizations on CICR and CDI. Blockers of Na^+ , K^+ , and other Ca^{2+} channels would be used to isolate P/Q-type currents. Experiments could be performed in the presence and absence of intracellular Ca^{2+} release blockers (heparin and ruthenium red) to determine the amount of enhancement of CDI that is caused by CICR. These experiments would establish the physiological significance of CICR in $\text{Ca}_v2.1$ channel regulation.

Potential consequences of altered $\text{Ca}_v2.1$ feedback regulation for neuronal function

Traditionally, the expression of Ca^{2+} -buffering proteins have been thought of as a mechanism for the neuron to buffer large Ca^{2+} influxes. Our results suggest that the role of these proteins is more complex than previously thought. These proteins may assist in Ca^{2+} shuttling by sequestering free Ca^{2+} ions in the cytoplasm, limiting their possible interactions with other Ca^{2+} -binding proteins, and allowing them to be released at more distal sites from the channel. This assisted diffusion would allow Ca^{2+} signaling to occur at sites more distant from the mouth of the channel.

One of the most widely recognized functions of $\text{Ca}_v2.1$ channels is their role in neurotransmitter release. Neurotransmitter release is proportional to the fourth power of Ca^{2+} concentration, and therefore will be affected by alterations in the influx of Ca^{2+} through $\text{Ca}_v2.1$ (Dodge and Rahamimoff, 1967; Mintz et al., 1995). A decreased role for CDI in determining the strength of coupling between $\text{Ca}_v2.1$ channels and exocytosis has been demonstrated in chromaffin cells (Wykes et al., 2007). In this case, $\text{Ca}_v2.1$ channels, which inactivate more slowly than $\text{Ca}_v2.2$, may play a dominant role in neurotransmitter release. Since they are more resistant to inactivation, $\text{Ca}_v2.1$ channels will continue to

mediate neurotransmitter release when Ca^{2+} concentration is elevated, thus prolonging neural signaling. The expression of Ca^{2+} buffering proteins could function to slow CDI and further prolong neurotransmitter release (Zaitsev et al., 2007). In this situation factors that modulate feedback regulation of $\text{Ca}_v2.1$ would have a direct impact on continued neurotransmitter release.

Paired pulse depression, associated with decreased neurotransmitter release, has been observed in paired neuronal recordings where PV was knocked out or removed by dialysis through the whole-cell recording electrode (Caillard et al., 2000; Muller et al., 2007). This effect of PV depends on its ability to increase the initial phase of the decay of Ca^{2+} transients. This prevents Ca^{2+} buildup upon subsequent stimulation and reduces facilitation. Our findings are generally consistent with these studies, since we observed increased inactivation in $\text{PV}^{-/-}/\text{CB}^{-/-}$ Purkinje neurons, which would lead to decreased Ca^{2+} influx. This would limit residual Ca^{2+} buildup in the presynaptic neuron, resulting in decreased neurotransmitter release, leading to a depression of the postsynaptic IPSP upon repetitive stimulation. However, the effects that we observed were mainly due to the change in subunit composition in $\text{PV}^{-/-}/\text{CB}^{-/-}$ mice and not directly due to the actions of Ca^{2+} buffering proteins.

To determine the effect of PV and CB on CDI, whole cell measurements of CDI in WT Purkinje neurons could be done before and after PV and CB are dialyzed out of the neuron by exchange of solution with the recording pipette. This approach would eliminate variability in measurement of CDI due to alterations in channel subunit composition in $\text{PV}/\text{CB}^{-/-}$ neurons. Another approach would be to create an inducible knockout mouse. This would allow $\text{Ca}_v2.1$ channels to express their normal subunit

profile, and recordings could be performed without having to wait for Ca^{2+} -buffering proteins to be dialyzed by the recording solution. Ideally, these methods could be combined with high-speed Ca^{2+} imaging to determine the effect of Ca^{2+} -buffering proteins on the spatial and temporal patterns of Ca^{2+} signaling. Additionally, the creation of fluorescently labeled PV or CB could be used to determine the subcellular localization and examine the mobility of these proteins. This would aid in determining the role that Ca^{2+} -buffering proteins play in Ca^{2+} shuttling.

Role of $\text{Ca}_v2.1$ in network function and pathological conditions

Since Ca^{2+} -buffering proteins are expressed only in specific populations of neurons, the lack of expression of these proteins will alter firing properties in only these specific populations. This could result in imbalanced firing in neural circuits. For example, loss of PV and CB has been shown to cause synchronous firing of Purkinje neurons along parallel fiber beams (Servais et al., 2005). This could indicate that precise control of Ca^{2+} signaling is required to maintain asynchronous firing in networks. Altered Ca^{2+} -buffering protein expression has also been shown to occur in some neurodegenerative diseases and mood disorders that involve altered firing in neural networks. For example, an increased number and proportion of PV positive GPi neurons and a decreased proportion in the caudate and putamen were found in patients with Tourettes syndrome (Kalanithi et al., 2005). In addition, a decreased proportion of PV interneurons were found in the entorhinal cortex of patients with bipolar disorder (Pantazopoulou et al., 2007). These findings may indicate a role for Ca^{2+} buffering proteins in the precise control of Ca^{2+} signaling and the maintenance of network firing.

One controversial aspect of Ca^{2+} -buffering proteins is the role that they play in protecting neurons from neurodegenerative diseases. Several studies have linked the expression of Ca^{2+} -buffering proteins with increased resistance to cell death brought about by Ca^{2+} -mediated excitotoxicity (Ho et al., 1996; Van Den Bosch et al., 2002). However, contradictory findings by other groups have indicated that the expression of Ca^{2+} buffering proteins may actually increase vulnerability to cell death by impairing Ca^{2+} sequestration (Yenari et al., 2001; Maetzler et al., 2004). These conflicting results may arise from the fact that CDI is increased in neurons that lack Ca^{2+} buffers, which limits the amount of Ca^{2+} influx. Our data from PV/CB^{-/-} Purkinje neurons support this idea, since the loss of Ca^{2+} buffering proteins not only increased CDI, but also signaled for compensatory changes to occur that also increased VDI. Based on our results, little evidence exists to support the idea that these proteins are important for neuroprotection.

$\text{Ca}_v2.1$ channels play a critical role in neuronal function by regulating physiological processes such as neurotransmitter release, synaptic plasticity, and neuronal excitability (Wheeler and Randall, 1994; Womack et al., 2004; Kang et al., 2006). Genetic alterations in $\text{Ca}_v2.1$ also produce pathological conditions such as migraine, epilepsy and ataxia (Zhuchenko et al., 1997; Kraus et al., 1998; Jouvenceau et al., 2001). We have shown that two potential modulators of $\text{Ca}_v2.1$, Ca^{2+} buffering proteins and Ca^{2+} release from intracellular stores, regulate the channel via multiple pathways. A more complete understanding of the mechanisms that underlie $\text{Ca}_v2.1$ regulation may permit new ways to pharmacologically manipulate these channels, which could be relevant to the treatment of pathological conditions involving aberrant Ca^{2+} signaling.

References

- Adkins C E, Morris S A, De Smedt H, Sienaert I, Török K, Taylor C W (2000) Ca^{2+} -calmodulin inhibits Ca^{2+} release mediated by type-1, -2 and -3 inositol trisphosphate receptors. *Biochem J* 345:357-363.
- Airaksinen MS, Eilers J, Garaschuk O, Thoenen H, Konnerth A, Meyer M (1997) Ataxia and altered dendritic calcium signaling in mice carrying a targeted null mutation of the calbindin D28k gene. *Proc Natl Acad Sci USA* 94:1488-93.
- Anderson K, Lai F, Liu Q, Rousseau E, Erickson H, Meissner G (1989) Structural and functional characterization of the purified cardiac ryanodine receptor- Ca^{2+} release channel complex. *J Biol Chem* 264:1329-1335.
- Arias-Montano JA, Floran B, Floran L, Aceves J, Young JM (2007) Dopamine D(1) receptor facilitation of depolarization-induced release of gamma-amino-butyric acid in rat striatum is mediated by the cAMP/PKA pathway and involves P/Q-type calcium channels. *Synapse* 61:310-9.
- Barski JJ, Hartmann J, Rose CR, Hoebeek F, Morl K, Noll-Hussong M, De Zeeuw CI, Konnerth A, Meyer M (2003) Calbindin in cerebellar Purkinje cells is a critical determinant of the precision of motor coordination. *J Neurosci* 23:3469-77.
- Bastianelli E (2003) Distribution of calcium-binding proteins in the cerebellum. *Cerebellum* 2:242-62.
- Bernatchez G, Talwar D, Parent L (1998) Mutations in the EF-hand motif impair the inactivation of barium currents of the cardiac $\alpha_1\text{C}$ channel. *Biophys J*

75:1727-39.

- Berrow NS, Campbell V, Fitzgerald EM, Brickley K, Dolphin AC (1995) Antisense depletion of beta-subunits modulates the biophysical and pharmacological properties of neuronal calcium channels. *J Physiol* 482 (Pt 3):481-91.
- Birnbaumer L, Campbell KP, Catterall WA, Harpold MM, Hofmann F, Horne WA, Mori Y, Schwartz A, Snutch TP, Tanabe T, Tsien RW (1994) The naming of voltage-gated calcium channels. *Neuron* 13:505-506.
- Black DF, Kung S, Sola CL, Bostwick MJ, Swanson JW (2004) Familial hemiplegic migraine, neuropsychiatric symptoms, and Erdheim-Chester disease. *Headache* 44:911-5.
- Blatow M, Caputi A, Burnashev N, Monyer H, Rozov A (2003) Ca^{2+} buffer saturation underlies paired pulse facilitation in calbindin- D28k-containing terminals. *Neuron* 38:79-88.
- Bodding M, Penner R (1999) Differential modulation of voltage-dependent Ca^{2+} currents by EGTA and BAPTA in bovine adrenal chromaffin cells. *Pflugers Arch Eur J Physiol* 439:27-38.
- Borst JG, Sakmann B (1998) Facilitation of presynaptic calcium currents in the rat brainstem. *J Physiol (Lond)* 513 :149-155.
- Bourinet E, Soong TW, Sutton K, Slaymaker S, Mathews E, Monteil A, Zamponi GW, Nargeot J, Snutch TP (1999) Splicing of alpha 1A subunit gene generates

phenotypic variants of P- and Q-type calcium channels. *Nature Neurosci* 2:407-15.

Brehm P, Eckert R (1978) Calcium entry leads to inactivation of calcium channel in *Paramecium*. *Science* 202:1203-1206.

Brice NL, Berrow NS, Campbell V, Page KM, Brickley K, Tedder I, Dolphin AC (1997) Importance of the different beta subunits in the membrane expression of the alpha1A and alpha2 calcium channel subunits: studies using a depolarization-sensitive alpha1A antibody. *Eur J Neurosci* 9:749-59.

Brody DL, Yue DT (2000) Relief of G-Protein Inhibition of Calcium Channels and Short-Term Synaptic Facilitation in Cultured Hippocampal Neurons. *J Neurosci* 20:889-898.

Bull R, Marengo JJ (1993) Sarcoplasmic reticulum release channels from frog skeletal muscle display two types of calcium dependence. *FEBS Lett* 331:223-7.

Bultynck G, Sienaert I, Parys JB, Callewaert G, De Smedt H, Boens N, Dehaen W, Missiaen L (2003-) Pharmacology of inositol trisphosphate receptors. *Pflugers Arch Eur J Physiol* 445:629-642.

Burgess DL, Biddlecome GH, McDonough SI, Diaz ME, Zilinski CA, Bean BP, Campbell KP, Noebels JL (1999) Beta subunit reshuffling modifies N- and P/Q-type Ca²⁺ channel subunit compositions in lethargic mouse brain. *Mol Cell Neurosci* 13:293-311.

- Caillard O, Moreno H, Schwaller B, Llano I, Celio MR, Marty A (2000) Role of the calcium-binding protein parvalbumin in short-term synaptic plasticity. *Proc Natl Acad Sci USA* 97:13372-7.
- Cao YQ, Tsien RW (2005) Effects of familial hemiplegic migraine type 1 mutations on neuronal P/Q-type Ca²⁺ channel activity and inhibitory synaptic transmission. *Proc Natl Acad Sci USA* 102:2590-5.
- Carbone E, Lux HD (1984) A low voltage-activated, fully inactivating Ca channel in vertebrate sensory neurones. *Nature* 310:501-502.
- Carter AG, Vogt KE, Foster KA, Regehr WG (2002) Assessing the Role of Calcium-Induced Calcium Release in Short-Term Presynaptic Plasticity at Excitatory Central Synapses. *J Neurosci* 22:21-28.
- Carter DS, Harrison AJ, Falenski KW, Blair RE, DeLorenzo RJ (2008) Long-term decrease in calbindin-D28K expression in the hippocampus of epileptic rats following pilocarpine-induced status epilepticus. *Epilepsy Res* 79:213-23.
- Castellano A, Wei X, Birnbaumer L, Perez-Reyes E (1993) Cloning and expression of a neuronal calcium channel beta subunit. *J Biol Chem* 268:12359-12366.
- Catterall WA (1999) Interactions of Presynaptic Ca²⁺ channels and snare proteins in neurotransmitter release. *Ann NY Acad Sci* 868(1):144-159.
- Cavelier P, Pouille F, Desplantez T, Beekenkamp H, Bossu JL (2002) Control of the propagation of dendritic low-threshold Ca²⁺ spikes in Purkinje cells from rat

cerebellar slice cultures. *J Physiol* 540:57-72.

Celio MR (1990) Calbindin D-28k and parvalbumin in the rat nervous system. *Neurosci* 35 :375-475.

Cens T, Restituito S, Charnet P (1999) Regulation of Ca-sensitive inactivation of a 1-type Ca^{2+} channel by specific domains of beta subunits. *FEBS Lett* 450:17-22.

Chard PS, Bleakman D, Christakos S, Fullmer CS, Miller RJ (1993) Calcium buffering properties of calbindin D28k and parvalbumin in rat sensory neurones. *J Physiol* 472:341-357.

Charnet P, Bourinet E, Dubel SJ, Snutch TP, Nargeot J (1994) Calcium currents recorded from a neuronal alpha 1C L-type calcium channel in *Xenopus* oocytes. *FEBS Lett* 344:87-90.

Chaudhuri D, Alseikhan BA, Chang SY, Soong TW, Yue DT (2005) Developmental activation of calmodulin-dependent facilitation of cerebellar P-type Ca^{2+} current. *J Neurosci* 25:8282-8294.

Chaudhuri D, Chang S-Y, DeMaria CD, Alvania RS, Soong TW, Yue DT (2004) Alternative Splicing as a Molecular Switch for Ca^{2+} /Calmodulin-Dependent Facilitation of P/Q-Type Ca^{2+} Channels. *J Neurosci* 24:6334-6342.

Chaudhuri D, Issa JB, Yue DT (2007) Elementary Mechanisms Producing Facilitation of $Ca_v2.1$ (P/Q-type) Channels. *J Gen Physiol* 129:385-401.

Chen G, Racay P, Bichet S, Celio MR, Egli P, Schwaller B (2006) Deficiency in

parvalbumin, but not in calbindin D-28k upregulates mitochondrial volume and decreases smooth endoplasmic reticulum surface selectively in a peripheral, subplasmalemmal region in the soma of Purkinje cells. *Neuroscience* 142:97-105.

Chen YH, Li MH, Zhang Y, He LL, Yamada Y, Fitzmaurice A, Shen Y, Zhang H, Tong L, Yang J (2004) Structural basis of the alpha1-beta subunit interaction of voltage-gated Ca^{2+} channels. *Nature* 429:675-80.

Cheney RE, Mooseker MS (1992) Unconventional myosins. *Curr Opin Cell Biol* 4:27-35.

Chin D, Means AR (2000) Calmodulin: a prototypical calcium sensor. *Trends Cell Biol* 10:322-328.

Cibulsky SM, Sather WA (1999) Block by Ruthenium Red of Cloned Neuronal Voltage-Gated Calcium Channels. *J Pharmacol Exp Ther* 289:1447-1453.

Cohen RM, Foell JD, Balijepalli RC, Shah V, Hell JW, Kamp TJ (2005) Unique modulation of L-type Ca^{2+} channels by short auxiliary beta1d subunit present in cardiac muscle. *Am J Physiol Heart Circ Physiol* 288:H2363-2374.

Copello JA, Barg S, Onoue H, Fleischer S (1997) Heterogeneity of Ca^{2+} gating of skeletal muscle and cardiac ryanodine receptors. *Biophys J* 73:141-156.

Copello JA, Barg S, Sonnleitner A, Porta M, Diaz-Sylvester P, Fill M, Schindler H, Fleischer S (2002) Differential activation by Ca^{2+} , ATP and caffeine of cardiac and skeletal muscle ryanodine receptors after block by Mg^{2+} . *J Membr Biol* 187:51-64.

- Craig PJ, McAinsh AD, McCormack AL, Smith W, Beattie RE, Priestley JV, Yip JL AS, Longbottom ER, Volsen SG (1998) Distribution of the voltage-dependent calcium channel alpha(1A) subunit throughout the mature rat brain and its relationship to neurotransmitter pathways. *J Comp Neurol* 397:251-267.
- Cui G, Meyer AC, Calin-Jageman I, Neef J, Haeseleer F, Moser T, Lee A (2007) Ca²⁺-binding proteins tune Ca²⁺-feedback to Cav1.3 channels in mouse auditory hair cells. *J Physiol* 585:791-803.
- Cuttle MF, Tsujimoto T, Forsythe ID, Takahashi T (1998) Facilitation of the presynaptic calcium current at an auditory synapse in rat brainstem. *J Physiol (Lond)* 512:723-729.
- Dargan SL, Parker I (2003) Buffer kinetics shape the spatiotemporal patterns of IP₃-evoked Ca²⁺ signals. *J Physiol (Lond)* 553:775-788.
- Dargan SL, Schwaller B, Parker I (2004) Spatiotemporal patterning of IP₃-mediated Ca²⁺ signals in *Xenopus* oocytes by Ca²⁺-binding proteins. *J Physiol (Lond)* 556:447-461.
- Darrow E, Strahlendorf JC, Strahlendorf HK (1991) Extracellular magnesium concentration alters Purkinje cell responsiveness to serotonin and analogues. *Eur J Pharmacol* 209:19-25.
- De Jongh K, Warner C, Catterall W (1990) Subunits of purified calcium channels. Alpha 2 and delta are encoded by the same gene. *J Biol Chem* 265:14738-14741.

- DeMaria CD, Soong TW, Alseikhan BA, Alvania RS, Yue DT (2001) Calmodulin bifurcates the local Ca^{2+} signal that modulates P/Q-type Ca^{2+} channels. *Nature* 411:484-489.
- Dick IE, Tadross MR, Liang H, Tay LH, Yang W, Yue DT (2008) A modular switch for spatial Ca^{2+} selectivity in the calmodulin regulation of Ca_v channels. *Nature* 451:830-834.
- Diverse-Pierluissi M, McIntire WE, Myung CS, Lindorfer MA, Garrison JC, Goy MF, Dunlap K (2000) Selective coupling of G protein beta gamma complexes to inhibition of Ca^{2+} channels. *J Biol Chem* 275:28380-5.
- Dodge FA, Rahamimoff R (1967) Co-operative activation of calcium ions in transmitter release at the neurotransmitter junction. *J Physiol* 193:419-432.
- Dunlap K, Luebke JI, Turner T.J. (1995) Exocytotic Ca^{2+} channels in mammalian central neurons. *Trends Neurosci* 18:89-98.
- Eberhard M, Erne P (1994) Calcium and magnesium binding to rat parvalbumin. *Eur J Biochem* 222:21-6.
- Edgerton JR, Reinhart PH (2003) Distinct contributions of small and large conductance Ca^{2+} -activated K^+ channels to rat Purkinje neuron function. *J Physiol* 548:53-69.
- Edmonds B, Reyes R, Schwaller B, Roberts WM (2000) Calretinin modifies presynaptic calcium signaling in frog saccular hair. *Nature Neurosci* 3:786-790.
- Elinder F, Nilsson J, Arhem P (2007) On the opening of voltage-gated ion channels.

Physiology & Behavior 92:1-7.

Erickson MG, Alseikhan BA, Peterson BZ, Yue DT (2001) Preassociation of Calmodulin with Voltage-Gated Ca^{2+} Channels Revealed by FRET in Single Living Cells.

Neuron 31:973-985.

Ertel EA, Campbell KP, Harpold MM, Hofmann F, Mori Y, Perez-Reyes E, Schwartz A, Snutch TP, Tanabe T, Birnbaumer L, Tsien RW, Catterall WA (2000)

Nomenclature of Voltage-Gated Calcium Channels. Neuron 25:533-535.

Fabiato A, Fabiato F (1975) Contractions induced by a calcium-triggered release of calcium from the sarcoplasmic reticulum of single skinned cardiac cells. J Physiol

249:469-95.

Fatt P, Katz B (1953) The electrical properties of crustacean muscle fibres. J Physiol

120:171-204.

Felix R, Gurnett CA, De Waard M, Campbell KP (1997) Dissection of functional domains of the voltage-dependent Ca^{2+} channel $\alpha_2\delta$ subunit. J Neurosci

17:6884-91.

Ferreira G, Yi J, Rios E, Shirokov R (1997) Ion-dependent inactivation of barium current through L-type calcium channels. J Gen Physiol 109:449-61.

Few AP, Lautermilch NJ, Westenbroek RE, Scheuer T, Catterall WA (2005) Differential Regulation of $\text{CaV}2.1$ Channels by Calcium-Binding Protein 1 and Visinin-Like

Protein-2 Requires N-Terminal Myristoylation. J Neurosci 25:7071-7080.

- Fierro L, Llano I (1996) High endogenous calcium buffering in Purkinje cells from rat cerebellar slices. *J Physiol (Lond)* 496 :617-625.
- Finch EA, Turner TJ, Goldin SM (1991) Calcium as a coagonist of inositol 1,4,5-trisphosphate-induced calcium release. *Science* 252:443-6.
- Forsythe ID, Tsujimoto T, Barnes-Davies M, Cuttle MF, Takahashi T (1998) Inactivation of presynaptic calcium current contributes to synaptic depression at a fast central synapse. *Neuron* 20:797-807.
- Fuentes O, Valdivia C, Vaughan D, Coronado R, Valdivia HH (1994) Calcium-dependent block of ryanodine receptor channel of swine skeletal muscle by direct binding of calmodulin. *Cell Calcium* 15:305-16.
- Gillis JM, Thomason D, Lefevre J, Kretsinger RH (1982) Parvalbumins and muscle relaxation: a computer simulation study. *J Muscle Res Cell Motil.* 3:377-398.
- Gruol DL, Netzeband JG, Quina LA, Blakely-Gonzalez PK (2005) Contribution of L-type channels to Ca²⁺ regulation of neuronal properties in early developing purkinje neurons. *Cerebellum* 4:128-39.
- Gurnett CA, Felix R, Campbell KP (1997) Extracellular interaction of the voltage-dependent Ca²⁺ channel alpha2delta and alpha1 subunits. *J Biol Chem* 272:18508-12.
- Hackney CM, Mahendrasingam S, Penn A, Fettiplace R (2005) The concentrations of calcium buffering proteins in mammalian cochlear hair cells. *J. Neurosci.*

25:7867-7875.

- Hagiwara S, Ozawa S, Sand O (1975) Voltage clamp analysis of two inward current mechanisms in the egg cell membrane of a starfish. *J Gen Physiol* 65:617-644.
- Haiech J, Derancourt J, Pechere JF, Demaille JG (1979) Magnesium and calcium binding to parvalbumins: evidence for differences between parvalbumins and an explanation of their relaxing function. *Biochemistry* 18:2752-2758.
- Hartley DM, Neve RL, Bryan J, Ullrey DB, Bak SY, Lang P, Geller AI (1996) Expression of the calcium-binding protein, parvalbumin, in cultured cortical neurons using a HSV-1 vector system enhances NMDA neurotoxicity. *Brain Res. Mol. Brain Res.* 40:285-296.
- Hashimoto T, Volk DW, Eggan SM, Mirnics K, Pierri JN, Sun Z, Sampson AR, Lewis DA (2003) Gene expression deficits in a subclass of GABA neurons in the prefrontal cortex of subjects with schizophrenia. *J Neurosci* 23:6315-26.
- Hernández Cruz A, Díaz Muñoz M, Gómez Chavarín M, Cañedo Merino R, Protti DA, Escobar AL, Sierralta J, Suárez Isla BA (1995) Properties of the Ryanodine-sensitive Release Channels that Underlie Caffeine-induced Ca^{2+} Mobilization from Intracellular Stores in Mammalian Sympathetic Neurons. *Euro J Neurosci* 7:1684-1699.
- Hirota J, Michikawa T, Natsume T, Furuichi T, Mikoshiba K (1999) Calmodulin inhibits inositol 1,4,5-trisphosphate-induced calcium release through the purified and reconstituted inositol 1,4,5-trisphosphate receptor type 1. *FEBS Letters* 456:322-

326.

- Ho BK, Alexianu ME, Colom LV, Mohamed AH, Serrano F, Appel SH (1996) Expression of calbindin-D28K in motoneuron hybrid cells after retroviral infection with calbindin-D28K cDNA prevents amyotrophic lateral sclerosis IgG-mediated cytotoxicity. *Proc Natl Acad Sci USA* 93:6796-801.
- Hobom M, Dai S, Marais E, Lacinova L, Hofmann F, Klugbauer N (2000) Neuronal distribution and functional characterization of the calcium channel α 2delta-2 subunit. *Eur J Neurosci* 12:1217-26.
- Hou TT, Johnson JD, Rall JA (1991) Parvalbumin content and Ca^{2+} and Mg^{2+} dissociation rates correlated with changes in relaxation rate of frog muscle fibres. *J Physiol (Lond)* 441:285-304.
- Houngaard J, Midtgaard J (1988) Intrinsic determinants of firing pattern in Purkinje cells of the turtle cerebellum in vitro. *J Physiol* 402:731-749.
- Huang M, Chida K, Kamata N, Nose K, Kato M, Homma Y, Takenawa T, Kuroki T (1988) Enhancement of inositol phospholipid metabolism and activation of protein kinase C in ras-transformed rat fibroblasts. *J Biol Chem* 263:17975-80.
- Imagawa T, Smith JS, Coronado R, Campbell KP (1987) Purified ryanodine receptor from skeletal muscle sarcoplasmic reticulum is the Ca^{2+} -permeable pore of the calcium release channel. *J Biol Chem* 262:16636-43.
- Imbrici P, Jaffe SL, Eunson LH, Davies NP, Herd C, Robertson R, Kullmann DM, Hanna

MG (2004) Dysfunction of the brain calcium channel $Ca_v2.1$ in absence epilepsy and episodic ataxia. *Brain* 127:2682-2692.

Inchauspe CG, Martini FJ, Forsythe ID, Uchitel OD (2004) Functional compensation of P/Q by N-type channels blocks short-term plasticity at the calyx of held presynaptic terminal. *J Neurosci* 24:10379-83.

Ito M (1984) *The Cerebellum and Neural Control*. New York: Raven Press.

Ito M, Kano M (1982) Long-lasting depression of parallel fiber-Purkinje cell transmission induced by conjunctive stimulation of parallel fibers and climbing fibers in the cerebellar cortex. *Neurosci Lett* 33:253-8.

Jay S, Sharp A, Kahl S, Vedvick T, Harpold M, Campbell K (1991) Structural characterization of the dihydropyridine-sensitive calcium channel alpha 2-subunit and the associated delta peptides. *J Biol Chem* 266:3287-3293.

Jen J, Wan J, Graves M, Yu H, Mock AF, Coulin CJ, Kim G, Yue Q, Papazian DM, Baloh RW (2001) Loss-of-function EA2 mutations are associated with impaired neuromuscular transmission. *Neurology* 57:1843-1848.

John LM, Mosquera-Caro M, Camacho P, Lechleiter JD (2001) Control of IP(3)-mediated Ca^{2+} puffs in *Xenopus laevis* oocytes by the Ca^{2+} -binding protein parvalbumin. *J Physiol (Lond)* 535:3-16.

Jouveneau A, Eunson LH, Spauschus A, Ramesh V, Zuberi SM, Kullmann DM, Hanna MG (2001) Human epilepsy associated with dysfunction of the brain P/Q-type

calcium channel. *Lancet* 358:801-7.

Jun K, Piedras-Renteria ES, Smith SM, Wheeler DB, Lee SB, Lee TG, Chin H, Adams ME, Scheller RH, Tsien RW, Shin HS (1999) Ablation of P/Q-type Ca^{2+} channel currents, altered synaptic transmission, and progressive ataxia in mice lacking the alpha(1A)-subunit. *Proc Natl Acad Sci USA* 96:15245-15250.

Kadowaki K, McGowan E, Mock G, Chandler S, Emson PC (1993) Distribution of calcium binding protein mRNAs in rat cerebellar cortex. *Neurosci. Lett.* 153:80-84.

Kalanithi PSA, Zheng W, Kataoka Y, DiFiglia M, Grantz H, Saper CB, Schwartz ML, Leckman JF, Vaccarino FM (2005) Altered parvalbumin-positive neuron distribution in basal ganglia of individuals with Tourette syndrome. *Proc Natl Acad Sci USA* 102:13307-13312.

Kang MG, Chen CC, Wakamori M, Hara Y, Mori Y, Campbell KP (2006) A functional AMPA receptor-calcium channel complex in the postsynaptic membrane. *Proc Natl Acad Sci USA* 103:5561-6.

Kano M, Garaschuk O, Verkhratsky A, Konnerth A (1995) Ryanodine receptor-mediated intracellular calcium release in rat cerebellar Purkinje neurones. *J Physiol* 487 :1-16.

Keynes R, Elinder F (1999) The screw-helical voltage gating of ion channels. *Proceedings of the Royal Society B: Biological Sciences* 266:843-852.

- Khodakhah K, Armstrong CM (1997) Inositol trisphosphate and ryanodine receptors share a common functional Ca^{2+} pool in cerebellar Purkinje neurons. *Biophysical J* 73:3349-57.
- Kohda K, Inoue T, Mikoshiba K (1995) Ca^{2+} release from Ca^{2+} stores, particularly from ryanodine-sensitive Ca^{2+} stores, is required for the induction of LTD in cultured cerebellar Purkinje cells. *J Neurophysiol* 74:2184-8.
- Kong H, Jones PP, Koop A, Zhang L, Duff HJ, Chen SR (2008) Caffeine induces Ca^{2+} release by reducing the threshold for luminal Ca^{2+} activation of the ryanodine receptor. *Biochem J*.
- Konnerth A, Dreessen J, Augustine GJ (1992) Brief dendritic calcium signals initiate long-lasting synaptic depression in cerebellar Purkinje cells. *Proc Natl Acad Sci USA* 89:7051-5.
- Kosaka T, Kosaka K, Nakayama T, Hunziker W, Heizmann CW (1993) Axons and axon terminals of cerebellar Purkinje cells and basket cells have higher levels of parvalbumin immunoreactivity than somata and dendrites: quantitative analysis by immunogold labeling. *Exp. Brain Res.* 93:483-491.
- Kraus RL, Sinnegger MJ, Glossmann H, Hering S, Striessnig J (1998) Familial hemiplegic migraine mutations change $\alpha_1\text{A}$ Ca^{2+} channel kinetics. *J Biol Chem* 273:5586-90.
- Kreiner L, Lee A (2006) Endogenous and Exogenous Ca^{2+} Buffers Differentially Modulate Ca^{2+} -dependent Inactivation of $\text{Ca}_v2.1$ Ca^{2+} Channels. *J Biol Chem*

281:4691-4698.

Krovetz HS, Helton TD, Crews AL, Horne WA (2000) C-Terminal Alternative Splicing Changes the Gating Properties of a Human Spinal Cord Calcium Channel alpha 1A Subunit. *J Neurosci* 20:7564-7570.

Kulik A, Nakadate K, Hagiwara A FY, Luján R, Saito H, Suzuki N, Futatsugi A, Mikoshiba K, Frotscher M, Shigemoto R (2004) Immunocytochemical localization of the alpha 1A subunit of the P/Q-type calcium channel in the rat cerebellum. *Eur J Neurosc* 19:2169-2178.

Kuwajima G, Futatsugi A, Niinobe M, Nakanishi S, Mikoshiba K (1992) Two types of ryanodine receptors in mouse brain: Skeletal muscle type exclusively in Purkinje cells and cardiac muscle type in various neurons. *Neuron* 9:1133-1142.

Lautermilch NJ, Few AP, Scheuer T, Catterall WA (2005) Modulation of CaV2.1 Channels by the Neuronal Calcium-Binding Protein Visinin-Like Protein-2. *J. Neurosci.* 25:7062-7070.

Laver DR, Baynes TM, Dulhunty AF (1997) Magnesium Inhibition of Ryanodine-Receptor Calcium Channels: Evidence for Two Independent Mechanisms. *J Memb Biol* 156:213-229.

Leao, Aristides A. P. Spreading Depression of Activity in the Cerebral Cortex. *J Neurophysiol* 7(6), 359-390. 44.

Lee A, Scheuer T, Catterall WA (2000) Ca²⁺/calmodulin-dependent facilitation and

inactivation of P/Q-type Ca²⁺ channels. *J. Neurosci.* 20:6830-6838.

Lee A, Westenbroek RE, Haeseleer F, Palczewski K, Scheuer T, Catterall WA (2002)

Differential modulation of Ca_v2.1 channels by calmodulin and Ca²⁺-binding protein 1. *Nature Neurosci* 5:210-7.

Lee A, Wong ST, Gallagher D, Li B, Storm DR, Scheuer T, Catterall WA (1999)

Ca²⁺/calmodulin binds to and modulates P/Q-type calcium channels. *Nature* 399:155-159.

Lee A, Zhou H, Scheuer T, Catterall WA (2003) Molecular determinants of

Ca²⁺/calmodulin-dependent regulation of Cav2.1 channels. *Proc. Natl. Acad. Sci. USA* 100:16059-16064.

Lee KS, Marban E, Tsien RW (1985) Inactivation of calcium channels in mammalian

heart cells: joint dependence on membrane potential and intracellular calcium. *J Physiol* 364:395-411.

Lee SH, Rosenmund C, Schwaller B, Neher E (2000a) Differences in Ca²⁺ buffering

properties between excitatory and inhibitory hippocampal neurons from the rat. *J Physiol (Lond)* 525:405-418.

Lee SH, Schwaller B, Neher E (2000b) Kinetics of Ca²⁺ binding to parvalbumin in

bovine chromaffin cells: implications for [Ca²⁺] transients of neuronal dendrites. *J Physiol (Lond)* 525:419-432.

Leveque C, Hoshino T, David P, Shoji-Kasai Y, Leys K, Omori A, Lang B, el Far O,

- Sato K, Martin-Moutot N (1992) The synaptic vesicle protein synaptotagmin associates with calcium channels and is a putative Lambert-Eaton myasthenic syndrome antigen. *Proc Natl Acad Sci USA* 89:3625-3629.
- Li-Smerin Y, Levitan ES, Johnson JW (2001) Free intracellular Mg(2+) concentration and inhibition of NMDA responses in cultured rat neurons. *J Physiol (Lond)* 533:729-743.
- Li Z, Decavel C, Hatton GI (1995) Calbindin-D28k: role in determining intrinsically generated firing patterns in rat supraoptic neurones. *J Physiol (Lond)* 488 (Pt 3):601-608.
- Li Z, Hatton GI (1997) Ca²⁺ release from internal stores: role in generating depolarizing after-potentials in rat supraoptic neurones. *J Physiol* 498 (Pt 2):339-50.
- Liang H, DeMaria CD, Erickson MG, Mori MX, Alseikhan BA, Yue DT (2003) Unified mechanisms of Ca²⁺ regulation across the Ca²⁺ channel family. *Neuron* 39:951-60.
- Linden DJ, Dickinson MH, Smeyne M, Connor JA (1991) A long-term depression of AMPA currents in cultured cerebellar Purkinje neurons. *Neuron* 7:81-9.
- Llano I, DiPolo R, Marty A (1994) Calcium-induced calcium release in cerebellar purkinje cells. *Neuron* 12:663-673.
- Llinas R, Hess R (1976) Tetrodotoxin-resistant dendritic spikes in avian Purkinje cells. *Proc Natl Acad Sci USA* 73:2520-2523.

- Llinas R, Nicholson C (1971) Electrophysiological properties of dendrites and somata in alligator Purkinje cells. *J Neurophysiol* 34:532-551.
- Llinas R, Sugimori M, Hillman DE, Cherksey B (1992) Distribution and functional significance of the P-type, voltage-dependent Ca^{2+} channels in the mammalian central nervous system. *Trends Neurosci* 15:351-355.
- Llinas R, Sugimori M, Lin JW, Cherksey B (1989) Blocking and isolation of a calcium channel from neurons in mammals and cephalopods utilizing a toxin fraction (FTX) from funnel-web spider poison. *Proc Natl Acad Sci USA* 86:1689-93.
- Luebke JI, Dunlap K TT (1993) Multiple calcium channel types control glutamatergic synaptic transmission in the hippocampus. *Neuron* 11:895-902.
- Lukyanenko V, Gyorke I, Wiesner TF, Gyorke S (2001) Potentiation of Ca^{2+} release by cADP-ribose in the heart is mediated by enhanced SR Ca^{2+} uptake into the sarcoplasmic reticulum. *Circ Res* 89:614-622.
- Luo D, Sun H, Xiao RP, Han Q (2005) Caffeine induced Ca^{2+} release and capacitative Ca^{2+} entry in human embryonic kidney (HEK293) cells. *Eur J Pharmacol* 509:109-15.
- Luisetto S, Fellin T, Spagnolo M, Hivert B, Brust PF, Harpold MM, Stauderman KA, Williams ME, Pietrobon D (2004) Modal Gating of Human $\text{Ca}_v2.1$ (P/Q-type) Calcium Channels: I. The Slow and the Fast Gating Modes and their Modulation by β Subunits. *J Gen Physiol* 124:445-461.

- Maeda H, Ellis-Davies GCR, Ito K, Miyashita Y, Kasai H (1999) Supralinear Ca^{2+} Signaling by Cooperative and Mobile Ca^{2+} Buffering in Purkinje Neurons. *Neuron* 24:989-1002.
- Maetzler W, Nitsch C, Bendfeldt K, Racay P, Vollenweider F, Schwaller B (2004) Ectopic parvalbumin expression in mouse forebrain neurons increases excitotoxic injury provoked by ibotenic acid injection into the striatum. *Exp Neurol* 186:78-88.
- Martone M, Zhang Y, Simpliciano V, Carragher B, Ellisman M (1993) Three-dimensional visualization of the smooth endoplasmic reticulum in Purkinje cell dendrites. *J Neurosci* 13:4636-4646.
- Matsuyama Z, Wakamori M, Mori Y, Kawakami H, Nakamura S, Imoto K (1999) Direct alteration of the P/Q-type Ca^{2+} channel property by polyglutamine expansion in spinocerebellar ataxia 6. *J Neurosci* 19:RC14.
- Matsuyama Z, Yanagisawa NK, Aoki Y, Black JL 3rd, Lennon VA, Mori Y, Imoto K, Inuzuka T (2004) Polyglutamine repeats of spinocerebellar ataxia 6 impair the cell-death-preventing effect of $\text{CaV}2.1$ Ca^{2+} channel--loss-of-function cellular model of SCA6. *Neurobiol Dis* 17:198-204.
- McDonough SI, Mintz IM, Bean BP (1997) Alteration of P-type calcium channel gating by the spider toxin omega-Aga-IVA. *Biophys J* 72:2117-28.
- Meuth SG, Kanyshkova T, Landgraf P, Pape H-C, Budde T (2005) Influence of Ca^{2+} - binding proteins and the cytoskeleton on Ca^{2+} -dependent inactivation of high-

voltage activated Ca^{2+} currents in thalamocortical relay neurons. *Pflugers Arch Eur J Physiol* 450:111-122.

Mikami A, Imoto K, Tanabe T, Niidome T, Mori Y, Takeshima H, Narumiya S, Numa S (1989) Primary structure and functional expression of the cardiac dihydropyridine-sensitive calcium channel. *Nature* 340:230-3.

Mintz IM, Adams ME, Bean BP (1992) P-type calcium channels in rat central and peripheral neurons. *Neuron* 9:85-95.

Mintz IM, Sabatini BL, Regehr W.G. (1995) Calcium control of transmitter release at a cerebellar synapse. *Neuron* 15:675-688.

Mintz IM, Venema VJ, Swiderek KM, Lee TD, Bean BP, Adams ME (1992) P-type calcium channels blocked by the spider toxin omega-Aga-IVA. *Nature* 355:827-9.

Miyakawa H, Lev-Ram V, Lasser-Ross N, Ross WN (1992) Calcium transients evoked by climbing fiber and parallel fiber synaptic inputs in guinea pig cerebellar Purkinje neurons. *J Neurophysiol* 68:1178-1189.

Miyazaki T, Hashimoto K, Shin H-S, Kano M, Watanabe M (2004) P/Q-Type Ca^{2+} Channel α_1A Regulates Synaptic Competition on Developing Cerebellar Purkinje Cells. *J Neurosci* 24:1734-1743.

Mochida S, Few AP, Scheuer T, Catterall WA (2008) Regulation of Presynaptic $\text{CaV}2.1$ Channels by Ca^{2+} Sensor Proteins Mediates Short-Term Synaptic Plasticity. *Neuron* 57:210-216.

- Mori MX, Vander Kooi CW, Leahy DJ, Yue DT (2008) Crystal Structure of the CaV2 IQ Domain in Complex with Ca²⁺/Calmodulin: High-Resolution Mechanistic Implications for Channel Regulation by Ca²⁺. *Structure* 16:607-620.
- Mori Y, Friedrich T, Kim MS, Mikami A, Nakai J, Ruth P, Bosse E, Hofmann F, Flockerzi V, Furuichi T, et al (1991) Primary structure and functional expression from complementary DNA of a brain calcium channel. *Nature* 350:398-402.
- Muller A, Kukley M, Stausberg P, Beck H, Muller W, Dietrich D (2005) Endogenous Ca²⁺ Buffer Concentration and Ca²⁺ Microdomains in Hippocampal Neurons. *J Neurosci* 25:558-565.
- Muller M, Felmy F, Schwaller B, Schneggenburger R (2007) Parvalbumin Is a Mobile Presynaptic Ca²⁺ Buffer in the Calyx of Held that Accelerates the Decay of Ca²⁺ and Short-Term Facilitation. *J Neurosci* 27:2261-2271.
- Murphy TH, Worley PF, Baraban JM (1991) L-type voltage-sensitive calcium channels mediate synaptic activation of immediate early genes. *Neuron* 7:625-635.
- N Maeda, M Niinobe, K Mikoshiba (1990) A cerebellar Purkinje cell marker P400 protein is an inositol 1,4,5-trisphosphate (InsP3) receptor protein. Purification and characterization of InsP3 receptor complex. *EMBO Journal* 9:61-67.
- Nagerl UV, Mody I, Jeub M, Lie AA, Elger CE, Beck H (2000a) Surviving granule cells of the sclerotic human hippocampus have reduced Ca(2+) influx because of a loss of calbindin-D(28k) in temporal lobe epilepsy. *J Neurosci* 20:1831-1836.

- Nagerl UV, Novo D, Mody I, Vergara JL (2000b) Binding Kinetics of Calbindin-D28k Determined by Flash Photolysis of Caged Ca^{2+} . *Biophys J* 79:3009-3018.
- Nakade S, Rhee S, Hamanaka H, Mikoshiba K (1994) Cyclic AMP-dependent phosphorylation of an immunoaffinity-purified homotetrameric inositol 1,4,5-trisphosphate receptor (type I) increases Ca^{2+} flux in reconstituted lipid vesicles. *J Biol Chem* 269:6735-6742.
- Nakanishi S, Fujii A, Kimura T, Sakakibara S, Mikoshiba K (1995) Spatial distribution of omega-agatoxin IVA binding sites in mouse brain slices. *J Neurosci Res* 41:532-539.
- Narita K, Akita T, Hachisuka J, Huang SM, Ochi K, Kuba K (2000) Functional Coupling of Ca^{2+} Channels to Ryanodine Receptors at Presynaptic Terminals - Amplification of Exocytosis and Plasticity. *J Gen Physiol* 115:519-532.
- Narita K, Akita T, Osanai M, Shirasaki T, Kijima H, Kuba K (1998) A Ca^{2+} -induced Ca^{2+} Release Mechanism Involved in Asynchronous Exocytosis at Frog Motor Nerve Terminals. *J Gen Physiol* 112:593-609.
- Nishizuka Y (1988) The molecular heterogeneity of protein kinase C and its implications for cellular regulation. *Nature* 334:661-665.
- Nowycky MC, Fox AP, Tsien RW (1985) Three types of neuronal calcium channel with different calcium agonist sensitivity. *J Gen Physiol* 86:440-443.
- Opatowsky Y, Chen CC, Campbell KP, Hirsch JA (2004) Structural analysis of the

voltage-dependent calcium channel beta subunit functional core and its complex with the alpha 1 interaction domain. *Neuron* 42:387-399.

Pantazopoulou H, Lange N, Baldessarini RJ, Berretta S (2007) Parvalbumin Neurons in the Entorhinal Cortex of Subjects Diagnosed With Bipolar Disorder or Schizophrenia. *Biological Psychiatry* 61:640-652.

Park D, Dunlap K (1998) Dynamic regulation of calcium influx by G-proteins, action potential waveform, and neuronal firing frequency. *J Neurosci* 18:6757-66.

Patel S, Morris SA, Adkins CE, O'Beirne G, Taylor CW (1997) Ca^{2+} -independent inhibition of inositol trisphosphate receptors by calmodulin: Redistribution of calmodulin as a possible means of regulating Ca^{2+} mobilization. *Proc Natl Acad Sci USA* 94:11627-11632.

Patterson M, Sneyd J, Friel DD (2007) Depolarization-induced calcium responses in sympathetic neurons: relative contributions from Ca^{2+} entry, extrusion, ER/mitochondrial Ca^{2+} uptake and release, and Ca^{2+} buffering. *J Gen Physiol* 129:29-56.

Pauls TL, Durussel I, Berchtold MW, Cox JA (1994) Inactivation of individual Ca^{2+} -binding sites in the paired EF-hand sites of parvalbumin reveals asymmetrical metal-binding properties. *Biochemistry* 33:10393-10400.

Pauls TL, Durussel I, Cox JA, Clark ID, Szabo AG, Gagne SM, Sykes BD, Berchtold MW (1993) Metal binding properties of recombinant rat parvalbumin wild-type and F102W mutant. *J Biol Chem* 268:20897-20903.

- Peng Y (1996) Ryanodine-Sensitive Component of Calcium Transients Evoked by Nerve Firing at Presynaptic Nerve Terminals. *J Neurosci* 16:6703-6712.
- Perez-Reyes E, Castellano A, Kim HS, Bertrand P, Baggstrom E, Lacerda AE, Wei XY, Birnbaumer L (1992) Cloning and expression of a cardiac/brain beta subunit of the L-type calcium channel. *J Biol Chem* 267:1792-1797.
- Peterson BZ, DeMaria CD, Adelman JP, Yue DT (1999) Calmodulin is the Ca^{2+} sensor for Ca^{2+} -dependent inactivation of L-type calcium channels. *Neuron* 22:549-558.
- Peterson BZ, Lee JS, Mulle JG, Wang Y, de Leon M, Yue DT (2000) Critical Determinants of Ca^{2+} -Dependent Inactivation within an EF-Hand Motif of L-Type Ca^{2+} Channels. *Biophys J* 78:1906-1920.
- Plogmann D, Celio MR (1993) Intracellular concentration of parvalbumin in nerve cells. *Brain Res* 600:273-279.
- Pragnell M, De Waard M, Mori Y, Tanabe T, Snutch TP, Campbell KP (1994) Calcium channel [beta]-subunit binds to a conserved motif in the I-II cytoplasmic linker of the [alpha]1-subunit. *Nature* 368:67-70.
- Qin N, Olcese R, Bransby M, Lin T, Birnbaumer L (1999) Ca^{2+} -induced inhibition of the cardiac Ca^{2+} channel depends on calmodulin. *Proc. Natl. Acad. Sci. USA* 96:2435-2438.
- Raman IM, Bean BP (1999) Ionic Currents Underlying Spontaneous Action Potentials in Isolated Cerebellar Purkinje Neurons. *J Neurosci* 19:1663-1674.

- Randall A, Tsien RW (1995) Pharmacological Dissection of Multiple Types of Ca^{2+} Channel Currents in Rat Cerebellar Granule Neurons. *Journal of Neuroscience* 15:2995-3012.
- Regan LJ (1991) Voltage-dependent calcium currents in Purkinje cells from rat cerebellar vermis. *J Neurosci* 11:2259-69.
- Reiken S, Lacampagne A, Zhou H, Kherani A, Lehnart SE, Ward C, Huang F, Gaburjakova M, Gaburjakova J, Rosemblyt N, Warren MS, He K, Yi G, Wang J, Burkhoff D, Vassort G, Marks AR (2003) PKA phosphorylation activates the calcium release channel (ryanodine receptor) in skeletal muscle: defective regulation in heart failure. *J Cell Biol* 160:919-928.
- Rettig J, Sheng ZH, Kim DK, Hodson CD, Snutch TP, Catterall WA (1996) Isoform-specific interaction of the $\alpha 1A$ subunits of brain Ca^{2+} channels with the presynaptic proteins syntaxin and SNAP-25. *Proc Natl Acad Sci USA* 93:7363-7368.
- Richards KS, Swensen AM, Lipscombe D, Bommert K (2007) Novel $\text{Ca}_v2.1$ clone replicates many properties of Purkinje cell $\text{Ca}_v2.1$ current. *Euro J Neurosci* 26:2950-2961.
- Roberts WM (1994) Localization of calcium signals by a mobile calcium buffer in frog saccular hair cells. *J Neurosci* 14:3246-62.
- Rousset M, Cens T, Gouin-Charnet A, Scamps F, Charnet P (2004) Ca^{2+} and phosphatidylinositol 4,5-bisphosphate stabilize a $\text{G}\beta\gamma$ -sensitive state of

Ca_v2 Ca²⁺ channels. J Biol Chem 279:14619-14630.

Sah P, McLachlan EM (1992) Potassium currents contributing to action potential repolarization and the afterhyperpolarization in rat vagal motoneurons. J Neurophysiol 68:1834-1841.

Sakurai M (1990) Calcium is an intracellular mediator of the climbing fiber in induction of cerebellar long-term depression. Proc Natl Acad Sci USA 87:3383-3385.

Sakurai T, Hell JW, Woppmann A, Miljanich GP, Catterall WA (1995) Immunochemical identification and differential phosphorylation of alternatively spliced forms of the alpha 1A subunit of brain calcium channels. J Biol Chem 270:21234-42.

Schiefer A, Meissner G, Iseberg G. (1995) Ca²⁺ activation and Ca²⁺ inactivation of canine reconstituted cardiac sarcoplasmic reticulum Ca²⁺-release channels. J Physiol 489:337-348.

Schmidt H, Brown EB, Schwaller B, Eilers J (2003a) Diffusional mobility of parvalbumin in spiny dendrites of cerebellar purkinje neurons quantified by fluorescence recovery after photobleaching. Biophys J 84:2599-2608.

Schmidt H, Stiefel KM, Racay P, Schwaller B, Eilers J (2003b) Mutational analysis of dendritic Ca²⁺ kinetics in rodent Purkinje cells: role of parvalbumin and calbindin D28k. J Physiol (Lond) 551:13-32.

Schneider MF, Chandler WK (1973) Voltage dependent charge movement of skeletal muscle: a possible step in excitation-contraction coupling. Nature 242:244-6.

- Schwaller B, Dick J, Dhoot G, Carroll S, Vrbova G, Nicotera P, Pette D, Wyss A, Bluethmann H, Hunziker W, Celio MR (1999) Prolonged contraction-relaxation cycle of fast-twitch muscles in parvalbumin knockout mice. *Am J Physiol* 276:C395-403.
- Schwaller B, Meyer M, Schiffmann S (2002) 'New' functions for 'old' proteins: the role of the calcium-binding proteins calbindin D-28k, calretinin and parvalbumin, in cerebellar physiology. Studies with knockout mice. *Cerebellum* 1:241-258.
- Sencer S, Papineni RVL, Halling DB, Pate P, Krol J, Zhang J-Z, Hamilton SL (2001) Coupling of RYR1 and L-type Calcium Channels via Calmodulin Binding Domains. *J Biol Chem* 276:38237-38241.
- Servais L, Bearzatto B, Schwaller B, Dumont M, De Saedeleer C, Dan B, Barski JJ, Schiffmann SN, Cheron G (2005) Mono- and dual-frequency fast cerebellar oscillation in mice lacking parvalbumin and/or calbindin D-28k. *Euro J Neurosci* 22:861-870.
- Sitsapesan R, Williams AJ (1990) Mechanisms of caffeine activation of single calcium-release channels of sheep cardiac sarcoplasmic reticulum. *J Physiol* 423:425-439.
- Soldatov NM, Zuhlke RD, Bouron A, Reuter H (1997) Molecular Structures Involved in L-type Calcium Channel Inactivation. Role of the Carboxyl-Terminal Region Encoded by Exons 40-42 in alpha 1C Subunit in the Kinetics and Ca²⁺ Dependence of Inactivation. *J Biol Chem* 272:3560-3566.
- Solem M, McMahon T, Messing RO (1997) Protein kinase A regulates regulates

inhibition of N- and P/Q-type calcium channels by ethanol in PC12 cells. *J Pharmacol Exp Ther* 282:1487-95.

Soong TW, DeMaria CD, Alvania RS, Zweifel LS, Liang MC, Mittman S, Agnew WS, Yue DT (2002) Systematic identification of splice variants in human P/Q-type channel $\alpha 1(2.1)$ subunits: implications for current density and Ca^{2+} -dependent inactivation. *J Neurosci* 22:10142-10152.

Sorrentino V, Giannini G, Malzac P, Mattei MG (1993) Localization of a novel ryanodine receptor gene (RZR3) to human chromosome 15q14-q15 by in situ hybridization. *Genomics* 18:163-5.

Starr TV, Prystay W, Snutch TP (1991) Primary structure of a calcium channel that is highly expressed in the rat cerebellum. *Proc. Natl. Acad. Sci. USA* 88:5621-5625.

Stea A, Tomlinson WJ, Soong TW, Bourinet E, Dubel SJ, Vincent SR, Snutch TP (1994) Localization and functional properties of a rat brain $\alpha 1A$ calcium channel reflect similarities to neuronal Q- and P-type channels. *Proc. Natl. Acad. Sci. USA* 91:10576-10580.

Stern MD (1992) Buffering of calcium in the vicinity of a channel pore. *Cell Calcium* 13:183-192.

Stout AK, Li-Smerin Y, Johnson JW, Reynolds IJ (1996) Mechanisms of glutamate-stimulated Mg^{2+} influx and subsequent Mg^{2+} efflux in rat forebrain neurones in culture. *J Physiol* 492 (Pt 3):641-57.

- Sutton KG, McRory JE, Guthrie H, Murphy TH, Snutch TP (1999) P/Q-type calcium channels mediate the activity-dependent feedback of syntaxin-1A. *Nature* 401:800-804.
- T J Cardy, C W Taylor (1998) A novel role for calmodulin: Ca²⁺-independent inhibition of type-1 inositol trisphosphate receptors . *Biochem J* 334:447-455.
- Takahashi M, Seagar MJ, Jones JF, Reber BF, Catterall WA (1987) Subunit structure of dihydropyridine-sensitive calcium channels from skeletal muscle. *Proc Natl Acad Sci USA* 84:5479-5482.
- Takahashi SX, Mittman S, Colecraft HM (2003) Distinctive Modulatory Effects of Five Human Auxiliary β_2 Subunit Splice Variants on L-Type Calcium Channel Gating. *Biophys J* 84:3007-3021.
- Takahashi T, Momiyama A (1993) Different types of calcium channels mediate central synaptic transmission. *Nature* 366:156-158.
- Takeshima H (1993) Primary structure and expression from cDNAs of the ryanodine receptor. *Ann NY Acad Sci* 707:165-177.
- Tanabe T, Takeshima H, Mikami A, Flockerzi V, Takahashi H, Kangawa K, Kojima M, Matsuo H, Hirose T, Numa S (1987-) Primary structure of the receptor for calcium channel blockers from skeletal muscle. *Nature* 328:313-318.
- Tang W, Sencer S, Hamilton SL (2002) Calmodulin modulation of proteins involved in excitation-contraction coupling. *Front Biosci* 7:d1583-9.

- Taverna E, Saba E, Rowe J, Francolini M, Clementi F, Rosa P (2004) Role of Lipid Microdomains in P/Q-type Calcium Channel (Cav2.1) Clustering and Function in Presynaptic Membranes. *J Biol Chem* 279:5127-5134.
- Tippens AL, Lee A (2007) Caldendrin, a Neuron-specific Modulator of Cav/1.2 (L-type) Ca²⁺ Channels. *J Biol Chem* 282:8464-8473.
- Tsien RY (1980) New calcium indicators and buffers with high selectivity against magnesium and protons: design, synthesis, and properties of prototype structures. *Biochemistry* 19:2396-2404.
- Tsujimoto T, Jeromin A, Saitoh N, Roder JC, Takahashi T (2002) Neuronal calcium sensor 1 and activity-dependent facilitation of P/Q-type calcium currents at presynaptic nerve terminals. *Science*. 295:2276-2279.
- Turner TJ, Dunlap K (1995) Pharmacological characterization of presynaptic calcium channels using subsecond biochemical measurements of synaptosomal neurosecretion. *Neuropharmacology* 34:1469-78.
- Uchitel OD, Protti DA, Sanchez V, Cherksey BD, Sugimori M, Llinás R (1992) P-type voltage-dependent calcium channel mediates presynaptic calcium influx and transmitter release in mammalian synapses. *Proc Natl Acad Sci USA* 89:3330-3333.
- Usowicz MM, Sugimori M, Cherksey B, Llinas R (1992) P-type calcium channels in the somata and dendrites of adult cerebellar Purkinje cells. *Neuron* 9:1185-99.

- Van Den Bosch L, Schwaller B, Vleminckx V, Meijers B, Stork S, Ruehlicke T, Van Houtte E, Klaassen H, Celio MR, Missiaen L, Robberecht W, Berchtold MW (2002) Protective effect of parvalbumin on excitotoxic motor neuron death. *Exp. Neurol.* 174:150-161.
- van den Maagdenberg AM, Pietrobon D, Pizzorusso T, Kaja S, Broos LA, Cesetti T, van de Ven RC, Tottene A, van der Kaa J, Plomp JJ, Frants RR, Ferrari MD (2004) A *Cacna1a* knockin migraine mouse model with increased susceptibility to cortical spreading depression. *Neuron* 41:701-10.
- Van Petegem F, Chatelain FC, Minor DL Jr (2005) Insights into voltage-gated calcium channel regulation from the structure of the $\text{Ca}_v1.2$ IQ domain- Ca^{2+} /calmodulin complex. *Nat Struct Mol Biol.* 12:1108-15.
- Van Petegem F, Clark KA, Chatelain FC, Minor DL Jr (2004) Structure of a complex between a voltage-gated calcium channel beta-subunit and an alpha-subunit domain. *Nature* 429:671-5.
- Varadi G, Lory P, Schultz D, Varadi M, Schwartz A (1991) Acceleration of activation and inactivation by the beta subunit of the skeletal muscle calcium channel. *Nature* 352:159-62.
- Vecellio M, Schwaller B, Meyer M, Hunziker W, Celio MR (2000) Alterations in Purkinje cell spines of calbindin D-28 k and parvalbumin knock-out mice. *European J Neurosci* 12:945-54.
- Velez P, Gyorke S, Escobar A, VEergara J, Fill M. (1997) Adaptation of single cardiac

ryanodine receptor channels. *Biophys J* 72:691-697.

Vendel AC, Terry MD, Striegel AR, Iverson NM, Leuranguer V, Rithner CD, Lyons BA, Pickard GE, Tobet SA, Horne WA (2006) Alternative Splicing of the Voltage-Gated Ca^{2+} Channel beta4 Subunit Creates a Uniquely Folded N-Terminal Protein Binding Domain with Cell-Specific Expression in the Cerebellar Cortex. *J Neurosci* 26:2635-2644.

Volsen SG, Day NC, McCormack AL, Smith W, Craig PJ, Beattie R, Ince PG, Shaw PJ, Ellis SB, Gillespie A, et al (1995) The expression of neuronal voltage-dependent calcium channels in human cerebellum. *Molecular Brain Research* 34:271-82.

Volsen SG, Day NC, McCormack AL, Smith W, Craig PJ, Beattie RE, Smith D, Ince PG, Shaw PJ, Ellis SB, Mayne N, Burnett JP, Gillespie A, Harpold MM (1997) The expression of voltage-dependent calcium channel beta subunits in human cerebellum. *Neuroscience* 80:161-174.

Walter JT, Alviña K, Womack MD, Chevez C, Khodakhah K (2006) Decreases in the precision of Purkinje cell pacemaking cause cerebellar dysfunction and ataxia. *Nature Neurosci* 9:389-397.

Wanaverbecq N, Marsh SJ, Al-Qatari M, Brown DA (2003) The plasma membrane calcium-ATPase as a major mechanism for intracellular calcium regulation in neurones from the rat superior cervical ganglion. *J Physiol* 550:83-101.

Westenbroek RE, Sakurai T, Elliott EM, Hell JW, Starr TV, Snutch TP, Catterall WA (1995) Immunochemical identification and subcellular distribution of the alpha

1A subunits of brain calcium channels. *J Neurosci* 15:6403-18.

Wheeler DB, Randall A, Tsien RW (1996) Changes in action potential duration alter reliance of excitatory synaptic transmission on multiple types of Ca^{2+} channels in rat hippocampus. *J Neurosci* 16:2226-2237.

Wheeler DB, Randall A TR (1994) Roles of N-type and Q-type Ca^{2+} channels in supporting hippocampal synaptic transmission. *Science* 264:107-111.

Wiser O, Trus M, Tobi D, Halevi S, Giladi E, Atlas D (1996) The $[\alpha]_2/[\delta]$ subunit of voltage sensitive Ca^{2+} channels is a single transmembrane extracellular protein which is involved in regulated secretion. *FEBS Letters* 379:15-20.

Womack MD, Chevez C, Khodakhah K (2004) Calcium-Activated Potassium Channels Are Selectively Coupled to P/Q-Type Calcium Channels in Cerebellar Purkinje Neurons. *J Neurosci* 24:8818-8822.

Womack MD, Khodakhah K (2004) Dendritic Control of Spontaneous Bursting in Cerebellar Purkinje Cells. *J Neurosci* 24:3511-3521.

Wykes RCE, Bauer CS, Khan SU, Weiss JL, Seward EP (2007) Differential Regulation of Endogenous N- and P/Q-Type Ca^{2+} Channel Inactivation by Ca^{2+} /Calmodulin Impacts on Their Ability to Support Exocytosis in Chromaffin Cells. *J Neurosci* 27:5236-5248.

Yang PS, Alseikhan BA, Hiel H, Grant L, Mori MX, Yang W, Fuchs PA, Yue DT (2006) Switching of Ca^{2+} -Dependent Inactivation of $\text{Ca}_v1.3$ Channels by Calcium

Binding Proteins of Auditory Hair Cells. *J Neurosci* 26:10677-10689.

Yenari MA, Minami M, Sun GH, Meier TJ, Kunis DM, McLaughlin JR, Ho DY, Sapolsky RM, Steinberg GK (2001) Calbindin d28k overexpression protects striatal neurons from transient focal cerebral ischemia. *Stroke* 32:1028-35.

Yoshimura H, Sugai T, Onoda N, Segami N, Kato N (2001) Synchronized population oscillation of excitatory synaptic potentials dependent of calcium-induced calcium release in rat neocortex layer II/III neurons. *Brain Res* 915:94-100.

Yue D, Backx P, Imredy J (1990) Calcium-sensitive inactivation in the gating of single calcium channels. *Science* 250:1735-1738.

Zaitsev AV, Povysheva NV, Lewis DA, Krimer LS (2007) P/Q-type, but not N-type, calcium channels mediate GABA release from fast-spiking interneurons to pyramidal cells in rat prefrontal cortex. *J Neurophysiol* 97:3567-73.

Zhou H, Kim S-A, Kirk EA, Tippens AL, Sun H, Haeseleer F, Lee A (2004) Ca²⁺-Binding Protein-1 Facilitates and Forms a Postsynaptic Complex with Ca_v1.2 (L-Type) Ca²⁺ Channels. *J Neurosci* 24:4698-4708.

Zhou H, Yu K, McCoy KL, Lee A (2005) Molecular Mechanism for Divergent Regulation of Ca_v1.2 Ca²⁺ Channels by Calmodulin and Ca²⁺-binding Protein-1. *J Biol Chem* 280:29612-29619.

Zhou YD, Turner TJ, Dunlap K (2003) Enhanced G protein-dependent modulation of excitatory synaptic transmission in the cerebellum of the Ca²⁺ channel-mutant

mouse, tottering. *J Physiol* 547:497-507.

Zhuchenko O, Bailey J, Bonnen P, Ashizawa T, Stockton DW, Amos C, Dobyns WB, Subramony SH, Zoghbi HY, Lee CC (1997) Autosomal dominant cerebellar ataxia (SCA6) associated with small polyglutamine expansions in the $[\alpha]1A$ -voltage-dependent calcium channel. *Nature Genetics* 15:62-69.

Zuhlke RD, Pitt GS, Deisseroth K, Tsien RW, Reuter H (1999) Calmodulin supports both inactivation and facilitation of L-type calcium channels. *Nature* 399:159-162.

Zuhlke RD, Pitt GS, Tsien RW, Reuter H (2000) Ca^{2+} -sensitive Inactivation and Facilitation of L-type Ca^{2+} Channels Both Depend on Specific Amino Acid Residues in a Consensus Calmodulin-binding Motif in the $\alpha 1C$ subunit. *J Biol Chem* 275:21121-21129.

Zuhlke RD, Reuter H (1998) Ca^{2+} -sensitive inactivation of L-type Ca^{2+} channels depends on multiple cytoplasmic amino acid sequences of the $\alpha 1C$ subunit. *Proc Natl Acad Sci USA* 95:3287-3294.